AN ISOTOPIC STUDY OF FIBER–WATER INTERACTIONS

A Dissertation
Presented to
The Academic Faculty

By

Frances Luella Walsh

In Partial Fulfillment
Of the Requirements for the Degree
Doctor of Philosophy in the
School of Chemical and Biomolecular Engineering

Georgia Institute of Technology

December 2006

AN ISOTOPIC STUDY OF FIBER–WATER INTERACTIONS

Approved by:

Dr. Sujit Banerjee, Advisor
School of Chemical and Biomolecular
Engineering
Georgia Institute of Technology

Dr. Timothy Patterson
School of Mechanical Engineering
Georgia Institute of Technology

Dr. Orlando J. Rojas
Forest Biomaterials Laboratory
College of Natural Resources
North Carolina State University

Dr. Yulin Deng
School of Chemical and Biomolecular
Engineering
Georgia Institute of Technology

Dr. Amyn Teja
School of Chemical and Biomolecular
Engineering
Georgia Institute of Technology

Date Approved: July 28th, 2006

To my husband Matt

In this world of ordinary people…
extraordinary people
I'm glad there is you
- Jimmy Dorsey and Paul Mertz
from "I'm Glad There is You"

ACKNOWLEDGEMENTS

And who can forget Major White, thanks for the stories, laughter, watching out for us, and thinking we were the best class IPST ever had.

TABLE OF CONTENTS

LIST OF TABLES

LIST OF FIGURES

LIST OF EQUATIONS

NOMENCLATURE

a	=	cross sectional area of a cylinder
BHWK	=	bleached hardwood kraft pulp
BSWK	=	bleached softwood kraft pulp
C	=	pulp consistency (%)
$C_{res,i}$	=	initial reservoir concentration
$C_{res,f}$	=	final reservoir concentration
c_i	=	initial concentration of blue dextran (as measured by UV-vis)
c_f	=	final concentration of blue dextran (as measured by UV-vis)
CL	=	curl index
CSF	=	corrected freeness (mL)
CSF_T	=	temperature corrected freeness (mL)
CSF_U	=	uncorrected freeness (mL)
cpm	=	counts per minute
D	=	percent activity in a fiber water suspension or diffusion coefficient
D_i	=	initial disintegrations per minute of the pulp-water system
D_w	=	disintegrations per minute in the water wash
DI	=	deionized water
DSC	=	differential scanning calorimetry
dpm	=	disintegrations per minute
$dpm_{control}$	=	disintegrations per minute of the water control
dpm_p	=	disintegrations per minute in the pulp fraction (DPM/g od pulp)

dpm_{sample}	=	disintegrations per minute of the water in the pulp sample
dpm_w	=	disintegrations per minute in the water fraction (DPM/g water)
FSP	=	fiber saturation point (g of water in pulp/g of od pulp)
FQA	=	fiber quality analysis
H	=	moles of hydrogen
HTO	=	tritiated water
KI	=	kink index
K_{pw}	=	pulp – water partition coefficient (g of water in pulp/g of od pulp)
L	=	number of hydration layers or projected fiber length
l	=	contour fiber length
L_i	=	individual fiber length
L_W	=	length weighted fiber length
M_∞	=	moles at equilibrium
MW_W	=	molecular weight of water (18.016g/mol)
MW_C	=	molecular weight of cellobiose (342g/mol)
N	=	number of kinked fibers
n_i	=	number of fibers
NMR	=	nuclear magnetic resonance
OD	=	deuterated hydroxyl group
od	=	oven dried sample
p	=	weight of od pulp (g)
q	=	weight of water in pulp (g)
q_i	=	water initially present in the pulp water system (g)

SEM	=	scanning electronic microscopy
s	=	weight of saturated or wet pulp (g)
T	=	temperature (°C)
UHWK	=	unbleached hardwood kraft pulp
USWK	=	unbleached softwood kraft pulp
V_{res}	=	volume of reservoir
w	=	weight of blue dextran solution (g)
WRV	=	water retention value (g of water in pulp/g of OD pulp)
WRV_{R0}	=	water retention value of unrecycled fiber
WRV_{RX}	=	water retention value of fiber recycled X times

SUMMARY

A new technique for measuring the water content of fiber is presented. Tritiated water is added to a pulp/water suspension whereupon the tritium partitions between the bulk water and the pulp. Through this technique a fiber:water partition coefficient is developed, K_{pw}. This thesis will cover the development of the K_{pw} procedure and three different case studies.

The first study involves comparing K_{pw} to traditional methods of fiber water content. The procedure provides a value of ten percent for the tightly bound water content of unrefined hardwood or softwood kraft fiber, either bleached or unbleached. If this water is assumed to cover the fiber surface as a monolayer, then an estimate of the wet surface area of fiber can be obtained. This estimate compares well to independent measurements of surface area.

K_{pw} has also been found to be valuable in furthering the understanding of refining. Based on the study, it is proposed that refining occurs in three discrete stages. First, refining removes the primary cell wall and S1 layer while beginning to swell the S2 layer. Next, internal delamination occurs within the S2 layer. Finally, fiber destruction occurs at high refining levels. By using K_{pw}, the three stages of refining are clearly recognized.

Lastly, K_{pw} is used to study the effect of hornification on bleached softwood kraft fiber. The recycling effects at three refining levels were characterized by K_{pw} and followed closely the findings of the refining study. At low and high refining levels, the impact of recycling was minimal according to K_{pw} results, but at 400 mL csf the impact

of recycling was much more pronounced. This could be attributed to the closing of

internal delaminations within the fiber.

CHAPTER 1: INTRODUCTION

The interaction between fibers and water has been a topic of interest for many years. In the literature, many studies have been performed and theories have been considered on topics such as the cellulose water interaction and hydrogen bonding within and between fibers. Many researchers have used complicated methods to decipher the fiber-hydrogen interaction. By using hydrogen to study hydrogen interactions and thus water to study water interactions, a simple, straight forward method has been developed to further our basic understanding of fiber-water systems.

Hydrogen isotopes give the researcher the ability to study the interaction between hydrogen and fibers without altering their present system. By exchanging hydrogen for one of its isotopes, such as tritium, the interaction between hydrogen and fibers can be traced and quantified. In the case of this research, tritiated water was used to further the understanding of the fiber water system and how fibers are affected by processing. Previously, researchers have used isotopes to quantify crystalline and amorphous regions of the fiber. But, rarely have studies been conducted using isotopes to understand how water interacts with fibers.

The hydrogen bonding nature between fibers and water is critical to the papermaking process. Water is a swelling medium for fibers. Fibers processed in water increase in surface area, conformability, and interaction with other fibers. Water also provides the mechanism to distribute fibers into a sheet and provides the means for bonding to occur during the drying process. Fibers processed in other solvents develop different properties and characteristics than those processed in water.

Processes such as refining and recycling affect the way fibers and water interact. Traditional measurement techniques such as freeness, water retention value, and solute exclusion have been used to quantify this interaction. However, each technique utilizes indirect data to quantify the interaction. Through the use of hydrogen isotopes, this interaction can be directly quantified.

Through this research, we hope to bring to light how the fiber-water interaction changes during processing and how monitoring these changes through the use of isotopes have the potential to improve the papermaking process. To monitor this relationship, a new experimental method utilizing tritiated water was developed. A comparison was performed between this new method and traditional measurements; including water retention value, solute exclusion, and freeness. Then this method was used to analyze fibers during the refining process and through recycling. Microscopy was also used to verify theories formulated during the course of study. Ultimately, the tritiated water method provides a different perspective from more traditional methods.

A number of questions, including the following, were put forth and addressed during the course of this research:

- Can the interaction between water and fibers be directly quantified?
- How does the quantification of the fiber water interaction add insight into the science of paper making?
- How does refining affect the fiber water interaction?
- How does recycling or drying affect the fiber water interaction?

This thesis will address these questions and thus provide further knowledge in one of the basic relationships in the papermaking process.

This thesis first analyzes the available literature to provide a background for the issues associated with fiber-water interactions. Then Chapter 3 provides an analysis of the literature and outline objectives of this research. Chapter 4 briefly discusses the experimental methods and materials associated with this study, while Chapter 5 discusses the development of the tracer technique. Chapters 6 through 9 discuss in detail the four portions of the thesis work, beginning with Chapter 6 which highlights the initial work validating the tritium tracer technique. Chapter 7 compares the tritiated water method with traditional methods by examining fiber saturation. Chapters 8 and 9 focus on the impact of refining and recycling on fiber, respectively. Chapter 10 provides the overall conclusions to this study.

By using isotopes to study fiber-water interactions, insights have been gained into how fibers interact with water and how this relationship changes during different processes.

CHAPTER 2: LITERATURE REVIEW

The impetus for this research came in the form of a figure provided by Neuman [1] during the Tenth Fundamental Research Symposium in 1993. This figure was a depiction of a cellulose surface in water, the "dangling tail" model of the cellulose surface, Figure 1 [1]. Neuman [1] suggested that in dilute suspensions, the "dangling tails" or cellulose fibrils extend into solution producing a rug-like effect surrounding the cellulose.
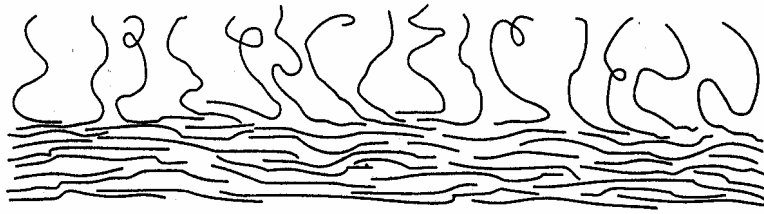
Figure 1: Neuman's Dangling Tail Model

Neuman [1] used a number of sources to validate his theory. He cited Clark [2] and his discussion of molecular fibrillation of cellulose and partial solubility in water. Neuman also discussed theories developed by Kibblewhite [3] and Alince [4]. Kibblewhite's [3] theory suggested that molecular fibrils could create high interfiber bonding and Alince [4] suggested that a surface roughness may prevent certain particles from having close contact with the fiber surface.

The following questions arose:

- How accurate is Neuman's theory?

- Could this water saturated surface be measured and quantified?

- How does processing affect the saturated surface of cellulose?

The answers to these questions began with a literature review covering many aspects of the fiber water relationship. First, an overview of the forms and characteristics of cellulose, the main component of fiber, is presented and relationships between cellulose and water introduced. This is followed by a discussion of fiber structure and softwood and hardwood characteristics with an introduction to water and its properties in various systems. This introduction leads into a discussion of water's relationship with fibers, which leads to a broader discussion of the accessibility of water, swelling of fibers, fiber saturation, bound water, and binding mechanisms. The concept of using isotopes to explore this relationship is then introduced. Lastly, a background on refining and paper recycling is provided.

2.1 Cellulose
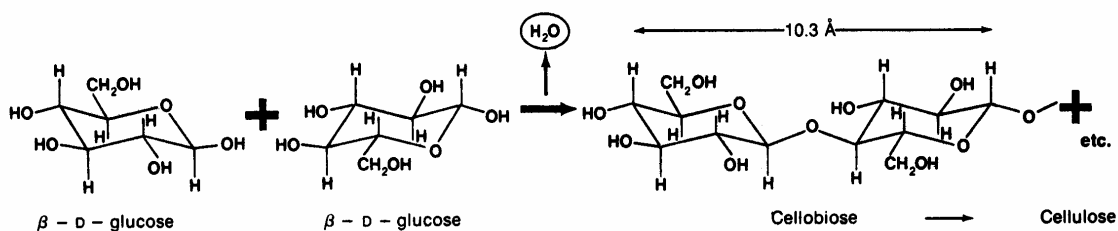
Figure 2: Cellulose formation

Paper consists primarily of cellulose fiber. This fiber comes from the cell wall of plants, primarily trees. The cell wall of a tree consists of approximately 40 % to 50 %

5

cellulose with the remaining percentages divided into lignin (15 % to 35 %) and

hemicelluloses (20 % to 30 %).[5, 6]
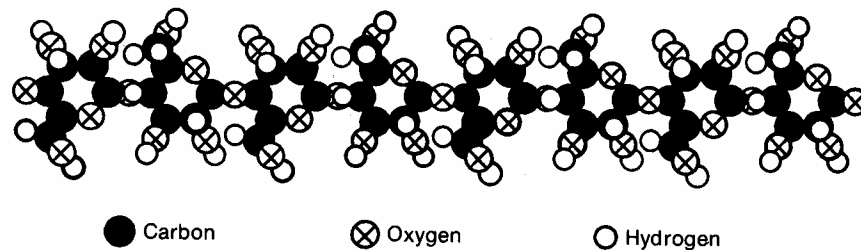
Figure 3: Cellulose molecule

Figure 2 depicts the chemical make up of the cellulose polymer [2]. Two glucose

molecules joined by a β-1,4 linkage form cellobiose, the base unit of cellulose. These

cellobiose units build upon each other forming chains of up to 5000 glucose units for raw

cotton. The alternating arrangement of glucose molecules results in a flat ribbon-like

structure held together by van der Waals forces and hydrogen bonding, Figure 3 [2]. It is

important to note the chemical configuration of the cellulose chain, which exposes the

hydroxyl groups of the molecule with the hydroxyls on the sixth carbon gaining

prominence in the structure [2]. The access of these hydroxyl groups to water creates the

strong cellulose water relationship.

Natural cellulose exists as an array of cellulose chains oriented parallel to one

another. These arrays are commonly known as microfibrils [7]. These molecules are

hydrogen bonded to one another and develop crystalline and amorphous regions [8]. The

microfibrils are approximately 3- 4 nm in diameter and further bundle themselves into

cellulose aggregates or fibrils that are 20 – 25 nm in diameter [9]. The strength and

rigidity of cellulose lies within the crystalline region, where the perfect bonding requires

a large amount of force to break the structure. The flexibility of cellulose lies in the

amorphous regions where the unaligned bonding creates movement within the molecule

[10]. Figure 4 indicates the hydrogen bonding points between two parallel cellulose

chains, primarily the hydrogen of carbon 6 is hydrogen bonded to the oxygen of carbon 3

[11]. The hydrogen bonding between the cellulose chains creates a water-inaccessible

crystalline structure.
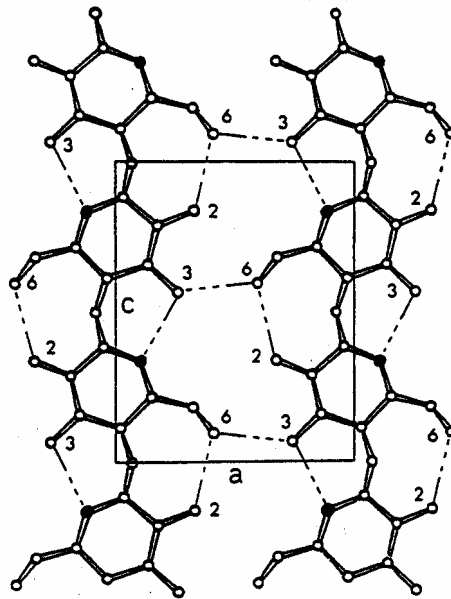
Figure 4: Hydrogen bonding between cellulose molecules

2.1.1 Cellulose Forms and Characteristics

Cellulose is a semicrystalline biopolymer with crystalline and amorphous regions.

The surface material is generally considered to be amorphous, although small crystallites

may form on the fiber surface [12]. The crystalline structure of cellulose is highly

ordered with extensive hydrogen bonding between the molecular chains. This degree of bonding causes the cellulose to be insoluble in water [13].

Cellulose can crystallize into several different polymorphs. Native cellulose is classified as cellulose I while regenerated cellulose is cellulose II. Cellulose I is thought to be made up of parallel chains of the previously described microfibrils. It can be converted to cellulose II through regeneration of dissolved cellulose or strong alkali treatment. A small amount can also convert during pulping. Within cellulose I there are two structural forms, I_α and I_β which differ from each other in terms of hydrogen bonding. I_α has a one-chain triclinic structure. This form is metastable and converts to I_β upon heating. The conversion accelerates during pulping where disordered cellulose may be transformed as well. I_β consists of a two-chain monoclinic structure. The I_β structure is energetically favored due to more favorable intermolecular bonding. Cellulose II is thought to consist of antiparallel chains instead of the parallel chains of cellulose I. A suggested result of this structure is chain folding [12].

Amorphous cellulose regions occur with substitutions and changes in hydroxyl groups in the base units of the cellulose molecule. The substitutions often involve various hemicelluloses consisting of hexoses and pentoses. The inability of these substitutions to fit tightly into the hydrogen bonded structure creates unstructured regions, which are accessible to water, and consequently become critical in the cellulose-water interaction [2].

2.1.2   Cellulose – Water Interaction

The interaction between cellulose and water is extremely important. This interaction allows bonds to form during paper making and gives the sheet strength during and after the paper making process. Water can be directly attached to cellulose through hydroxyl groups and indirectly through modified water structure [13]. Some of the hydrogen atoms present in the cellulose structure are exchangeable with those atoms present in the water. Seventy percent of the hydrogen atoms in the cellulose structure are bonded to carbon. These atoms are considered non-exchangeable. The remaining hydrogen atoms are attached to oxygen. Approximately 15 % of these atoms are in an amorphous structure and readily exchange with water. The remaining 15 % are in a crystalline structure, but they still exchange slowly with water and some exchange more readily than others do. Refining helps enhance the interaction between water and cellulose by imparting mechanical actions on the cellulose fiber [8].   This relationship will be discussed further in Section 2.4.

2.2 Fiber Structure

Besides cellulose, fibers are also made up of hemicelluloses and lignin. Within this section, hemicelluloses and lignin will be briefly discussed, as well as the fiber construction and characteristics of softwood and hardwood.

2.2.1   Fiber components

Cellulose, discussed in Section 2.1, exists as microfibrils within the cell wall, or fiber. These microfibrils are strings of aggregated cellulose chains of approximately 3.5

nm in diameter and consist of amorphous and crystalline regions [14]. Microfibrils are found throughout the fiber in various amounts in combination with hemicelluloses and lignin [2, 6, 14, 15].

Hemicelluloses consist of a number of different types of sugar monomers, which vary with wood species. These monomers consist of six-carbon sugars including mannose, galactose, and glucose, as well as, five-carbon sugars xylose and arabinose [14]. Typical hemicellulose polymers include glucomannan, galactoglucomannan, arabinogalactan, glucuronoxylan, and glucuronarabinoxylan. These structures are amorphous in nature [16]. The average degree of polymerization for hemicellulose is between 100 and 200 sugar units. This, in combination with its amorphous nature, makes hemicelluloses much more soluble than cellulose. During kraft pulping much of the hemicelluloses are dissolved [14].

Lignin is the glue that holds the cell wall together. It consists of a complex polymer made up of phenylpropane units in a completely amorphous structure. Delignification of fibers occurs during kraft pulping resulting in a lignin content of 3.0 – 5.2 % for bleachable pulp grades. Bleaching of kraft pulps further decreases the lignin content of the pulp. [14]

2.2.2 Cell wall structure
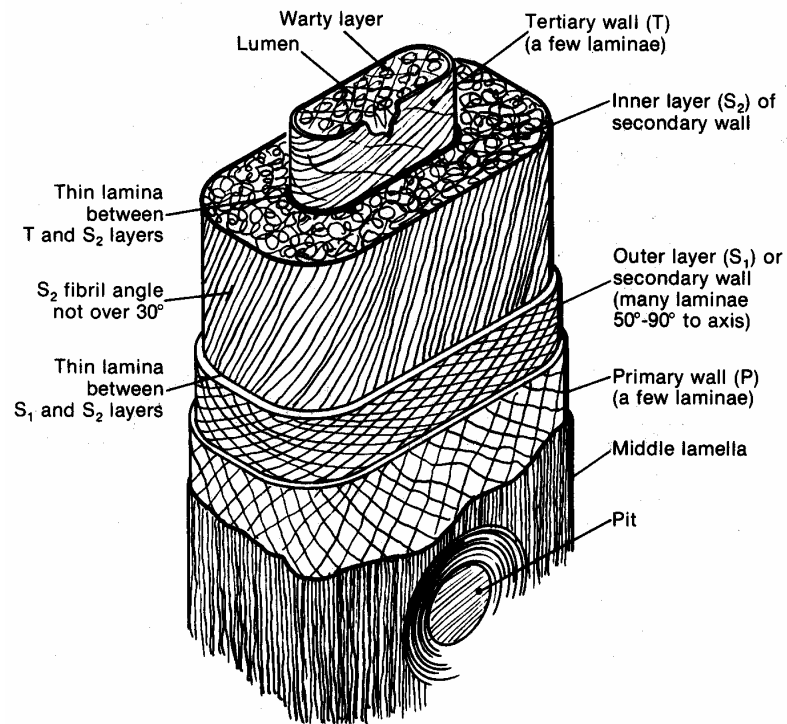
Figure 5: Cell wall structure

The cell wall is a complicated structure made up of three primary parts; the primary wall, secondary wall, and tertiary wall. The open space in the middle of each cell is called the lumen. The space within the lumen is generally used to transport fluids throughout the tree. Surrounding the outside of the cell is the middle lamella [2, 6, 14, 15]. This thin band, approximately 1 to 2 μm thick, cements the fibers together and consists mainly of lignin. This composition allows the fibers to easily separate during chemical pulping as the lignin is dissolved [2]. A depiction of the cell wall is shown in Figure 5 [2].

11
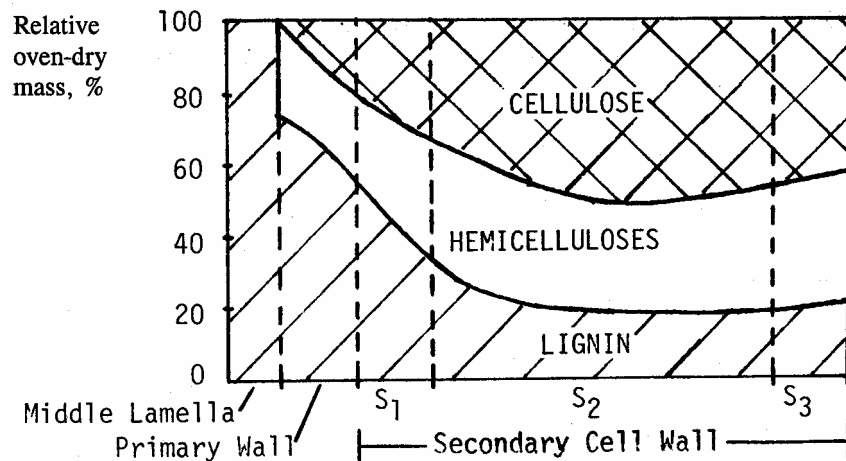
Figure 6: Chemical makeup of cell wall

The cell wall is built from the outside, starting with the primary wall. This thin wall, of the order of 0.1µm thick, is made up primarily of lignin and hemicellulose as shown in Figure 6 [14]. Inside the primary wall is the first part of the secondary wall, or the S1 layer. The S1 layer is also very thin approximately 0.1 – 0.3 µm. The cellulose in this area is wound almost perpendicular to the axis of the fiber [2]. The thickest part of the cell wall is the S2 layer, 2 – 8 µm thick [2]. This portion of the cell wall contains the most cellulose, Figure 6 [14]. These cellulose microfibrils are oriented closest to the fiber axis, at no more than a 30º angle. The smaller the angle, the higher the tensile strength of the fiber [2]. The tertiary wall, or S3 layer, is on the inside of the secondary wall. This wall, like the S1 layer, is very thin, 0.1 µm [6]. On the inside of the fiber, lining the lumen, may be a warty membrane [2].

2.2.3 Softwood characteristics

Softwoods, or gymnosperms, are characterized by their simple anatomy, Figure 7 [2]. The wood contains mainly longitudinal fiber tracheids, approximately 90-95 %. These tracheids, or fibers, range between 2.5 – 7 mm long and 25 – 60 µm wide [14]. The tracheids are used to move fluids throughout the living tree, hence the large open tube structure and the prominent pits to conduct fluids horizontally through the tree [2]. Ray cells, 5 – 10 %, and resin cells, 0.5 - 1.0 % make up the remaining anatomy [14]. Most of the ray cells, also know as parenchyma cells, are removed during washing steps after pulping [2]. Therefore, softwood pulp is made up almost exclusively of tracheids.

2.2.4 Hardwood characteristics

Hardwoods, or angiosperms, are deciduous trees and have a much more complex structure than softwoods. Figure 7 also displays a schematic of a section of hardwood [2]. As shown, hardwoods contain vessel elements, fiber tracheids, libriform fibers, and ray and parenchyma cells. The wood consists of 36-70 % fibers, 20-55 % vessel elements, 6-20 % ray cells, with approximately 2 % parenchyma cells [14]. Because of the presence of vessel elements, the fibers within hardwood are shorter, 1 – 1.5 mm, and possess less open area than softwood fibers [2]. These properties lead to lower overall strength, but a much smoother sheet of paper [14].
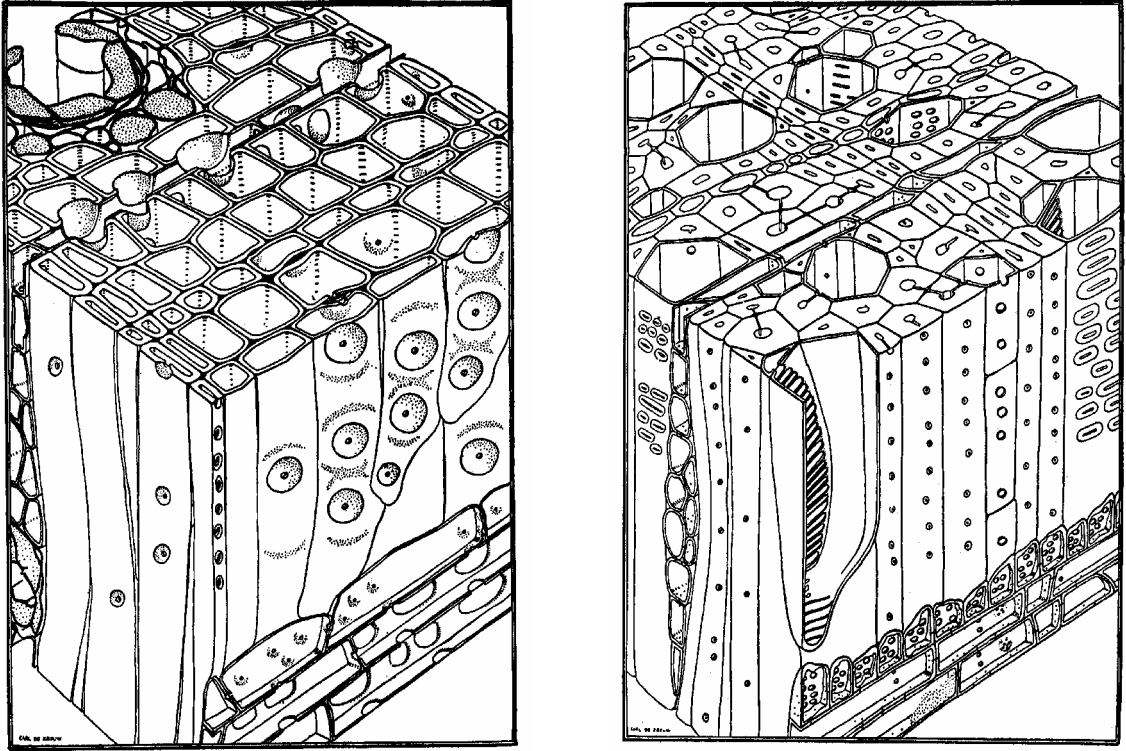
Figure 7: Softwood structure (left) and hardwood structure (right)

2.3 Water

Cellulose and water are similar in many regards, which provides for the strong interaction between the two. Cellulose has even been called "water with a backbone" [17]. The hydroxyl regions of cellulose interact easily with water due to the dipole nature of water.

2.3.1 Water

Water, a key to life on earth, has many unique properties. When compared to other liquids, it has higher density, viscosity, surface tension, specific heat, and latent heat. These properties are due to an asymmetrical orientation of the two hydrogen

and one oxygen atoms resulting in a permanent dipole. Although molecules of its size are often gases at room temperature, the dipole allows water molecules to attract one another creating large aggregates and aligning into a denser more ordered structure, thus the higher than normal properties [16].

The dipole results from the non-linear configuration of the oxygen and two hydrogen molecules. The attraction between neighboring oxygen and hydrogen atoms bonds the two molecules together forming a hydrogen bond, Figure 8 [2]. This hydrogen bonding allows for the formation of ice and the bonding of paper fibers.
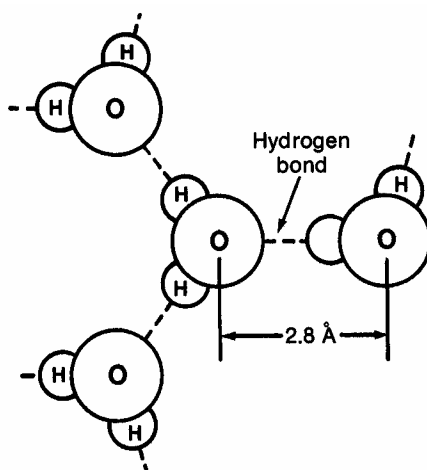
Figure 8: Hydrogen bonding of water molecules

2.3.2 Hydrogen bonds

Hydrogen bonds are deemed present when either, there is evidence of bond formation or that the bond connecting molecule A to molecule B specifically includes a hydrogen atom covalently bonded to molecule A. Hydrogen bonds can occur between two electronegative atoms, commonly oxygen, nitrogen, and fluorine.

15

Typically, the bond strength of a hydrogen bond is one sixth to one tenth that of a strong chemical bond [18]. The bonding ability of hydrogen is a short range interaction of less than 0.2 nm and the angle between donor and acceptor must be within a narrow range [19].

The presence of hydrogen bonds has been confirmed through infrared vibration spectra within cellulose. The free hydroxyl groups in cellulose vibrate at about 3630 cm^{-1} [18]. While, the restrained hydrogen bonded groups vibrate at a lower frequency, approximately 3500 cm^{-1} [18, 20]. Within paper, the hydroxyl groups of hemicelluloses and lignin can also hydrogen bond [18, 21]. It is important to note that these hydrogen bonds occur not only between fibers but also within fibers. The hydroxyl groups present on the surface of the fiber have the ability to bond with other hydroxyl groups of the same fiber or with groups from an adjacent fiber. This bonding may be impeded by the presence of lignin or other impurities interrupting possible hydrogen bonding conformations between fibers. The strength of the fiber – fiber bond is determined by the hydrogen bonding present between the fibers [21].

2.3.3   Structured and confined water

The hydrogen bonding nature of water also leads to interesting phenomena when water is in the presence of a surface, structured, or contained between two closely placed surfaces, confined. The following section will discuss some theories on the interaction between the fiber surface and surrounding water, but before looking

at fibers specifically, a general discussion of water and surfaces will be presented here. This discussion will focus mainly on structured and confined water.

Structured water is found on the surface of particles suspended in water and in a humid atmosphere. Many theories have been proposed on the structure of this water. This structure differs depending on the chemistry of the solid. The relationship between metals, hydrophobic and hydrophilic polymers and water will briefly be introduced. Cellulose or fibers, which are mainly hydrophilic, will be discussed in more detail in Section 2.4 and throughout this thesis.

Metals, especially catalysts, have been studied due to the effect on water on the catalytic nature of the metal. Traditionally, it has been assumed that a buckled bilayer ice-like structure covers the surface of metals [22]. However, it has been shown that water forms in a single layer on platinum, forming a flat ice-like surface, with both the oxygen and the hydrogen of the water participating in bonding. Each hydroxyl group of the water participates in bonding either by bonding directly to the metal or by hydrogen bonding to a water molecule in the overlayer. This bonding does result in weakening of the internal bonding structure of water [22]. Jacob and Goddard [23] discussed the possibility of partially dissociated water on the platinum surface, also determining that the monolayer structure is the lowest energy structure. Michaelides, et al. [24], also found a partially dissociated OH-H_2O overlayer to be the most thermodynamically stable.

Hydrophobic polymers have very limited interaction with the water molecules. Thus, ice formation occurs at 0 °C and any water that may be interacting with the polymer is limited [25].

The adsorption of water onto a hydrophilic polymer can change the mechanical and physical properties of that polymer. The water acts as a plasticizer lowering the glass transition temperature and increasing mobility within the polymer. Adams and Lerner [26] showed that in sucrose the hydroxyl groups interact almost exclusively with the surrounding water and not between and within sucrose molecules. Water is often present in three forms, classified by differential scanning calorimetry (DSC), non-freezing bound water, freezing bound water, and free water. The amount of water is dependent on the polar interaction of the polymer with the water molecules. There is also a set amount of nonfreezing bound water for each polymer determined by the hydrogen bonding ability of the polymer. Above that point water can interact with the surface as freezing bound water. The nonfreezing bound water and freezing bound water represent two types of hydrogen bonding, water attached directly to the surface and water attached to this and subsequent hydration layers [25].

Hydrophilic polymers such as cellulose generally have two types of water within their system bound and free. Bound water is structured by the hydrophilic polymer, consisting of the nonfreezing and freezing bound water, while free water has properties similar to bulk water. Exchange between these two types of water is quite rapid [27].

Confined water can be found within the pores of a solid or between solid surfaces. The changes in behavior of water within these spaces is thought to be dependent on the size and geometry of the space [28]. The space may structure the water due to geometric constraints. In turn, this water may subsequently order the

18

surrounding water [29]. One interesting phenomena of confined water is supercooling. Crupi et al. [28] discussed that water within sol-gel silicas has the ability to supercool to between -15 and -25 ºC. When ice formation does occur within the silica, the structure is cubic rather than the normal hexagonal shape [28]. The size and shape of the confining space also reduce the ability for a water molecule to form all of its potential hydrogen bonds. Urbic, Vlachy and Dill [29] found that this restriction is present until a separation of around 10 water molecule diameters occurs between solid surfaces. As the space between the surfaces decreases, the properties of water change from fluid-like to solid-like. Leng and Cummings [30] determined that at approximately three hydration layers, or a separation of three water molecule diameters, the water retains fluid-like characteristics, although with increased shear viscosity. At a distance of one or two hydration layers, monolayer or bilayer ice can form [30].

Density profiles have commonly been used to model and further understand the changes in confined water. The density of water will oscillate between parallel surfaces due to steric packing and hydrogen bonding. This density and hydrogen bonding oscillation will occur even when the pore or channel is ten times the size of the water molecule [29]. Leng and Cummings [30] determined that beyond 10 Å the water density oscillations subside and approach bulk densities. This oscillation pattern compares well with that of a single surface [30]. Urbic et al. concluded that due to the hydrogen bonding ability of water, confinement alters the orientation and distribution of water molecules [29]. Force oscillations correspond with the density oscillations [29, 31]. Israelachvili and Pashley [31] concluded that these forces

represent a breakdown of continuum theories DLVO (Derjaguin, Landau, Verwey and Overbeek [32, 33]) and van der Waals forces as the space between surfaces decreases to bi and monolayer proportions. This breakdown corresponds well to the thin stable layers observed in soil science, but is not understood.   Israelachvili and Pashley felt this was due to the existence of water molecules forming ordered layers on the surfaces of hydrated substrates [31].

The confined water can be held in the space in a low density or high density state, see Figure 9 [29]. Urbic et al. found that within the low density state (c), the water was in a gas-like state with high compressibility. In the high density case (a), the water was in a liquid-like state and was highly incompressible and in a highly connected hydrogen bonded network. The third state (b), represents the transition between densities. This state is highly volatile and has increased fluctuations in its density and hydrogen bonding profile [29].

Child [34] briefly described confined water within cellulose. Sorbed water of cellulose initially replaces weakly bonded intermolecular hydrogen bonds. As more water diffuses into the system these molecules bond to the sorbed water forming water bridges. These bridges increase in size until chain motion causes the bridges to break [34].
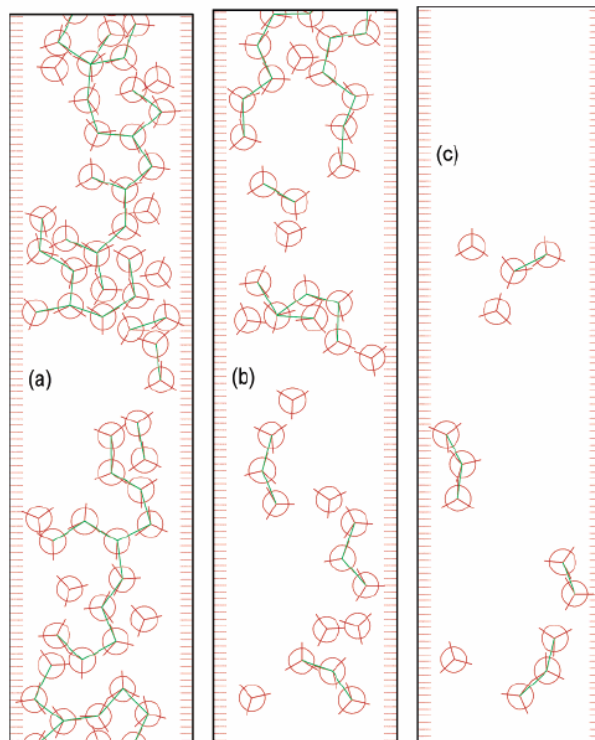
Figure 9: Densities of confined water

2.4 Fiber-Water Relationship

Now that the properties of fibers and water have been introduced, this section will introduce their relationship. Interaction theories, different classifications of water and bonding theories will be discussed. A basic understanding of present theories is critical to this thesis as it gives the foundation to begin our research.

2.4.1   Fiber-water interaction theories and models

Much difficulty lies in truly determining the interaction between fibers and water. First, there are many different ways in which water and fiber interact. Through the years, different types of water have been defined based on their

interaction with fiber. The way that water changes during its interaction with fibers has also been characterized.

First, a few definitions of water in relation to fiber, Stone and Scallan [35] physically classified the water fiber relationship, while Christensen and Giertz [16] chemically classified water.

Stone and Scallan [35] used Figure 10 to describe the physical relationship between water and fiber. V_C is considered the water held within the cell walls of a saturated fiber. Water in the lumen of the fiber is V_L and V_F is water held by the fibril surface of the fiber. Lastly, V_I consists of water held between fibers. Stone and Scallan felt that the volume of water in V_C indicated the amount of swelling within the fiber [35].
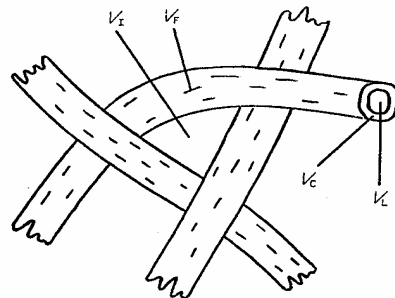
Fig. 1. Ways in which water may be held by fibers.

Figure 10: Ways water physically interacts with fiber

Christensen and Giertz [16] used the general term imbibed or sorbed water to define any water chemically held by a fiber. Free water is classified as any water surrounding, but not associated directly with the fiber. The transition between

22

imbibed and free water provides a general definition for the fiber saturation point [16]. The imbibed water can then be divided into different categories as defined by Stamm [36]. First, the most firmly held water is the water of constitution. This is the water attached to the most thermodynamically attractive sites [37]. This water is held so strongly by the fiber that it cannot be removed until thermal degradation of the fiber occurs. The second most strongly held water is monomolecularly adsorbed water, which forms a monolayer surrounding the fiber held in place by hydrogen bonds. These hydrogen bonds are associated with hydroxyl and carboxyl groups present in the fiber [37, 38]. The water adsorbed beyond the monolayer, from a relative vapor pressure of 0.2 to approximately 0.9, is considered to be polymolecularly held in solid solution by Stamm [36]. This water forms a disordered ice structure when freezing occurs [37]. Stamm [36] resisted calling this polymolecularly held water capillary-condensed water since capillary condensation occurs only to a limited degree within the cell wall. Other authors referred to this water as multilayer water [39]. In Stamm's opinion, the majority of capillary condensation occurs after the cell walls are saturated in microscopically visible capillaries [36]. It is important to note as dried fiber takes on water, water sorption begins with the imbibed water, followed by capillary condensed water and is finally surrounded by bulk or free water. Also, as this water is added to cellulose, the intermolecular forces present within the cellulose diminish, decreasing the glass transition temperature [39].

Through these definitions, theories can begin to take shape on the effect of water on cellulose. Christensen and Giertz [16] summarized three theories in their

paper from the 3rd FRS (Fundamental Research Symposium); the surface adsorption theory, the capillary condensation theory, and swelling theory. All three of these theories observe the effect of adding water to a dry fiber.

First, the surface adsorption theory considers the large amount of internal surface present within the cell wall, including microfibrils, and the surfaces of accessible voids and capillaries. Under the assumption that these surface areas contain many active hydroxyl and other polar groups, the initial water is sorbed in a monolayer, becoming complete at a relative vapor pressure of approximately 0.2. Then at higher relative vapor pressures, water forms multilayers. This theory does not account for the dramatic increase in moisture content at high relative vapor pressures of 0.995 and above [16, 36].

The capillary condensation theory utilizes capillary action to determine that small capillaries will cause water vapor to condense inside these capillaries at a relative vapor pressure of approximately 0.7. The amount of water will continue to increase as the relative vapor pressure increases with the cell wall lumens filling close to 1.0 relative vapor pressure. It is questionable whether this condensation can occur from moist air or rather if wet fibers can retain water within the capillaries as the fiber dries [16].

The last theory discussed by Christensen and Giertz [16] is the swelling theory in which disordered regions of the cell wall consisting mainly of amorphous hemicelluloses acting like a gel where the accessible hydroxyl groups hydrogen bond with the water. This theory was first used to describe the uptake of substances such as viscose rayon which is largely amorphous, but contains very few capillaries [16].

While the previous paragraphs discussed the effect of water on cellulose, the opposite approach can also be taken by considering the effect of cellulose on water. Two opposing view points on this topic were presented at the 6th FRS. Goring [40] proposed that cellulose fibers disrupt the structure of water creating a perturbed layer. This perturbed layer is hydrogen bonded to the hydroxyl groups on the cellulose surface. Caulfield [41] also proposed a hydrogen bonding interaction between the fiber and water, but he suggested that this hydrogen bonding structured the water around the fiber rather than perturbing it.

Goring [40] developed a theory that the cellulose surface disturbs the self hydrogen bonding nature of water. The water molecules surrounding the cellulose surface make up the perturbed hydration layer depicted in Figure 11 [40]. The perturbed layer is indicated by the lack of hydrogen bonded ring structures which are present in the free water or unperturbed layer. The perturbed layer consists of more fluid-like water compared to the unperturbed layer which is much more solid-like. These two layers have different thermal expansions and when cellulose fibers are added to water the fluid-like water increases. Thus, calculations utilizing the proportions of fluid-like and solid-like water resulted in determining a perturbed layer of 0.17 g of water /g of cellulose [40]. Goring then estimated that on average each available hydroxyl group is attached to 1.9 water molecules [40].
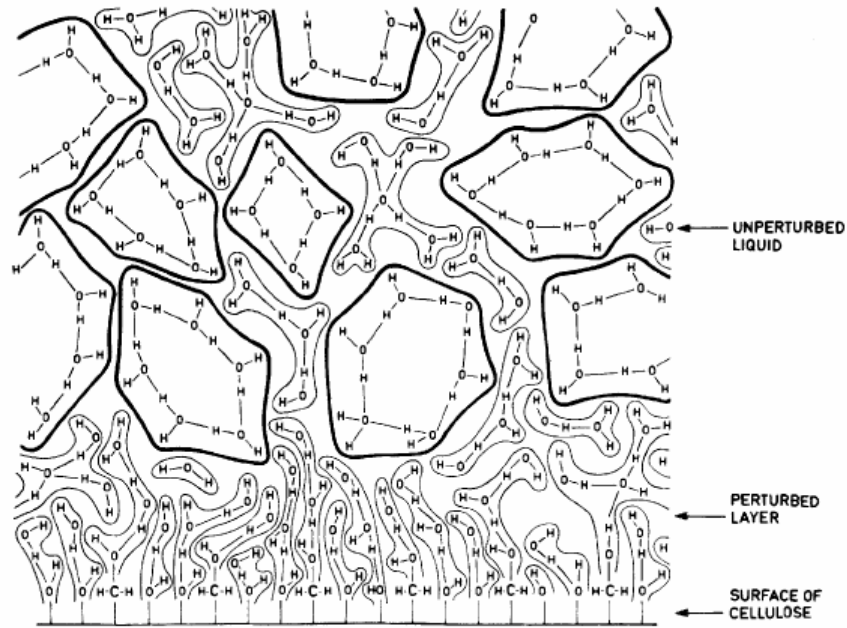
Figure 11: Goring's model of fiber water interaction

Caulfield [41] developed a different theory of water / cellulose interaction utilizing the polarization theory of Polanyi. Caulfield [41] theorized that instead of destructuring water, cellulose actually structures water. With this theory, only the first layer of water is attracted strongly by the cellulose surface. The following layers do not interact with the cellulose surface but with the preceding water layer, Figure 12 [41]. The force of attraction in each layer becomes increasingly weaker until the layers are destructured by the surrounding water. Thus, bound water measurements can be obtained utilizing relative vapor pressure [41].
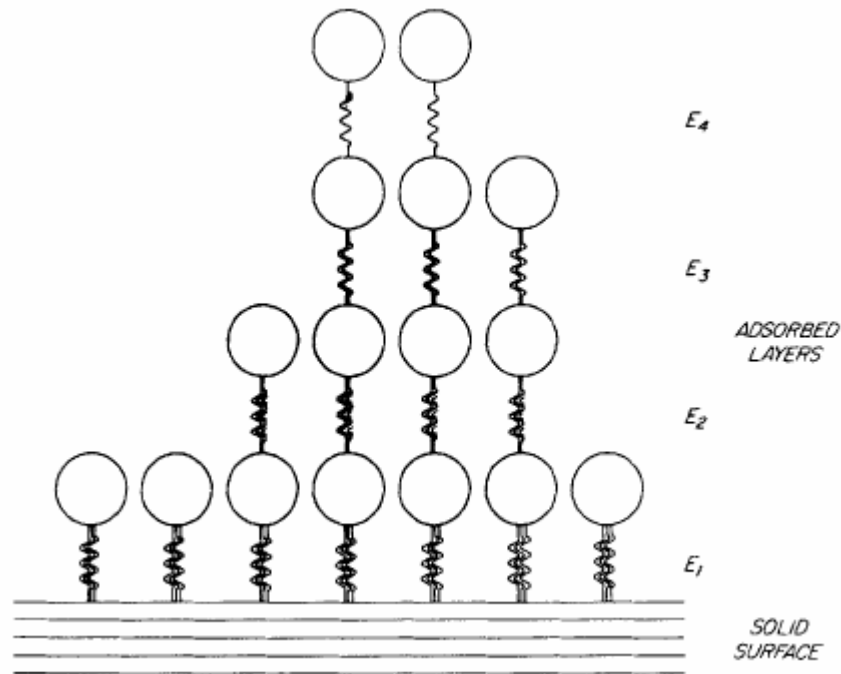
Figure 12: Caulfield's fiber water theory

Christensen and Giertz [16] also presented a theory similar to Caulfield's [41] when excess water is present in the fiber-water system. They determined that water would be bound to the cellulose within the cell wall and also to the surface of the fiber. The line between bound water and free water would be almost indistinguishable. The cellulose surfaces would not be in direct contact with one another, but would more likely share a layer of bound water [16]. As in Caulfield's theory [41], multiple layers surround the fiber with each layer becoming less bound and ordered as the layers progress from the fiber surface [16].

Hartley et al. [42] used aspects of both Goring [40] and Caulfield's [41] theories to develop their theory of water cluster adsorption. This theory stems from initial monolayer theories, BET [43] and Dent [44], but focuses on the energy of the

available bonding sites to determine the bonding potential. Thus, although monolayer adsorption will occur first, a second or third layer may attach prior to all monolayer sites being filled, depending on the energy of the available sites. As this adsorption continues, the additional water will begin behaving more like free water. Another portion of their theory involved the residence time of these clusters. As the hydration of other polymers is quite dynamic, it can be surmised that the same is true for wood and fiber with microsecond movement and exchange occurring [42].

2.4.2   Accessibility of Water

Accessibility of water is often categorized under the term swelling, or the increase in volume of a material due to liquid uptake, temperature or pressure changes [38]. It is believed that the amorphous regions of the fiber largely control accessibility [36]. As fibers do not completely disintegrate when brought into contact with water, it can be considered that swelling within the fiber is restricted. This swelling can be restricted for many reasons including the isotropic nature of the primary wall, the fibril angle of the S1 layer, disorder within the S2 layer, and crystalline regions within the fiber [16]. Water is held by the fiber in a number of ways, as discussed previously. Water is also held in a number of places within the fiber; the amorphous regions of the cell wall, cracks and pores, in the lumen, on the surface of the fiber as well as the fibril surface surrounding the cell. In general, fibers in an excess of water will swell until equilibrium occurs between the water within the fiber and the water surrounding the fiber. This swelling is dependent on the

mechanical properties of the fiber, temperature, and the ionic strength of the solution [38].

During processing, fibers swell as more surfaces open up and become available for contact with water. This opening occurs as forces upon the restricting elements cause failure and bond breakage [16]. Swelling is an important part of the measurement of fiber wet cohesion. By plotting swelling versus beating time, the slope of the line becomes a measure of the wet cohesion of the fiber wall. Different methods are available for testing the degree of fiber swell. These include the pressure plate method, inverse size exclusion chromatography, differential scanning calorimetry, water retention value, and the solute exclusion technique. The amount of swelling measured is dependent upon the test method [38].

The fiber preparation process also has an effect on how the fiber swells during refining. Kraft fibers swell slightly at the start of beating and then remain constant. This is true regardless of beating time and freeness changes. One theory is that the fiber walls have greater integrity and, after the initial swelling, the walls resist further expansion. Overall, the kraft pulp continues to swell throughout refining, but the swelling occurs in the fines rather than in the fibers. Fines have a different internal structure than fibers; they are not short pieces of fiber, but are pieces of the fiber cell wall. Fines become much more swollen than the parent fiber and fiber segments [45].

2.4.3 Fiber saturation

The fiber saturation point (FSP) is a fundamental property of fiber. Christensen and Giertz [16] define the fiber saturation point as the amount of water

required to completely fill the cell wall without filling the lumen. The term was first defined by Tiemann [46] in 1906 in reference to the moisture content below which wood would begin shrinking. Since then, the definition has adapted to a number of moisture systems including pulp fibers.

Measurement of this fiber saturation point has proven difficult. Christensen and Giertz [16] defined it thermodynamically by stating the fiber saturation point occurs when the heat of sorption becomes zero. Any additional water is without heat effects and is called free water. FSP measurements are made through water permeability, treatment with a salt solution, and determination of the latent heat of fusion [16]. Two methods have become the most prevalent ways of measuring fiber saturation point: water retention value (WRV) and solute exclusion (FSP).

WRV, although often used to measure fiber saturation point, actually measures the amount of water contained within a fiber mat, not distinguishing between interfiber spaces and within the fiber. WRV is measured by centrifuging a wet sample at 900 g for 30 minutes [47]. During this process, the centrifugation drives the free water out and the moisture content of the sample is reduced to the water retention value. However, care must be taken not to compress the fiber. As the fiber swelling increases, compression becomes more of an issue. The pulping process, pulp yield, drying and rewetting, as well as refining can also affect WRV. Therefore, WRV tracks the progress of these various processes. In refining, it has been found that WRV correlates with an increase in breaking length [48]. WRV is often used to determine the swelling power or potential of a pulp [49].

Scallan [50] utilized solute exclusion, a method developed by Samuelson [51]

and modified by Scallan and Stone [35, 45] for wood and pulp fibers, to determine

the fiber saturation point. He defined fiber saturation point as the amount of water

within a fiber that is totally inaccessible to a completely excluded macromolecule

[50].   This concept is depicted in Figure 13 [50] where different yield pulps are

subjected to solute exclusion. As shown, each curve levels off at a particular point

where the macromolecule is first completely excluded from pulp sample. Thus, the

volume of water, indicated on the y-axis, gives the fiber saturation point.
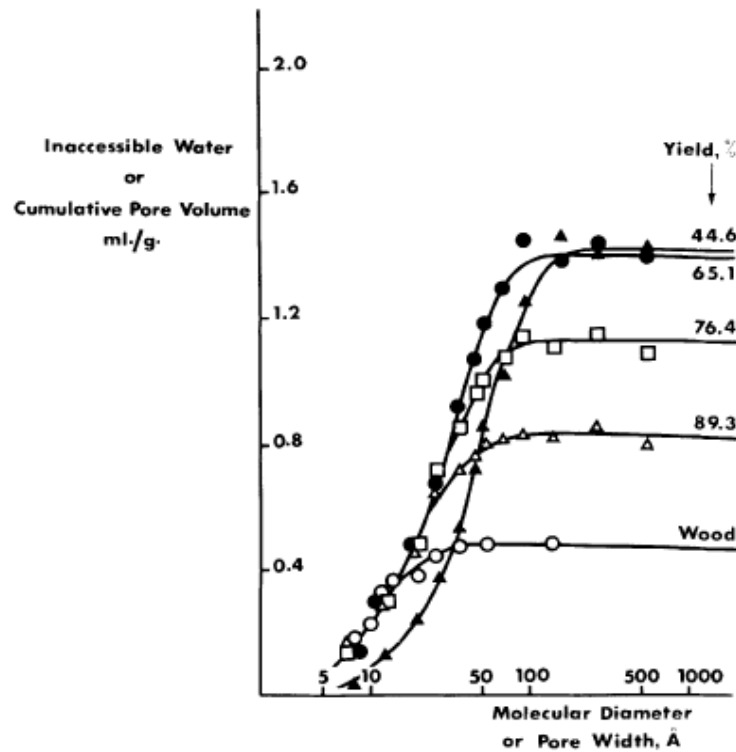
Figure 13: Fiber saturation point using solute exclusion

The development of solute exclusion filled a need to more accurately depict the water swollen nature of fiber. The process involves equilibration of wet pulp and macromolecules of a known hydrodynamic size. The concentration of the macromolecules is then measured and inaccessible and accessible water calculated. A range of molecular sizes is used, as the larger the molecule, the more inaccessible the water in the fiber becomes. This range of molecules allows for two aspects of the fiber to be calculated, pore size distribution and FSP. FSP is the point where the smallest molecule becomes completely excluded from the cell wall. As with WRV, this method also has some problems. First, low yield pulps do not have a distinct FSP. Secondly, fibrils have diffuse outer boundaries. Thus, the probe molecule can have difficulty approaching the fiber and water between fibrils could be deemed inaccessible [45]. Thirdly, the smallest probe molecule usually employed is glucose. Thus, inaccuracies can be created [38, 45]. There is also the inkbottle theory of pore shape. In this theory, the molecule may not be able to fit through the neck of the pore into the wider space inside. Thus, the pore size is inaccurately calculated [52]. Of the two methods, solute exclusion is deemed the more accurate method, but WRV can give an exact measure of FSP up to 1.80 grams of water/ gram of solids according to Scallan and Carles [48].

Oftentimes the results of FSP or WRV are deemed to be "bound water" however, in actuality this is not the case. These measurements give the total amount of water within the pores of the fiber. Thus, there is a great potential that some and possibly most of the water measured with FSP and WRV is not chemically bound to the fiber.

2.4.4 Bound water

The difficulty in defining bound water of fibers resides in the fact that the cellulose residing in those fibers, while having a great affinity for water, does not form a true hydrate. Thus, there is not a concrete number of water molecules that surround the fiber as there is in the case of a hydrated salt. Instead, the hydrophilic nature of the fiber adsorbs surrounding water molecules. The number of water molecules is greatly affected by the state and exposed surface of the fiber. The amount of bound water present in the fiber depends almost exclusively on accessible sites of amorphous regions in the fiber [53]. Also, the adsorption of these water molecules changes the nature of the dried fiber causing it to swell and allow for the adsorption of more water [2]. Thus defining bound water of fibers has become the focus of many studies. Table 1 provides examples of bound water measurements performed during various studies. Due to the many different determinations of the relationship between water and fiber the general term interfacial water was used to generally describe the results of each study, while the authors definition is included under the heading 'Determination'.

Table 1: Historical bound water measurements

Authors	Material	Interfacial water (g/g)	Determination	Method
Hernadi [54]	Cotton Bleached Spruce Bleached Poplar Bleached Straw	0.05 / 0.05 0.06 / 0.06 0.06 / 0.07 0.07 / 0.06	Monolayer Coverage	Water vapor adsorption
Mange, et al. [55]	Acala Cotton Rowden Cotton Mercerized Cotton Rayon	0.04 0.06 / 0.06 0.12 0.19 / 0.19	Bound Water	DSC
Mange, et al. [55]	Acala Cotton Rowden Cotton Mercerized Cotton Rayon	0.20 0.19 / 0.14 0.22 0.39 / 0.31	Total nonfreezing water	DSC
Maloney, et al. [56]	Unbleached Kraft Cotton Microcrystalline Cellulose	0.34 0.24 0.20	Nonfreezing bound water	DSC
Nakamura, et al.[57]	Cotton Yarn Cotton lint Wood Cellulose	0.14 0.18 0.19	Nonfreezing bound water	DSC
Carles and Scallan [58]	Cotton Wood Sulfite pulp Kraft pulp	0.15 0.23 0.30 0.33	Maximum value of bound water	NMR

Hernadi utilized Caulfield's theory along with equations developed by Jefferies [59] and Zwikker - de Boer [60] to determine the water content necessary for monolayer coverage. While plotting adsorption at different partial vapor pressures, Hernadi noticed a change in slope at low partial pressures. He theorized that this change in slope indicates the point at which monolayer coverage is achieved [54]. One difficulty with using Hernadi's method to measure bound water is that the method starts with dried pulp. Thus, some surface area maybe lost due to drying.

Other researchers focused on nonfreezing water, which can be considered "total bound water" as determined by differential scanning calorimetry (DSC) [55-57, 61]. There are many theories proposed on why water near the fiber does not freeze. Maloney, et al. [56] summarized a number of the theories in their 1998 paper. These theories range from limited molecular motion to kinetic effects to capillary forces in nanoscale pores to site adsorption theory, which is the theory Maloney [56] proposed as best explaining their results. Site adsorption theory is based on the premise that nonfreezing bound water corresponds to the number and type of accessible hydration sites in the fiber, primarily hydroxyl groups [56]. Nakamura et al. [57] also subscribed to the site adsorption theory by characterizing bound water as that restricted by the hydroxyl groups of the cellulose, resulting in a lower transition temperature. Nonfreezing water is considered a subset of this bound water, the water that is most tightly associated with the cellulose. Therefore, it has no detectable peak in cooling or heating process associated with DSC [49, 57]. In a recent study, Nakamura along with Hatakeyama and Hatakeyama [62], found a decrease in specific heat between $0.5 - 0.10$ g H_2O/g cellulose Figure 14 [62]. They determined that a

change in the amorphous structure caused the unusual behavior. Calculations were used to determine the amount of the nonfreezing water by subtracting the total amount of water in the sample from the two discernable peaks. There are two problems that are associated with DSC. First, the nonfreezing water is determined indirectly. Secondly, freezing has the potential to alter a fiber due to the expansion of water during ice formation.
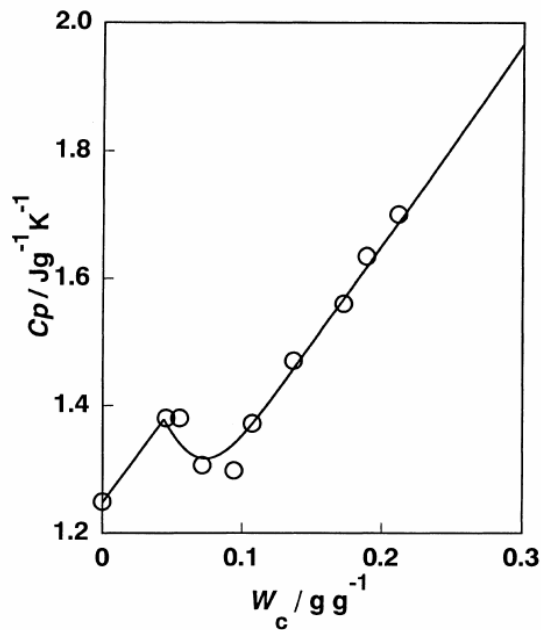
Figure 14: Specific heat during vaporization of water from cellulose

Nelson and Mange et al. [61] also differentiated between this "total bound water" and bound water. Mange et al. [55] determined that the "total bound water" or nonfreezing water is dependent on the freezing temperature of the study. He studied nonfreezing water at -4.5 °C and -13 °C for Rowden Cotton and Rayon (Table 1). It is interesting to note that the change in temperature only affected the total

36

nonfreezing water and did not have any effect on Mange's [55] bound water determination. Nelson [61] also determined that 0.09 g/g can be considered the saturation of primary bound water sorption sites using DSC, confirming his conclusions in a previous study with Froix [63] using NMR. A difficulty in using DSC to determine fiber saturation properties is that the fiber must be stressed. While the nonfreezing water may prevent modification of the micropore structure of the fiber wall, the gross structure of the fiber can be distorted by the formation of ice crystals, potentially altering the overall surface of the fiber. Also, because DSC deals with the interpretation of various peaks and other indirect information the overall results may be subject to error.

Carles and Scallan [58] used NMR to study bound water in a variety of fibers. Their results fall in line with the nonfreezing water results determined by DSC. They also stated that due to experimental difficulties in determining the spin-spin relaxation times of protons in bound water, the results give the maximum amount of bound water in the fiber. Again, the findings using NMR reflect indirect measurements, although the fibers are studied in various wet states which should minimize fiber alteration. One other issue with NMR is the need to orient the studied fibers in a particular direction for readings. Carles and Scallan [58] end their discussion with an interesting question; do hydroxyl groups cause the water adsorption on the cellulose surface or does the presence of a surface alone cause water adsorption?

2.4.5 Fiber surface bonding theories

Retulainen [11] provides a brief review of the theories of adhesion of polymeric materials in his thesis, in which, he names seven adhesion theories: mechanical interlock, adsorption, chemical bonding, electric, acid-base, diffusion, and the weak boundary layer theory. He concludes that in terms of fibers, hydrogen bonding is key to adhesion while van der Waal's forces are also very important.

There are three basic types of bonding between fiber surfaces. First, chemical bonds, or hydrogen bonds, found within the cellulose molecules and also from acid-base interactions between the molecules. Second, intermolecular bonds caused by van der Waals forces. Van der Waals forces have a smaller bonding energy than hydrogen bonds [64]. These forces contribute to the cohesion present within the cellulose chain and the solute [10]. The third type of bonding is entanglement or interdiffusion between polymeric chains on the surface of the fiber. Lastly, these three types of bonding can occur when two fibers are brought into close contact with one another [64].

As previously discussed, chemical or hydrogen bonding occurs between cellulose chains and microfibrils. It also occurs between cell wall elements and between fibers. Thus, almost all hydroxyl groups within a fiber are engaged in productive hydrogen bonding. This bonding either is involved in holding the cellulose structure together, reinforcing the structure, or creating the bonded network of fibers present in a sheet of paper. The remaining available hydroxyl groups are usually associated with water [10, 64].

Within the dried state, fibers are held together by the means of hydrogen bonds [10, 19, 64-69].   Byrd [66, 68] proved the importance of hydrogen bonds by studying strength in a series of dry-formed handsheets. During press-drying, the sheets needed a moisture content of 40 % for adequate bonding [68]. Under normal pressing conditions, a moisture content of over 60 % was necessary [66]. Johansson [67] observed bonding characteristics in various solvents, utilizing the solvents to break up the hydrogen bonding nature of the pulps studied, resulting in a method to characterize the bonding nature of various pulps.

Campbell [70, 71], introduced a theory of bonding now known as the Campbell Effect. He concluded that there are three factors important to cellulose bonding: available area, contact, and hydrogen bonding. His theory involved the impact of drying on contact. As water is removed from the sheet, free water is first removed in the form of evaporation. This free water has no impact on the bonding of the cellulose fibers, but its removal is required for the remaining water to assist in fiber – fiber contact. The remaining water is also removed through evaporation, but as it is removed, shrinkage occurs, setting up surface tension forces between the fiber and fibril surfaces. The forces are the result of the formation of capillaries between fibril surfaces. According to Campbell [70], as the water is removed the tension between the fibrils increases. The pressure between fibrils begins at approximately 142 atm at 90 % relative humidity and increases to around 3110 atm at 10 % relative humidity. This increase in pressure draws the fibrils closer together until they are in contact range with one another and bonding can occur [70]. Figure 15 [2] depicts the capillary forces present during the drying process.
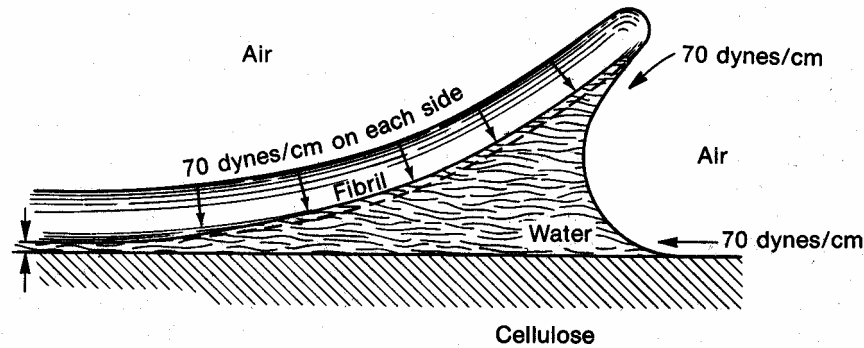
Figure 15: Capillary forces in interfiber bonding

Entanglement or interdiffusion utilizes external fibrillation to link two fibers close together while in the wet state. Thus, when water is removed a chemical bond can form [64], as shown in Figure 16 [2]. McKenzie [65] first adapted Voyutskii's theory of autohesion and adhesion for high polymers [72] to paper. The theory is developed from the idea that adhesion will occur between two plasticized surfaces due to the mingling or diffusion of molecular segments from both surfaces. Upon a change of state; drying, cooling, etc.; bonds form within this intermingled region, thus bonding the two surfaces together [65]. McKenzie [65] felt that contact and surface tension, as described by Campbell [70, 71], do not facilitate enough molecular alignment to form bonds. However, the fibrils, present in the wet state during paper making, are in a plastic state and the diffusion theory can be applied to paper making [65]. Pelton et al. [19] agreed with McKenzie's assessment. They considered that the polymers involved in bonding must be above their glass transition temperature for diffusion to occur. Considering that water is an effective plasticizer for fiber

40

constituents, diffusion occurs between fibers while free water is present, and bonds

form as that water is removed [19]. Robertson [69] further confirmed this study by

observing the bonding potential of fibers in different solutions, concluding that

plasticizing along with high surface tension forces provides the means for interfiber

adhesion. Kibblewhite further extends it by stating that the intensity of bonding

depends on the quantity and quality of the molecular and micro fibrils [3].
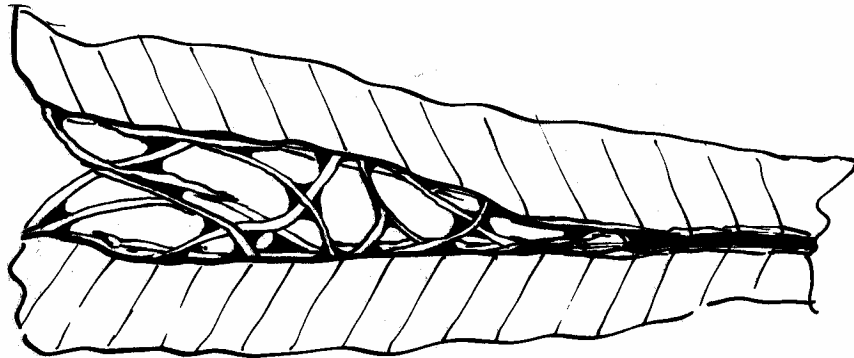
Figure 16: Bonding of two fibrillated surfaces

This adhesion bonding theory employs the ideas of Neuman [1]. According to

Neuman, the external fibrillation exists in the form of microfibril tails. These tails

can extend 65-75 nm into solution, thus there is a high probability that diffusion

between tails occurs. However, this length measurement is only an estimate due to

the ambiguous boundary of swollen cellulose [1].

It is important to remember the physical characteristics of the fiber also

contribute to their overall bonding nature. The flexibility and collapsibility of

individual fibers are significant in bonding and forming the over all paper network

[73]. Paavilainen [73] determined that more flexible fibers create a consolidated network resulting in an increase in the number and area of fiber – fiber bonds. This increase in consolidation is due to the enhanced response of flexible fibers to Campbell's forces. The formation of external fibrillation and fines also contribute to the increased Campbell's forces. While thin walled fibers can be considered ten times more flexible than thick walled fibers, 55 % of thick walled fibers collapse completely while only 24 % of thin walled fibers fully collapse during sheet formation. The collapse of fibers also increases the area of fiber – fiber bonds [73].

2.5 Isotopes

Tracer studies utilizing isotopes have rarely been used within paper industry studies, although they have been recommended from time to time. In 1965, Christensen and Giertz [16] recommended a switch from a thermodynamic view point to a more mechanistic approach, including the utilization of tracer experiments to study fiber water interaction. This thesis will take the approach of using a tracer to further the understanding of the interaction between fibers and water.

Isotopes are characterized as two or more atoms which have the same atomic number but have different mass numbers resulting in the same chemical behavior, but different physical properties [74]. Thus isotopes of hydrogen, deuterium and tritium, are useful in understanding the fiber water relationship.

42

2.5.1 Studies utilizing deuterium

Deuterium, an isotope of hydrogen, has been used to study cellulose. Deuterium exchanges with the labile hydrogen of the cellulose polymer. Hydroxyl groups are almost equivalently exchanged into OD groups during the deuteration process [75]. This exchange results in the ability to characterize cellulose accessibility and crystallinity due to the different exchange rates of crystalline and amorphous regions [76]. It is important to note, although expected, that experimentally the same molar quantities of deuterated water and ordinary water are adsorbed by cellulose. When this experiment was performed at different relative vapor pressures, the adsorption results were consistent across all relative vapor pressures [36]. Also important, the exchange rate between hydroxyl groups and deuterium happens at the same or faster rate than the diffusion of deuterated water through the system [77].

This deuterium exchange is similar with all types of cellulose. The reaction is minimally affected by pH and temperature. The amorphous regions of the polymer react quickly in solution since the reaction rate is limited only by the diffusion of the deuterated water through the suspension [77]. However, one study suggests running the experiment at standard temperature and exchanging for one hour will exchange all of the amorphous cellulose [76]. The crystalline exchange happens at a much slower pace, without complete exchange. One such study allowed the exchange to take place over a sixty-four day period after which over 80 % of the hydroxyl groups in cellulose had been exchanged [8]. Another hypothesis is that only the perfectly crystalline regions will remain inaccessible to the deuterium [13].

Heavy water is a useful probe into cellulose structure and accessibility. Exchange will occur with hydroxyl groups that are accessible to water such as crystalline microfibrils and accessible faults as well as the amorphous regions. In Child and Jones' [13] study a correlation was found between deuterium accessibility and BET results. Gutherie and Heinzelman [78] used heavy water with another isotope, ^{18}O, to determine accessibility. The advantage of ^{18}O is that it will not exchange with the oxygen on the cellulose so they can verify exchange of deuterium onto the fiber by the ^{18}O containing water [78]. Hatakeyama and Hatakeyama [77] utilized deuterium to observe the changes in amorphous cellulose during water and heat treatment. They focused on the re-crystallization of amorphous cellulose during treatment and the impact on hydrogen bonding. Their study determined that molecular rearrangement occurs throughout cellulose, but hydrogen bonding occurs randomly [77]. Hishikawa et al. [75] used deuterium to classify three different types of amorphous regions within cellulose. Ioelovitch and Gordeev determined that there is a monolayer of a less ordered crystalline or paracrystalline surface between amorphous and crystalline regions [79].

Other studies involved determining monolayer adsorption and diffusion characteristics. Wong and Ang [27] found that water contents less than 0.8 g of D_2O/g of macroscopically oriented cellulose could not be resolved by NMR. This may correspond to monolayer adsorption. Li [80] determined that the average residence time for absorbance of D_2O on the cellulose surface is approximately 1.5 ms. Tsuchikawa and Siesler [81, 82] used deuterium to monitor the diffusion of water in softwood and hardwood.

There are a number of methods to measure the degree of deuterium exchange. Spectroscopy is often used to measure the amount of water exchange. Water accessibility can also be measured through this process. NMR, mass spectroscopy, and refractive index are a few of the techniques [13, 83] that have been used. There are also methods of measuring deuterium exchange without spectroscopy. In one study, Frilette [84] measured the decrease in density of the D_2O/H_2O mixture after exchange with cellulose. In another study, Jefferies [85] observed weight differences in dried cellulose after deuterium exchange. However, deuterium can re-exchange with atmospheric water vapor, thus making these measurements less accurate [76]. Schott [86] utilized tensile tests to determine the strength of hydrogen bonds formed by hydrogen and deuterium. Through testing the wet strength of paper he determined that water formed stronger bonds.

2.5.2   Studies utilizing tritium

Tritium has the same chemical properties as deuterium and hydrogen, but tritium is a radioactive isotope. Tritium's radioactive nature facilitates measurement of tritium tracers through beta decay. The decay of tritium can be measured through scintillation counting, thus tritium concentrations are easily measured [87].

Examples of using tritium relative to fibers are few, but tritium has been used for a number of other applications. Sakai et al. [87] utilized tritiated water to characterize dialysis membranes. They were able to measure the permeability of water in the dialysis system without the complication of reaction with the membrane, which had been an issue with previous studies. Sumi et al. [88] determined the

accessibility of water in wood through the use of tritiated water. They determined that spruce and birch woods have accessibilities of approximately 60 % and 50 % respectively. Converting the wood into holocellulose increased the accessibility by a few percentage points.

In one study involving cellulose and tritiated water, Wahid and Ali [89] determined the molecular weight of cellulose by cleaving it in a acidic medium containing tritiated water. Recently, Jacobson [90] utilized tritiated water to understand diffusion of water through green wood.

2.6 Refining

One of the cases studied in this thesis is the effect of refining on the fiber water relationship. Refining, while a fundamental element of the papermaking process is a complex and incompletely understood process. Many researchers have focused on the effects of refining. Thus many theories have been developed through the years. This section will define the refining process, touch on a few historic theories, and lastly discuss the current theories on the effect of refining on fibers. For more information on refining there are a number of reviews and books available [91-98].

2.6.1   Refining Definition

Refining is the process of imposing cyclic deformation on cellulose fiber. Rotating bars or rotating surfaces with bars perform this deformation. The primary effects of refining are irreversible. Currently most mills use specific energy to

characterize the refining process. However, specific energy does not accurately quantify the changes that the fibers go through during the refining process. A number of factors influence refining. The swelling of chemical pulps and solubility of cell walls components are dependant on temperature and the glass transition temperature on the fiber. Water, a swelling medium, also influences refining. If refining occurred in a non-swelling medium only cutting would occur. Consistency, pH, and electrolyte concentration also influence refining [94, 97].

Refining is a random process in two ways. Randomly selected fibers undergo the refining action and the action occurs randomly along the length of the fiber. Refining action also occurs between fibers as well as along the bar edge of the refiner. Therefore, as the consistency of the stock changes, so do the effects of refining. At low consistencies, the fiber is refined as part of a floc where the refining action occurs along the bar edge rather than between the fibers. At higher consistencies, more action occurs between the fibers than along the bar edge, thus the refining action becomes more uniform among the fibers. The variety of action performed results in the problem of characterizing the beating or refining process. It is impossible to characterize the beating result by only one parameter or to develop a parameter so it completely describes the refining process. Thus, a number of different theories have been developed which has resulted in a number of disagreements. Currently there is no universally accepted theory relating refining process variables to structural changes in the fiber's cell wall [94, 97].

2.6.2 Historical Refining Theories
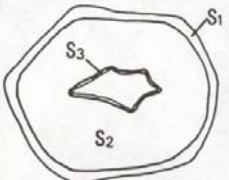
Through the years, there have been two major divisions in refining theory, chemical and physical. During the first quarter of the twentieth century, the chemical theory of beating dominated the literature. This theory suggested that beating increased the strength of paper by modifying the surface cellulose into a chemically distinct cellulose hydrate. In the early 1930's Campbell [71] determined that beating had very little effect on forming true cellulose hydrates. Instead, the theory developed that beating increasingly exposed the fiber surface allowing for water adsorption onto the exposed area, thus increasing the wetness of the pulp. This wetness was determined not to be due to hydrate formation. In 1926 Strachan [99] developed a physical theory of beating. He theorized that the strength increase was due to the mechanical entanglement of fibrils on the surfaces of the fibers. The wetness increased because of water being retained within this felted fibril surface [92]. The shortcomings of these oversimplified theories soon came to light as new theories developed.

2.6.3 Refining Effects on Fiber

Overall, there are three major classifications of refining: the creation of new surfaces, the creation of new particles, and generation of structural damage and modifications. Each of these general classifications have been further divided and explored. In terms of chemistry, fundamental beating responses can be described as the breakage of hydrogen bonds and breakage of covalent bonds [97]. Table 2

depicts the stages of virgin fiber beating or refining in terms of changing fiber

characteristics [100].

Table 2: Fiber Development during Refining

	Cross Section	Characteristics of Fiber
Unbeaten	S1 S3 S2	Deformation of lumen Swelling of S2
Beating		Initiation of S1 delamination Initiation of external fibrillation Initiation of S2 delamination Separation of S3
		Progress of S1 delamination Swelling of S1 Progress of external fibrillation Destruction of S1 Progress of S2 delamination
		Disappearance of S1 Progress of S2 delamination Swelling of outer S2 Destruction of S2 External fibrillation of S2

New surface creation, one of the major classifications, can be divided into three classes: external fibrillation, internal fibrillation, and molecular fibrillation. External fibrillation involves partial detachment of the lamella and macrofibrils from the outer layers of the cell wall. Internal fibrillation involves the tangential splitting of the coaxial structure of the cell wall and water adsorption. A large lumen enhances internal delamination and swelling, dislocations in the fiber wall increases external fibrillation [73]. The water adsorption results in swelling and flexibility. Robertson [101] notes that with low degrees of beating, swelling enhances the strength of the resulting paper, but at high degrees of beating, swelling can actually correlate with a decrease in strength. A number of tests have been developed to quantify the degree of fiber swell and adsorption. These tests were introduced in Section 2.4 and will be further discussed later in this dissertation.

Unfortunately, there is little visual evidence of internal fibrillation. The main source of confirmation is the observation of collapsed beaten fibers and the comparison of the unbeaten fibers, which do not collapse. Emerton [92] described internal fibrillation and cell wall modification as the breaking of lateral bonds between adjacent coaxial lamellae in the cell wall. Permitting the entry of water and the sliding of one lamella over another increasing flexibility [45]. Molecular fibrillation is defined as a partial solubilization of the polymeric structure of the components of the cell wall matrix. This type of fibrillation involves molecules that are attached to the cell wall at one end while the other end is in solution. Currently there is no direct evidence of molecular fibrillation occurring in refining. However, previous studies have found that some cell wall material does dissolve during

refining. This evidence provides a basis for molecular fibrillation as molecular fibrillation is a prerequisite for total dissolution of the polymeric components of the cell wall. Thus, researchers felt that molecular fibrillation may be one of the most important effects of refining [97].

New particle creation involves the cutting of fibers and the cutting or splitting loose of cell wall lamellae and macrofibrils. This cutting and splitting action results in fine and crill generation. New particles are also created through dissolution or cutting away of individual polymers from the cell wall [97].

The third major class of refining is structural damage and fiber modification. This class includes cutting of fibers and lamellae, partial cleavage of the cell wall, the generation of axially compressed zones, creation of invisible weak zones and changes in crystalline sites and microfibril orientation. Currently the only photographic evidence exists of partial cell wall cleavage. Axially compressed zones consist of misalignment zones, dislocations and kink bands. The misalignment zones are significant to sheet consolidation. During consolidation, microcompressions and Jentzen's effects become mechanisms within these zones. Thus, these zones allow paper structure opportunities for strain energy dissipation. Invisible weak zones lower the cell wall rigidity. This loss in rigidity results in localized collapse during drying and initiation of the final rupture during tensile and tear testing. Extensive refining can lead to cellulose mobility and the possibility of cellulose II structure formation in highly refined areas [97].

Table 3 displays refining effects elucidated by previous researchers [97]. These primary structural effects were discussed in the previous paragraphs. Figure 17

51

[98] relates these primary effects to fiber properties, the fiber – water relationship, and finished paper properties.

The area of changes in crystallinity has been studied a number of times. One such study by Liitia et al [12], used solid state NMR to observe these changes. In this study, changes after refining were not observed although a lower degree of crystallinity was found in the fines fractions as compared to the whole pulp. However, the small fraction of fines present in the pulp prevented accurate measurement of the increase in fines during refining. The study also found that fines might have a higher percentage of cellulose II than the bulk fiber. These observations lead to the conclusion that either a mechanical force breaks crystallites during refining or the degree of crystallinity on the surface is lower than inside the fiber, thus resulting in the lower crystallinity of fines [12].

Table 3: Primary Structural Effects of Refining

Historical	Fahey	Higgins & Young	Giertz	Clark	Ebeling	Page
Cutting/ splitting	Breaking of covalent bonds	Fiber shortening	Cutting and crushing	Shortening	Fiber shortening	Fiber straightening plus those listed by Ebeling
External fibrillation		External fibrillation	Successive cleavage of external layers of the cell wall & subsequent breaking away of these layers	External splitting	Successive cleavage of external layers of the cell wall & their subsequent breaking away	
Hydration	Intrafiber H-bond breaking	Intrafiber H-bond breaking	Intrafiber H-bond breaking	Internal Splitting	Delamination of internal cell wall layers	
		Production of fines		(Production of debris)		
			Creation of dislocations	(Longitudinal compression)	Local dislocations of the cell wall structure	
					Dissolution of chemical components of cell wall and simultaneous formation of colloidal carbohydrate solution (molecular fibrillation)	
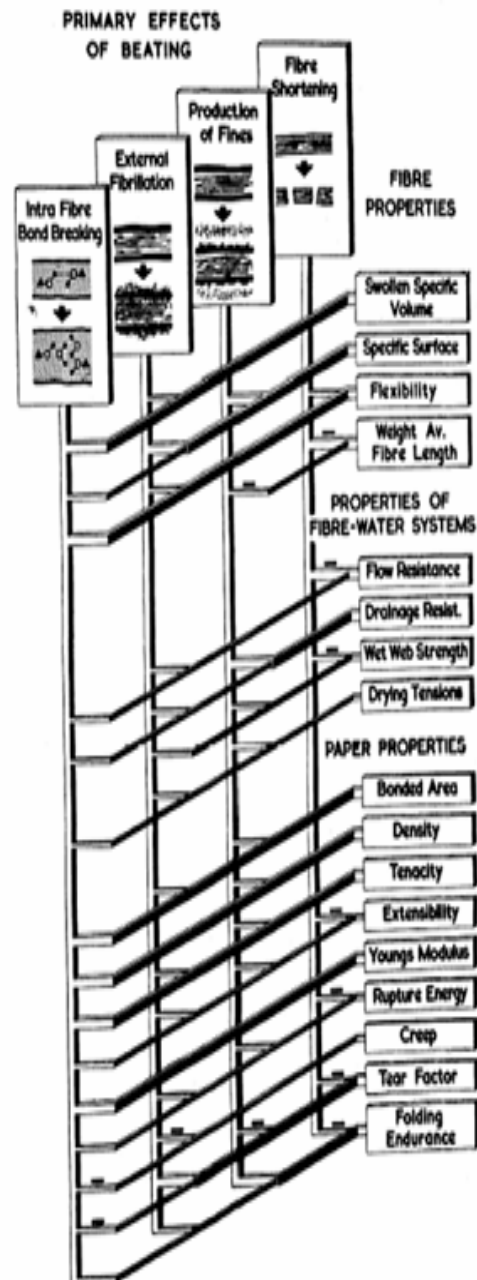
The primary effects are shown in a highly idealised way. A thick connecting member indicates that the primary effect is considered to exert a major influence, a thin member indicates a lesser influence. The absence of any connecting member does not necessarily mean that there is no relationship whatsoever, but it indicates that any such influence is considered to be quite small compared to the others that determine the property in question. A minus sign indicates an inverse relationship.

Figure 17: Primary effects of beating

A recent study used CP/MAS 13C-NMR spectroscopy with spectral fitting to study the crystallinity of refined unbleached kraft fibers [102]. They chose to refine the fibers in a laboratory refiner and separate out the fine fractions for study during processing. The results of the study showed a small decrease in the percent crystallinity of the fines as refining progresses, with a slight increase in the crystallinity of the fiber after the completion of the refining process. This slight increase may correspond to the removal of the amorphous cellulose surface of the fiber, which corresponds with the decreased crystallinity of the fines [102].

2.6.4   Measuring the effects of refining on fiber

The most common wet method for measuring the effects of refining on pulp is freeness. Freeness is used throughout the mills of today. Freeness works very well for measuring changes in a pulp as it is refined under standard conditions, however there are drawbacks to using the method.

Freeness is an indirect measure of fiber drainage, but as fiber changes during refining, freeness also becomes a measure of fiber swell and surface area. As refining increases, the ability of the fiber to freely drain decreases due to the swollen nature, water carrying ability, and increased surface area of the fiber. Thus, freeness can be used as a measure of fiber swell and surface area. However, freeness measurements become increasingly variable at the ends of the refining spectrum. The measurements also can only be applied to one type of pulp at a time; they do not correlate between different types of fiber or pulping techniques. Therefore, freeness testing can be used

to characterize a frequently run furnish in a mill, but does not work well for studies involving different types of pulp, thus the development of methods such as WRV and solute exclusion.

The BET method of surface area measurement [43] has also been used in the area of refining. BET surface area increases with water accessibility, and thus, changes through refining. The one difficulty with BET is that it is a dry measurement and it is difficult to preserve the swollen structure of the fiber. In Child and Jones' study, leaching the pulp with methanol followed by hexane removed the water present in the system. The sample was then dried over nitrogen and the samples were evacuated at room temperature. This process helped to maintain the swollen structure of the fiber and minimize collapsed pores [13].

The impact of refining can also be found in the testing of handsheets and finished products. Figure 18 [6] illustrates how tensile, burst, and tear strength of the finished sheet change during refining. It is important to note that Figure 18 only shows trends down to a freeness of 500 CSF, these trends may not hold true at lower freenesses.
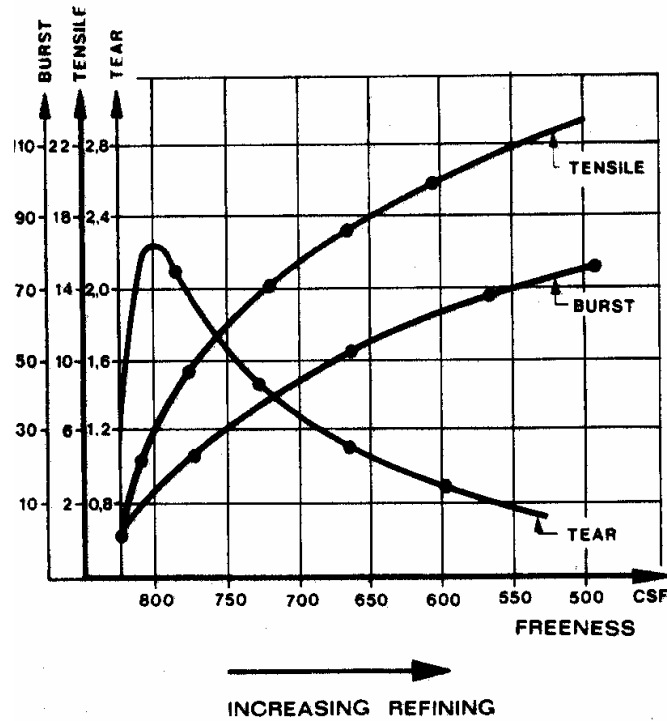
Figure 18: Changes in strength properties during refining

2.7 Recycling

Recycling fibers is prevalent with in the paper industry. Whether the fibers are pre or post consumer, the properties of the fibers have changed from their virgin state during processing. Through pressing and drying the fiber structure is altered, thus the fibers relationship with water changes. One of the cases studied in this thesis is how this relationship changes through successive drying. The bonding nature is influenced by drying as it alters fiber strength and swelling ability. Tensile and burst decrease with recycling, while tear strength can increase depending on conditions. Overall, it is understood that the biggest shift in fiber properties occurs after the fibers have been dried once. Subsequent recycling does not as dramatically change fiber properties [103].

The effect of drying on fibers is often classified as hornification and is discussed in the following section.

2.7.1 Hornification

The original definition of hornification is defined as the percent decrease in water retention value (WRV) from the original value after drying and reslushing [49, 104, 105]. Using the original definition of hornification; Weise, Maloney and Paulapuro [49]; developed three levels of 'wet hornification'. First, between 25 and 45 % solids, there is no hornification effect. At higher solids WRV decreases linearly with increased solids content. During the final phase between 60 and 75 % solids, WRV becomes constant despite increased solids [49]. These phases give evidence to interior pore closure and bonding during drying phases.

Currently, hornification refers to the changes that occur to a fiber during pressing and drying, both physically and chemically. This definition focuses on fiber shrinkage and the formation of irreversible internal hydrogen bonding [6, 49, 77, 104]. The hydrogen bonds formed between and within fibers during the drying process cause shrinkage and an increased rigidity of the fibers. These hydrogen bonds slightly increase the crystallinity index of the fibers [53]. The irreversible hydrogen bonds formed during this process decrease the flexibility of the fibers to one half that of the never dried fibers and also reduce fiber collapsibility [73]. There is a loss of pore structure resulting in surface area reduction [104]. The loss of pore structure also lowers the reswelling capabilities of the fiber [53]. Hornification occurs to a much larger extent in low yield pulps [103, 104]. Wistara and Young

found that the higher the initial bonding ability of the pulp, the greater the degree of hornification [103].

Hornification occurs as the fibers and fibrils pack together during drying forming hydrogen bonded layers and closing capillaries within the fiber caused by polysaccharide hardening [103]. This cocrystallization results in a crosslinked fiber structure [106]. Microstructural changes within the fiber are also possible during hornification [103]. These changes may influence the interaction between fibers and water [103]. However, while hornification is often considered irreversible, limited swelling does occur upon rehydration. Thus, not all bonds formed within and between fibers can be fully crystalline in nature. Some of these bonds are removed in the presence of water. One possible explanation is the esterification of hydroxycarboxylic acid resulting in a lactone. Latones have been found in hornified pulps, but not in never-dried material. These covalent lactone bridges disappear under certain chemical conditions [104].

Many studies have focused on reversing the effects of hornification [107]. The four most common methods of reducing the effect of hornification in the final product involve refining, chemical treatment, the addition of virgin fibers, and fiber fractionation [103]. Care must be taken when refining hornified fibers as oftentimes refining increases drainage time and can lower the strength of the fibers [103]. Swelling has been the focus of many of these studies. By swelling the fibers in various solutes bonds can be broken re-exposing the hydroxyl sites for bonding between fibers [107]. Alkali treatments can force water into the hornified fiber through osmotic pressure, thus swelling and opening the fiber [103].

CHAPTER 3: PROBLEM ANALYSIS AND OBJECTIVES

3.1 Problem Statement

Through the use of hydrogen isotopes, the interaction between fiber and water can be directly quantified. This quantification of the fiber water relationship can lead to new insights on the effect of processing on fibers.

3.1.1 Key Questions

- Can the interaction between water and fibers be directly quantified?

- Can the water saturated surface of a fiber be measured and quantified?

- How does processing affect the saturated surface of cellulose?

  - How does refining affect the fiber-water interaction?

  - How does recycling or drying affect the fiber-water interaction?

- How does the quantification of the fiber-water interaction add insight into the science of paper making?

3.2 Problem Analysis

The primary goal of the study is to quantify the interaction between fiber and water. With this quantification, insights into the fiber-water relationship will be gained. These insights can then be used to further understand the effect of processing on fibers.

Hydrogen bonding is a key force in fiber and sheet strength. Paper consists of fibers bonded through a hydrogen bond matrix with covalent bond reinforcement.

Without hydrogen bonding, fibers will not network into a sheet.[17] Figure 19 [108] displays how fiber and water interact during the process of sheet formation. Therefore, understanding fiber processing in terms of its effect on hydrogen accessibility and bonding is key to understanding how processing affects the properties of fibers and ultimately those of the paper sheet.
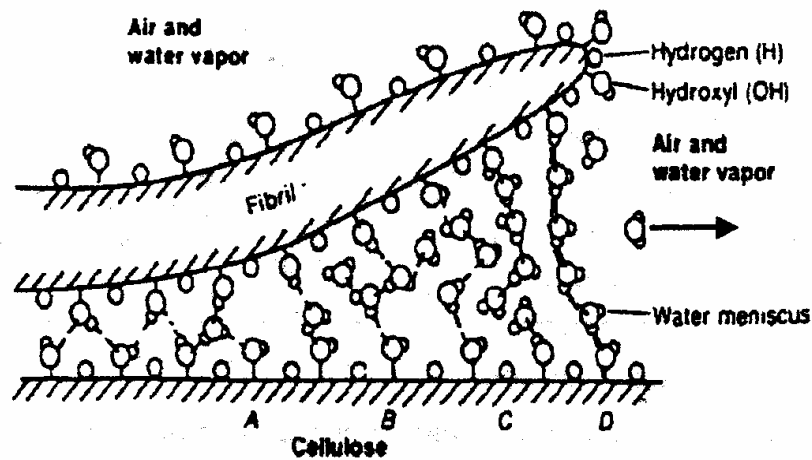
Figure 19: Fiber and Water Interaction

Neuman's dangling tail theory, described earlier in this thesis, provides a theoretical basis for this study. Based on this theory, cellulose has microfibrils, or tails, extended into solution.[1] The forces present in processing fibers should affect the fiber surface and, therefore, increase or decrease the concentration of cellulose tails, and thus the number of available hydrogen bonding sites. The change in hydrogen bonding sites should affect the macro properties of the fiber such as freeness, water retention value, and swelling.

The "dangling tail" theory is compatible with the Diffusion Theory of Adhesion. The diffusion theory states that above the glass transition temperature, two polymer bodies when pressed together will fuse into one body through the diffusion, or migration, of individual amorphous polymers within the two bodies.[109] The individual amorphous polymers are the dangling tails of Neuman's theory. Cellulose, with its hydrothermoplastic nature, as well as, its amorphous and crystalline sections, fits very well into both theories, especially in terms of paper formation and strength. The act of refining should increase the number of dangling tails, thus increasing the amorphous regions of the fiber as well as accessible hydrogen bonding sites. This should result in greater diffusion between fibers, increasing sheet strength.

3.2.1 Hydration Layer Theory

The monomer unit of cellulose is cellobiose, two glucose molecules joined by a β-1,4 linkage. This chemical configuration results in six hydroxyl groups that are available for exchange with surrounding hydrogen and thus creates a strong bond between other cellulose chains and surrounding molecules.

Using the Polanyi's polarization theory, as discussed by Caulfield [41], multilayer sorption of water and other molecules occurs on the surface of these cellulose units. The initial layer of molecules is attracted strongly to the cellulose surface and adsorbs directly to that surface. The successive layers are adsorbed by the prior layer of molecules and bond less strongly to the system with each molecular layer. Cellulose has the potential to adsorb up to 8 layers at the fiber saturation point.[41] Due to the bipolar nature of water molecules, these successive layers align

61

above the hydroxyl groups of the cellulose forming H-bonds and produce a hydrated matrix around the cellulose molecule. Other studies, using non-freezing bound water, have shown that an average of 5 to 6 layers of hydration can surround the cell. However, the adsorption is not even and sites may hold up to 10 layers. The number of layers decreases as temperature increases.[110]

A fiber saturation point for a cellobiose unit can be calculated using Equation 1. Considering that each layer will consist of 6 attached water molecules, the number of layers (L) can be multiplied by 6 to generate the number of moles of water surrounding the cellobiose unit. Then converting the water to a mass basis (MW_W) and dividing by the molecular weight of cellobiose (MW_C) will give an estimate of the fiber saturation point. Using Caulfield's estimate of 8 hydration layers and 1 mole of cellobiose a total of 48 moles of water can hydrate 1 mole of cellobiose. This leads to a fiber saturation point of 2.53 g/g. Increasing the maximum number of layers to 10 yields a fiber saturation point of 3.16 g/g.

Equation 1: Fiber saturation point estimate

$$FSP = 6L\left(\frac{MW_w}{MW_C}\right)$$

3.2.2 Isotope theory

The fiber-water interaction can be monitored through the use of hydrogen isotope markers. These markers will chemically behave like the hydrogen present in water. The chemical similarity allows for minimal impact of the fiber-water system,

thus maintaining the integrity of the system. The ability to quantify the amount of water interacting with a fiber changes the theoretical estimates of fiber saturation point into an actual number representing the amount of water truly interacting with the fiber. Equation 2 gives a representative equation for fiber water interaction. The moles of hydrogen (H), determined by isotope interaction, is multiplied by the molecular weight of water (MW_W) and divided by the molecular weight of cellobiose (MW_C) to give a g of water / g of cellobiose or fiber. The equations necessary to generate H are discussed in Chapter 4, with the experimental development discussed in Chapter 5.

Equation 2: Isotope calculation for fiber water interaction

$$FSP = H\left(\frac{MW_W}{MW_C}\right)$$

3.3 Hypothesis

Mechanical forces generated during the processing of fiber alter the fiber surface chemistry, or reactivity, and thus, the fiber-water interaction. The available hydrogen bonding sites on the fiber decrease or increase with the mechanical processing and therefore, change the fiber-water relationship.

3.3.1 Refining Discussion

Morphological changes to the fiber occur during the beating or refining of pulp. In the case of virgin fiber, four stages occur during the beating process. First the lumen is deformed and the S2 layer begins to swell. Secondly, the S1 and S2

layers begin to delaminate, external fibrillation starts, and the S3 layer separates. In the third stage, the S1 layer swells as it continues to delaminate and destruction of the layer begins, external fibrillation continues, and S2 layer delamination progresses. In the final stage, the S1 layer disappears, and the S2 layer continues with delamination, swelling, external fibrillation, and destruction of the layer.[111] The refining process should result in an overall increase in surface area of the fiber. Thus there should be a general increase in available hydrogen bonding sites. The effects of refining were discussed in Chapter 2.

3.3.2 Recycling Discussion

Morphological changes also occur during the drying of fibers. As water is removed from the fiber, hydrogen bonds form within and between fibers. These bonds cause the fibers to shrink and create more crystalline areas within the fiber. Upon readsorption of water, the fibers do not fully regain their swollen state. This phenomenon is known as hornification and should result in a general decrease in hydrogen bonding sites. Hornification is also discussed in more detail in Chapter 2.

3.3.3 Isotopes

By using hydrogen isotopes to quantify the changes during refining and recycling, insight should be gained into how these two processes affect fibers.

3.4 Objectives

1) Develop an experimental procedure to measure the amount of hydrogen interacting with the fiber

2) Test this method with unrefined fiber to determine the basic fiber water interaction

3) Utilize the method to quantify the changes that occur during refining

4) Utilize the method to quantify the changes that occur during recycling

CHAPTER 4: EXPERIMENTAL MATERIALS AND PROCEDURES

Chapter 4 briefly describes the experimental materials and methods used to complete the research discussed in subsequent chapters.

4.1 Experimental Materials

4.1.1 Softwood

All experiments pertaining to softwood used northern softwood. A bleached softwood kraft pulp was produced at Stora Enso's Wisconsin Rapids mill and received in slush form. A bleachable grade softwood kraft pulp was produced in Maine at International Papers Androscoggin mill and received in fluff pulp form.

4.1.2 Hardwood

All experiments pertaining to hardwood used northern hardwood. Bleached and bleachable grade hardwood kraft pulp were produced at Stora Enso's Wisconsin Rapids mill and received in slush form.

4.2 Test Methods

4.2.1 PFI Mill Refining

PFI refining was performed following IPST method Procedure 401B [112] which follows the CPPA method [113]. Samples were taken from the PFI mill at specific revolutions. The consistency of the stock was 10% for all samples.

4.2.2   Recycling Procedure

Sheets were prepared for recycling and testing by making handsheets following TAPPI Test Method T 205 [114]. Six of these handsheets were pressed and dried following standard conditions and were reserved for AFM testing. The other six handsheets were couched off of the handsheet mold and reserved in their wet state for K_{pw} and WRV measurements. The remaining pulp was made into 3 g handsheets following TAPPI Method 272 [115]. These handsheets were reserved for recycling. This procedure was repeated for all recycling levels. This method removed the majority of fines through the handsheet mold and minimized freeness changes that occurred during recycling.

4.2.3   Freeness

TAPPI Test method T 227 om-99 was used to perform the freeness testing [114]. All freeness tests were corrected for temperature and consistency using Equation 3 and Equation 4. Where T stands for temperature in Celsius and C represents the consistency of the sample. Figure 20 [14] give an operational schematic of the freeness tester.

Equation 3: Temperature Corrected Freeness

$$CSF_T = CSF_U + 4.6(20 - T)\left[1 - \frac{(400 - CSF_U)^2}{61000(CSF_U)^{0.25}}\right]$$

Equation 4: Fully Corrected Freeness

$$CSF = CSF_T + 590(C - 0.3)\left[1 + \left(\frac{0.4 - C}{0.2}\right)\left(\frac{CSF_T}{1000}\right)\right]\left[\frac{1 - (CSF_T - 390)^2}{87000(CSF_T)^{0.2}}\right]$$
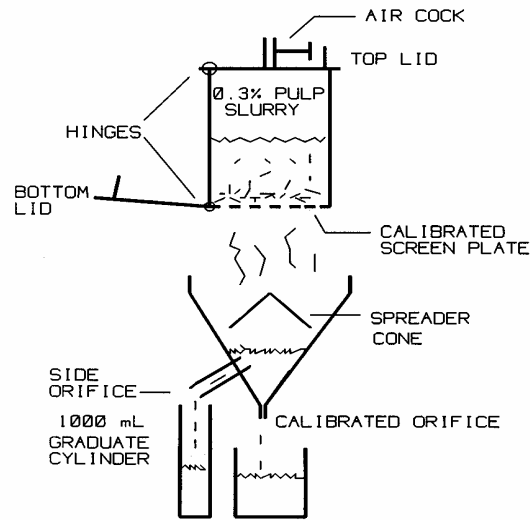
Figure 20: Freeness Test Schematic

4.2.4 Water Retention Value

The water retention value (WRV) was determined using TAPPI UM 256 [47]
and IPST Procedure No. 416 [116] which are based on the work by Jayme [47, 116,
117]. After processing the pulp, four 0.63 g (OD weight) samples were diluted to 0.5
% consistency. These samples were each drained onto a fine mesh screen in a
centrifuge cup. The cups were placed in a centrifuge at 900 g for 30 minutes. After
centrifuging, the pulp pad was weighed and dried. Once dry, the pulp pad was

weighed again. From the weights of the wet (s) and dry (p) samples, the WRV was

calculated using Equation 5.

Equation 5: Water Retention Value

$$WRV = \frac{(s-p)}{p}$$

4.2.5   Solute Exclusion Technique

The solute exclusion technique used for this study was developed from the

work of Stone and Scallan, and Frazier.[35, 118]

The solute exclusion technique is based on the premise that the pores of the

cell wall have a maximum size. Stone and Scallan developed this technique to

determine the amount of water held in the cell walls while excluding any water found

in the lumen, microfibrils, or capillary spaces between fibers. To quantify the water

in the cell wall, they employed a chemically inert polymer small enough to infiltrate

the water in the lumen, microfibrils, and capillary spaces but large enough to be

excluded from the cell walls. The polymer is introduced to the fiber in a dilute

suspension and allowed to equilibrate with the water in the fiber suspension. The

polymer suspension is then removed from the fiber and its concentration calculated.

From the change in concentration of the polymer suspension, the volume of water

accessible to the polymer is determined. The inaccessible water, or water within the

cell wall, is calculated by subtracting the accessible volume from the total volume of

water in the fiber/polymer suspension.

Further work by Stone, Scallan, and Abrahamson defined the fiber saturation point as the water contained within the fiber that is inaccessible to dextran with a molecular weight of 2 x 10^6 and a molecular diameter of 560 Å. The size of this molecule corresponds with a plateau in their graph of polymer molecular diameter versus inaccessible water Figure 21 [45].
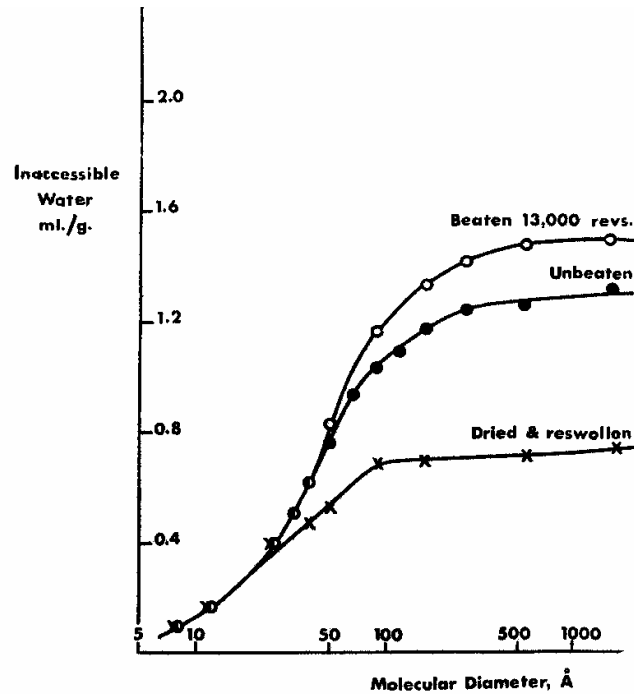
Figure 21: Molecular diameter versus inaccessible water

Böttger, Thi and Krause [119] modified the work of Stone, Scallan, and Abrahamson [45] by utilizing blue dextran, also with a molecular weight of 2 x 10^6 and molecular diameter of 560 Å, to determine the fiber saturation point in their study. The advantage of using blue dextran comes with the ease of concentration measurement, the absorbance of the solution at 610 nm. Frazier [118] utilized the

70

work of Böttger, Thi and Krause [119] to determine the fiber saturation points for his thesis research. His method was modified for this study.

For this study, 0.5 g (OD weight) samples were drained to approximately 20 % consistency. Once the desired consistency was obtained, the sample was placed in a preweighed 30 mL Nalgene bottle and weighed. Approximately 6 mL of a 1 g/L blue dextran solution was then added to the bottle. This was weighed again and the mixture was vortexed for 30 seconds and placed in an automated wrist action shaker for 2 hours. The sample was then allowed to sit overnight to create a homogeneous mixture.   The next day, the sample was filtered through a fritted glass filter and the filtrate passed through a syringe fitted with a 1 μm filter to remove any fines that might have escaped the fritted glass. The filtrate concentration was tested using a UV-visible spectrometer set at 620 nm. The fiber saturation point was calculated using Equation 6.

Equation 6: Fiber Saturation Point - Solute Exclusion Method

$$FSP = \frac{\left(w + q - \frac{w * c_i}{c_f} \right)}{p}$$

One issue that occurred when developing a FSP procedure from the literature was the issue of consistency. Literature references ranged from 6 % final consistency to 2 % final consistency. However, our initial experiments showed excessive error at low consistencies. In order to determine the correct experimental consistency a

computer simulation was conducted. Using Equation 6, calculations were performed
at various initial and final consistencies and the percent coefficient of variance was
determined.

Both final and initial consistencies proved to be factors in experimental error,
as seen in Figure 22. Figure 22 has the initial consistency of the pulp on the x-axis
with the percent coefficient of variance (% COV) on the y-axis. The final
consistency of the solution is listed on the right side of each respective trend. The %
COV was calculated by varying the final absorbance (c_f) by 0.002 in either direction
of a standard FSP of 2.21 g/g. Obviously, the final consistency had a rather large
impact on the variation of the results, but the impact of the initial consistency was
surprising. Through these calculations, it became apparent that using the highest
initial consistency was important.

By keeping the initial consistency above 20 %, a final consistency as low as 5
% could potentially give very accurate results. Proper mixing becomes a concern
with the higher consistency solutions, vortexing the mixture for 30 seconds prior to
shaking helped the solution become more homogeneous. Thus, it was determined
that a final consistency of 6 % and an initial consistency of at least 20 % would be
used for all future experiments.
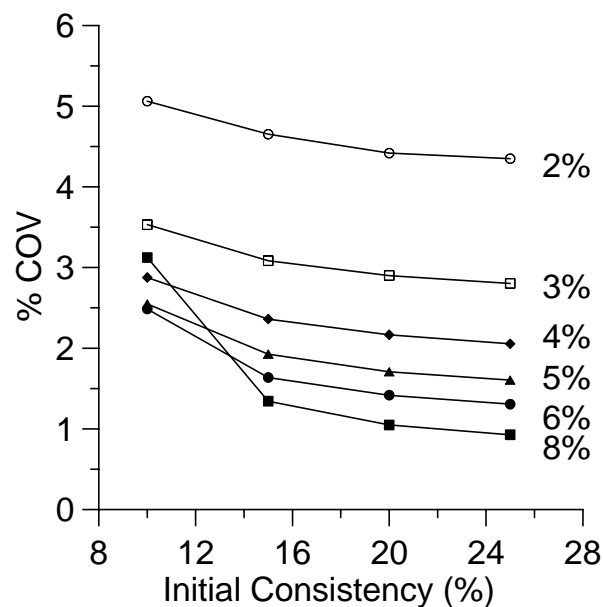
Figure 22: FSP equation error correlations with consistency

4.2.6 AFM Procedure

AFM, or atomic force microscopy, was preformed by Adam Brancato. AFM uses a small cantilever beam to tap against a surface, such as a sheet of paper. The interaction of the tip of the cantilever beam with the surface is measured by deflection of the lever [120]. This deflection can be quantified and the interaction of the surface with the tip can be plotted to give a chemical map of the surface [120]. Thus, this tool can be used to measure the hydrophilicity of the surface of a sheet of paper.

To determine the hydrophilicity of the paper surface, a sample was placed on a glass slide then the cantilever with a silicone dioxide tip was lowered into place. This tip first scanned the surface of the paper in the tapping mode to image the surface. If the image produced a reasonable contact area without static, the AFM was switched to contact mode and force measurements were taken. The adhesive force

was tested and recorded at various points on the sheet. Each point was tested twice for agreement before accepting the data point. This process was repeated on a second area of the sheet for a total of 60 points, prior to statistical analysis, and three sheets were tested for each recycling stage [121].

4.2.7 Tritium Tracer Technique

The pulp was brought to 8 % consistency and divided into four 1.2 g (OD weight) samples for tritium testing. Each individual sample was placed in a funnel fitted with a fritted glass filter. To the sample, 25 mL of DI water spiked with 300 μl of tritiated water, containing approximately 20 μCi of activity was added. The tritiated water was allowed to equilibrate for 1 minute prior to draining excess water. The fiber was washed with 25 mL aliquots of acetone until the activity in the filtrate was below 1000 dpm. The acetone washing was done to insure all free water is removed from the sample. Then the fiber was washed with two 25 mL aliquots of DI water. The *dpm* of each wash was recorded and from this information, the partition coefficient of pulp to water (K_{pw}) was calculated using Equation 7, Equation 8, and Equation 9.

Equation 7: Tritium Pulp Water Coefficient

$$K_{pw} = \frac{dpm_p}{dpm_w}$$

Equation 8: dpm of Pulp

$$dpm_p = \frac{\sum D_W}{p}$$

Equation 9: dpm of Water

$$dpm_w = \frac{D_i - \sum D_W}{q_i}$$

4.2.8 K_{pw} Sample Preparation Modifications for Recycled Handsheets

The tritiated water technique was used to monitor changes in the bulk phase during recycling. The experimental technique remained the same as described in Chapter 5, but the sample preparation was modified to better detect recycling changes.

The main issue in comparing AFM measurements to K_{pw} involved the differing states of the fiber in the two test methods. For the AFM method, samples from dried handsheets were used. Prior experiments using dried samples with the tritiated water provided inconclusive results. Therefore, samples needed to be in the wet state for the K_{pw} measurements.

To allow for the same fiber composition in both tests, 1.2 g handsheets were made. For each recycling level, four of these handsheets were couched off the handsheet mold and placed in a plastic bag for K_{pw} testing. Thus, the virgin samples for K_{pw} were made up in the process of forming the virgin handsheets and so on and

so forth. These wet handsheets were each diluted to a consistency of 8 % (or 15 g total weight) prior to performing the K_{pw} test on each handsheet.

4.2.9   Fiber Quality Analysis

Fiber quality was measured with the OpTest Laboratory Fiber Quality Analyzer. This machine analyzes 5,000 individual fibers, returning information on fines percentage, average length (arithmetic, length weighted and weight weighted), mean curl and kink, as well as a fiber length distribution. For this thesis, the average length-weighted length, mean curl, and kink index were used to categorize the properties of the fiber and the effect of processing on the fiber.

The following equations are used to calculate the properties described above. Equation 10 is used to calculate the average fiber length while minimizing the effects of fines. The length-weighted average is most commonly used to compare fiber lengths.   Equation 11 determines the curl index for an individual fiber. Curl is considered to be the ratio between the contour length of the fiber and the projected length or the farthest span of the fiber when allowed to freely form. Equation 12 determines the kink index. Kink is determined by the number of kinked fibers divided by the total length of all the fibers. A kink is defined as a sharp change in direction and is divided into three angle divisions; 21-45º, 46-90º, and 91-180º for this equation. Each fiber may count once in each angle division, but will not be counted multiple times in that division [122].

Equation 10: Length Weighted Fiber Length

$$L_W = \frac{\sum n_i L_i^2}{n_i L_i}$$

Equation 11: Curl Index

$$CI = \frac{L}{l} - 1$$

Equation 12: Kink Index

$$KI = \frac{\left(2N_{(21-45)} + 3N_{(46-90)} + 4N_{(91-180)}\right)}{\sum L}$$

4.2.10 Britt Jar Fines

The Britt jar was used to separate the pulp into fines and fiber fractions for microscopy. Following TAPPI Test Method T 261 [115] the fibers and fines were separated. The fines suspension was then drained onto filter paper and dried to determine the fraction of fines in the pulp. The fiber fraction was concentrated and reserved in a wet state for microscopy.

4.2.11 Light Microscopy

Light microscopy was performed for a portion of this thesis by Rob Lowe. Lowe gives a full description of this method and procedures in his paper presented at

the 2005 Fundamental Research Symposium [123]. The work presented within this thesis was used to highlight the external changes taking place during refining.

The structure of the external surface was observed by wet pressing a dilute suspension of fibers onto a glass slide, where the fibers were allowed to dry. Image of the fibers were then taken by using a Leica DM-IRM inverted, reflected light microscope with a Hamamatsu ORCA-ER digital camera and a 50 watt metal halide lamp. A mica sheet created polarized light, removing excess light rays. The fibers were dyed prior to producing the slide to increase contrast within the image [123]. Figure 23 gives a representation of the images produced with this technique.
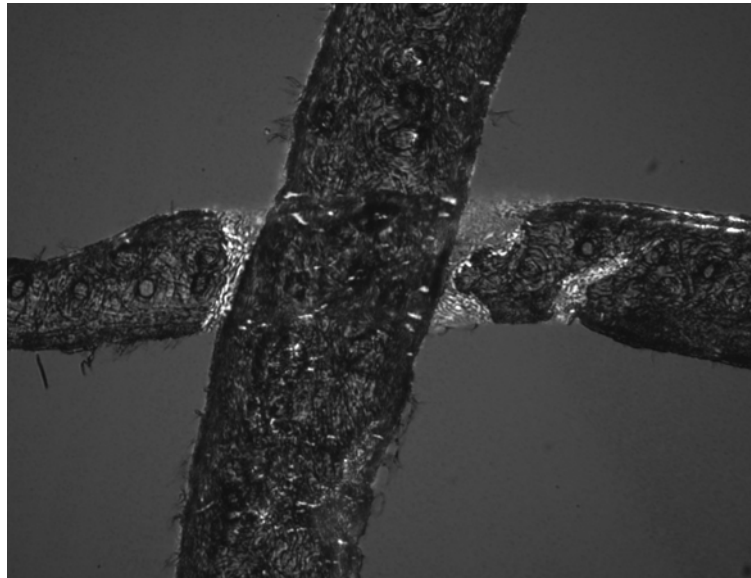
Figure 23: Representative light microscopy image

4.2.12 Scanning Electron Microscopy

Scanning electron microscopy or SEM was performed by Shaobo Pan. This microscopy was used to highlight the external changes of the fiber. The SEM used is JEOL JSM-6400, the product of JEOL LTD.

The procedure used is a modification of the process as discussed by Williams and Drummond [124, 125]. The procedure to develop the images is as follows. First wet fines-free pulp is sandwiched between sheets of blotter paper. The water is removed from the fiber sandwich through a series of ethanol exchanges beginning with 10 % EtOH for ten minutes. This first exchange is followed by successive ten minute exchanges with 25, 50, 75, and 90 % ethanol. The ethanol exchange ends after three 100 % EtOH exchanges each lasting ten minutes. Three Ethylene Oxide ten minute exchanges are performed prior to soaking the fibers in epoxy resin overnight while shaking the suspension at room temperature [126]. The shaking aligns the fibers in one general direction. This allows for the observation of the interior cell wall.

The blotter paper is removed from each side of the fiber sandwich and in fresh epoxy resin the fiber pad is rolled into a rod aligning the fibers with the axis. Multiple rods are sandwiched together and placed perpendicularly in the mold. The spaces between the rods are filled with epoxy resin and heated for one day (24 hours) at 70 ºC. The sample is removed from the mold and polished with 120 #, 320 #, 800 #, 1200 #, 2400 # and 4000 # sandpaper respectively. The surface is then etched with a mixture of 10 mL EO, 20 mL MeOH and 4 g NaOH for 20 seconds. Finally the

sample is coated with OsO_4. The sample is then ready for the SEM [126]. Figure 24

gives a representation of the images produced by SEM.
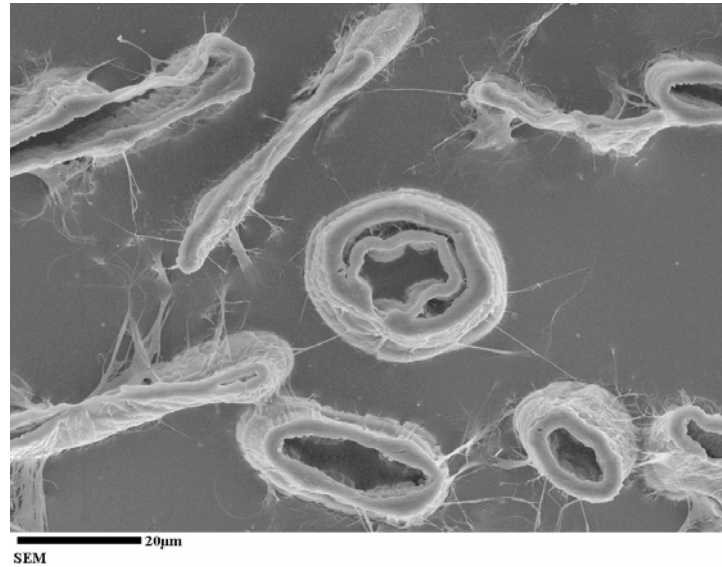
Figure 24: Representative SEM image

CHAPTER 5: TRACER TECHNIQUE DEVELOPMENT

5.1 Advantages of Isotopes

Isotopes of elements contain slightly more or less neutrons than their respective elements, but exhibit the same chemical behavior. Hydrogen has two isotopes, deuterium and tritium. While a hydrogen atom does not contain any neutrons, deuterium and tritium contain one and two neutrons respectively.

5.1.1   Isotope Theory

Cellulose consists of six hydroxyl groups per cellobiose group. The protons in these hydroxyl groups can readily exchange with those in other hydroxyl groups and in water. The cellulose chains bond together to form microfibrils, which in turn bond together forming cellulose fibers. The surface of these cellulose fibers consist of crystalline, semi-crystalline, and amorphous regions of cellulose, all with exposed hydroxyl groups available for exchange.

As a fiber is processed, the surface and internal structure of the fiber changes to expose more exchangeable groups. By using an isotope of hydrogen as a tracer, the number of groups and the fibers accessibility to water can be calculated.

5.1.2   Deuterium Experiments

This study began with using deuterium as a tracer, but soon moved on to tritium due to the difficulty of accurately tracing the deuterium through mass spectroscopy. The deuterium process was modified from the original experiments

developed by Jacobson to accommodate the use of pulp fibers [90]. The initial results of these experiments proved inconclusive. Various concentrations of fibers and D_2O were tried to address this issue, but in the end, the mass spectroscopy method proved to be too imprecise. Although the results of these experiments proved unusable, they laid the ground work for the tritium portion of this thesis work.

5.2 Tritium Experiment Development

The tritium content of a liquid system can be directly measured through scintillation counting. By using scintillation counting, direct measurements could be taken throughout the experimental process. Tritium, like hydrogen and deuterium, is able to exchange in three areas of the fiber:

- The hydroxyl groups on the fibers surface
- The hydroxyl groups in the amorphous regions of the cell wall, any pores or exposed areas due to processing
- Water attached to the fiber through hydrogen bonding also exchanges with tritium

5.2.1 Initial Tests

Initial experiments were conducted by comparing a tritiated water – fiber suspension versus a tritiated water control of the same total activity based on weight. Results were generated by comparing the activity of the control to the activity of the tritium-fiber suspension given by Equation 13, where $dpm_{control}$ refers to the tritium activity in the control and dpm_{sample} refers to the tritium activity in the water phase of

82

the fiber sample. In general, tritium increased in the fiber sample as compared to the control. This conclusion coincides with the decrease in hydrogen content available in fiber, however the variation in this method lead to further iterations.

Equation 13: Initial tritium calculation

$$D = \frac{\left(dpm_{control} - dpm_{sample}\right)}{dpm_{control}} * 100$$

The first issue was the presence of fiber in the scintillation sample, which leads to two-phase effects and increases counting uncertainty. Normally, the fiber can be separated out through a variety of methods, but as we were dealing with a radioactive substance more care was needed. Centrifuging was the first attempt to separate the fiber and water layers. Using a bench top centrifuge the system separated into two phases, but the boundary was easily disturbed and sample contamination still occurred. Filtering provided a method to separate water from pulp. Two methods were employed. First a syringe with a glass filter was used but the filter plugged with the suspended pulp. Second, small amounts of tritiated pulp were placed in a glass wool packed Pasteur pipette and the excess water was removed from the system. The water was fiber free, but there was still a large amount of variability between samples.

The major problem with measuring the change in tritium in the water phase of the fiber:water system was that the changes were small. The fiber in the sample only made up between 1 and 5 % of the total mixture. Changes in the samples containing

fiber were found to range between -44 % and 83 % when compared against a control, again giving inconclusive results. Hence, the fiber was assayed instead of the water.

5.2.2 Acetone Test Method Development

In order to count the activity in the fiber, the free water needed to be removed from the pulp. To do so a water-miscible aprotic solvent was needed. Acetone was chosen as the wash solvent because although the methyl protons can potentially enolize and exchange with tritium, the rate of exchange is far too slow to be significant under our conditions [127]. Also, it swells pulp to a relatively small extent. With compressed samples, Mantanis, Young, and Rowell found that acetone increased the thickness of a kraft pulp pad by 43 % while the corresponding increase with water was 373 %.[128] Therefore, the addition of an acetone wash to a water saturated pulp pad should minimize swelling and the exposure of additional surface area. Thus, the fiber became chemically dried without bound water being removed from the system. Rehydration of the pulp would generate a liquid where the tritium content came only from the fiber. From this liquid, the tritium concentration on the fiber could be determined.

Investigation of this method began with simulating the acetone/water/pulp system through a computer model. Figure 25 displays the interaction of acetone, represented by the squares, and water, represented by the unfilled circles, with the pulp fibers in the system. The upper graph shows the activity in the pulp, which remains constant as long as only acetone is used to wash the system. This is due to the lack of hydrogen exchange between the pulp fibers and the acetone. If the washes

are changed to water the activity in the pulp drops substantially and will continue

dropping until the tritium is completely removed from the system, due to hydrogen

exchange occurring between the pulp fibers and the water washes. This interaction is

reflected in the lower graph where activity in the washes is represented. As shown,

the acetone is continually removing activity from the water phase of the system

through removing free water. Thus removal of the free water by acetone does not

impact the activity in the pulp phase as indicated by the upper graph. When the

washes are changed to water, the wash activity increases substantially, indicating the

amount of hydrogen available in the pulp fibers and bound water.
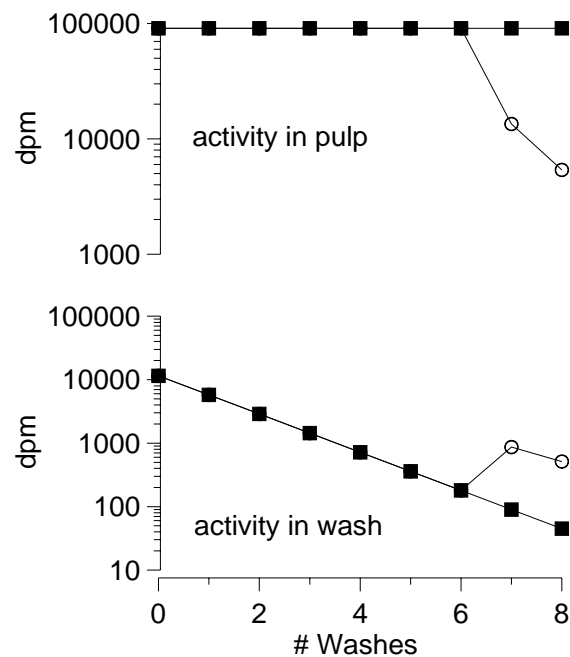
Figure 25: Model simulation of activity in pulp and washes

This model is a simplistic view of the fiber-water system, but it indicates that

these experiments should work and provide a basis for experimental procedure. First,

the system was modeled to remove approximately 99 % of the tritium in the system (filled squares in Figure 25). Once 99 % of the tritium was removed, two water washes (unfilled circles in Figure 25) were introduced to remove the tritium in the pulp. Notice the decrease in activity of the pulp and the resultant increase in the wash activity. This provided a basis for experimental parameters. It is however important to note, that this is just a representative system. The impact of bound water is not modeled within this system. Nor is the impact of water introduced to the system with acetone. The impact of bound water proved experimentally to be the main component of tritiated water interacting with the fiber, not the tritium exchanging with the fiber surface as depicted with this computer simulation.

The experimental method went through a number of iterations before determining the most consistent method. During these experiments two key process elements were determined. First, as noted earlier, the samples for counting must be free of any fiber fragments. Thus, all washes needed to be filtered. Secondly, acetone must be water free to minimize removal of bound water prior to the water washes.

5.3 Final Acetone Test Method

To perform the fiber:water distribution measurements, each sample was placed in a 30 mL Buchner funnel fitted with a 100-70 μm fritted glass filter 30 mm in diameter. This filter is attached to a low vacuum supply and empties into a 60 mL graduated addition funnel with a 500 mL round bottom flask below the funnel to collect the excess wash. Samples for testing are taken by separating the Buchner

funnel from the addition funnel and removing a sample using a 100 μL fixed volume pipette. By including the addition funnel in the system, isolated samples can be taken before they mix with the previous washes and the amount removed with each wash can be measured. The 500 mL flask allows for containment of the waste and separation between the acetone and water washes, two flasks are used for each experiment.

For the fiber:water distribution measurements, the pulp was brought to 8% consistency and divided into four 1.2 g (OD weight) samples. Each sample was placed in the Buchner funnel and water (25 mL) containing 20 μCi of tritiated water was added. The system was allowed to equilibrate for one minute with 30 seconds of stirring to distribute the tritiated water. During this time, gravity drainage could occur, but the fritted glass filter would prevent the majority of water from leaving the system. Once one minute had passed, the excess water was drained off using the low vacuum source. This drainage was timed and measured using the graduated addition funnel. The fiber was then flushed with 25 mL aliquots of acetone under low vacuum, until the activity in the filtrate dropped to below 1,000 dpm, which represents less than 1% of the initial radioactivity applied. The fiber was then back-washed twice with 25 mL of water each time allowing one minute of equilibration without mixing.

The activity in all measured washes was determined by liquid scintillation counting, mixing the 100 μL sample taken from the addition funnel with 10 mL of Scintiverse-E scintillant. The activity was measured with a Perkin-Elmer Tri-Carb 2800 TR scintillation counter. For the first fiber sample the activity in all the washes

was measured to develop a wash curve. For the remaining samples, the initial

drainage, the first and last acetone washes and both water washes were counted.

The overall procedure consists of the three steps defined by the following

equations.

Equation 14: Equilibration

$$fiber + HTO \leftrightarrow fiber - T + HTO$$

Equation 15: Wash

$$fiber - T + acetone \leftrightarrow dry\ fiber - T + wet\ acetone$$

Equation 16: Backwash

$$dry\ fiber - T + H_2O \leftrightarrow HTO + wet\ fiber$$
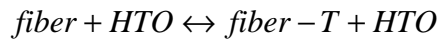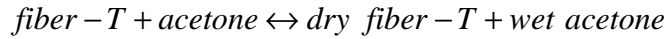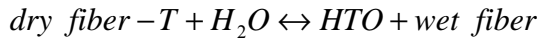
First, the fiber needs to be equilibrated with the radioactive water, Equation

14. Next, the excess radioactive water needs to be removed from the system to leave

a dry (water-free) fiber, Equation 15. Last, the radioactivity associated with the fiber

needs to be back-exchanged into water and counted, Equation 16. This allows us to

determine a term $K_{pw} = [T]_{pulp}/[T]_{water}$, which is the distribution coefficient of tritium

between fiber and water, *i.e.* [fiber-T]/[HTO] in Equation 16.

The equilibration step is straightforward. The fiber is mixed with water

containing a known amount of tritium, whereupon some of the protons associated

with the fiber (either directly or through bound water) exchange with the tritiated water to give partially tritiated fiber, fiber-T. The washing step is more difficult because all the free water must be removed from the fiber; otherwise, the tritium in the free water would also be counted.

5.3.1 Equilibration

The fiber is equilibrated for one minute prior to draining. The drainage time for the various pulps ranged from a few seconds to around ten minutes based on the fibrillation and self-packing of the fiber in the funnel. Li et al. determined the diffusion rate of water in kraft fiber to range between 1.31×10^{-9} to 0.16×10^{-9} m^2/s.[129] The rate of diffusion in the fiber-water system was determined using Crank's equations for uptake by a cylinder from stirred solution using Figure 26 and Equation 17, Equation 18, and Equation 19 [130]. With the discussed system, $M_\infty =$ 0.30 and at equilibrium, $(Dt/a^2)^{1/2} = 0.92$. Therefore, using the most restrictive diffusion case given by Li, water can diffuse through a fiber in our system in approximately 21 ms.[130] Thus, a minute provides ample time for equilibration to occur.

Equation 17: M_∞ calculation

$$M_\infty = V_{res}\left(C_{res,i} - C_{res,f}\right)$$

Equation 18: Calculation for determining the correct curve

$$Curve\# = \frac{M_\infty}{V_{res} C_{res,i}}$$

Equation 19: Time needed for equilibration

$$t = \frac{\left(a X_{int\,ercept}\right)^2}{D}$$

Subscripts (multiple uses)
res = reservoir
no subscript or p = polymer
sur = interface between poly
          and external bath
i or 0 = initial
1 = reservoir conc. if constant
f, ∞, or * = final, equilibrium

At Equilibrium,
$M_t = M_\infty$
$M_\infty = V_p [C_f - C_i] = V_p [C_1 - C_0]$
          $= V_{res} [C_{res,i} - C_{res,f}]$
#'s on curves $= M_\infty/(V_{res} C_{res,i})$
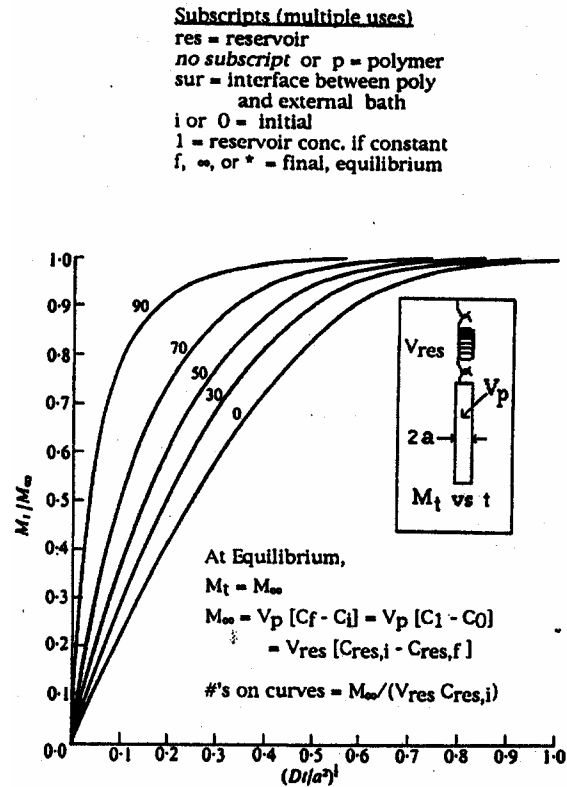
Figure 26: Crank's method for determining uptake by a cylinder from a stirred solution of limited volume

90

5.3.2 Washing

The excess water is flushed out in the second step.   It is essential that the wash acetone be completely dry; otherwise the fiber-associated tritium will begin to back exchange with any water present. In other words, the process represented in Equation 16 will start while the acetone wash step (Equation 15) is still taking place. Acetone containing 5 % water will allow approximately 10 % of pulp-associated tritium to be removed during the acetone wash. Even at 99 % purity 2 % exchange may occur. This problem was minimized through the use of nanograde acetone (99-100 % min) from Mallinckrodt. Efforts were made to keep the acetone dry throughout the experiment. Finally, the fiber is washed with two 25 mL aliquots of DI water to exchange off the tritium bound to the pulp and to bound water.

Equation 15 assumes that the bound water is not displaced by acetone; i.e. the tritium in the bound water remains associated with the fiber during the acetone wash. This bound tritium exchanges to water during the back-wash step represented by Equation 16. In order to demonstrate this difference, fiber was equilibrated with tritiated water as described above. One fraction of the fiber was washed with successive aliquots of acetone. A second fraction was washed with water, i.e. the acetone washing was omitted. The activity contained in the separate acetone and water washes are illustrated in Figure 27. The acetone is able to remove much less activity because it cannot access the tritium exchanged into the functional groups in the fiber and to the bound water. However, the water is able to wash out the tritium associated with the fiber phase and the activity in the initial wash water is correspondingly higher.
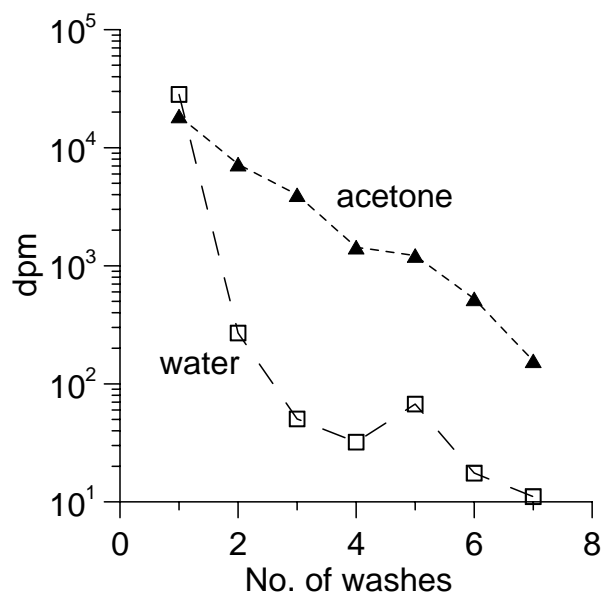
Figure 27: Removal of tritium from refined bleached hardwood pulp by acetone or water washes

Proof of the excess water flushing is shown in Figure 28, where water washes preceded by acetone washes can remove as much or more tritium from the system as the prior acetone wash. The curve was created by first measuring the activity in the tritiated water, wash 1 on the x-axis, then the activity that remained in the water phase after equilibrating the fiber with the tritiated water, wash 2. The fiber was then rinsed first by 25 mL acetone, washes indicated by the triangles, then 25 mL DI water, washes indicated by the squares. This acetone / water cycle was repeated until no activity remained in the acetone washes. The lack of activity is indicated by the two consecutive water washes at the end of the curve and the missing wash 11(0 dpm) on the figure. The increase in activity in washes 8, 10, and 12 when compared to their

preceding acetone washes indicate that the water in these washes, and most likely

previous water washes, is exchanging with the tritium attached to the fiber.
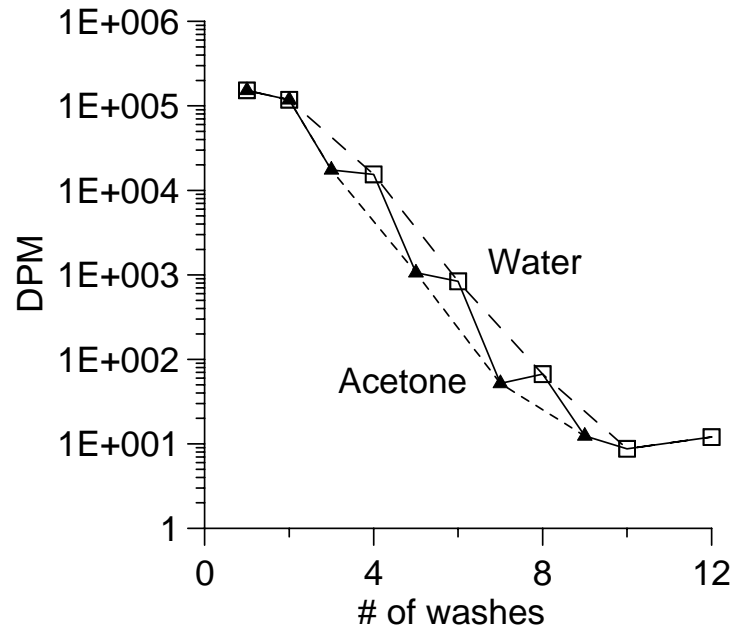
Figure 28: Acetone/Water Washes

Based on this information, curves were developed for each sample as shown

in Figure 29. Initial samples for each fiber type and refining level were used to

determine the number of washes needed to decrease the wash DPM to less than 1000

DPM. Then, two water washes were performed to exchange all tritium out of the

fiber and bound water. To standardize between small variations in pulp weight

between samples the activity is given per gram of od pulp. Therefore, no initial

activity is given prior to equilibrating with the pulp.   The first wash on the graph

indicates the amount of activity left in the water phase after equilibration. The next

series of washes are the acetone washes, which continue until the activity is under

1000 dpm/g od pulp. Then the fiber is equilibrated with water as shown in the last

section of the figure. Again, the order of magnitude jump shown between the acetone

and water washes indicates the reaction of water with the fiber.
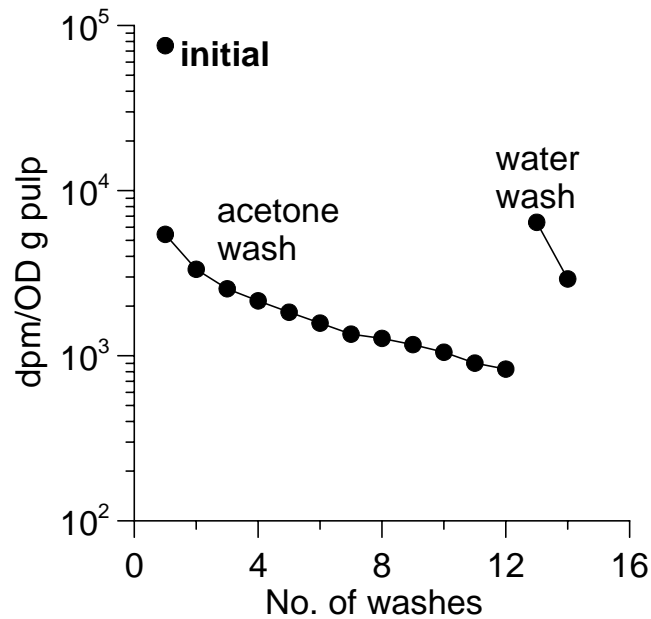
Figure 29: Experimental wash results

5.3.3   Backwash

The backwash is a critical step in measuring the fiber:water distribution. In

this step, the tritium ions bound to the fiber are re-equilibrated with water. DI water

(25 mL) is introduced into the fiber and allowed to equilibrate without vacuum for

one minute. Then the water is removed by vacuum from the system. This removal

can take from a few seconds to over 15 minutes; all samples in this study had a

drainage time of a few seconds. To fully remove the tritium the backwash is

repeated. The two washes is standard practice and extra washes often result in background activity levels.

5.3.4 Scintillation Counting

Scinitillation counting was performed using QuantaSmart™ software and a TriCarb® 2800TR Liquid Scintillation counter from PerkinElmer. Using this system an assay, or program, was developed to determine the disintegrations per minute (dpm) of the sample [131].

The dpm of a sample is first determined by introducing a beta-emitting radionuclide to a scintillator. The beta particle emitted from the radionuclide is converted to a photon by the scintillator. The scintillation counter contains a photosensitive device that converts the photon light into an electrical pulse. These pulses are counted and a count per minute, or cpm, is tabulated. Some of the beta particles are not converted in the scintillation process and are thus quenched. This quenching creates a discrepancy between the cpm and the actual disintegrations in the sample. To convert from cpm to dpm a quench curve is necessary. This curve is based on the counting efficiency of known quench standards.[131] From this curve, a counting efficiency is determined and the dpm of the sample is calculated using Equation 20.

Equation 20: Calculating dpm

$$dpm = \frac{cpm}{counting\ efficiency}$$

5.3.5 Calculations

K_{pw}, the fiber:water partition coefficient, is directly calculated from the activity counted in the washes. The pulp is initially mixed with radioactive water with a total tritium content of D_i dpm. The pulp picks up the tritium and is then washed sequentially with acetone and water. The tritium in the combined water washes contains the tritium captured by the pulp and bound water, ΣD_p dpm, so that the activity in the pulp phase (without the free water) is given by Equation 21 where p is the weight of the pulp. The difference between the initial activity, D_i, and that retained in the pulp, ΣD_p, is the amount of activity in water not associated with pulp. Hence the activity remaining in the water after the fiber addition is given by Equation 22 where q is the weight of water in the mixture. The ratio of the activity in the two phases, the partition coefficient K_{pw}, is expressed by Equation 23.

Equation 21: dpm in fiber phase

$$dpm_p = \frac{\sum D_W}{p}$$

Equation 22: dpm in water phase

$$dpm_w = \frac{D_i - \sum D_W}{q_i}$$

Equation 23: Determination of K_{pw}

$$K_{pw} = \frac{dpm_p}{dpm_w}$$

5.3.6 Efficiency of Method

The following mass balance for a bleached softwood run is representative of the distribution and recovery of tritium.

Initial tritium added to pulp (as 10^6 dpm)	=	4.172
Tritium recovered in filtrate after equilibration with pulp	=	3.133
Tritium recovered from acetone washes	=	0.880
Tritium recovered from water washes	=	<u>0.011</u>
Sum of recovered tritium	=	4.024
Percent tritium recovered	=	96.5 %

The tritium in the system is recovered almost completely from the water fiber system, thus the recovered washes can be used to determine the amount of tritium contained in the fiber and water phases of the system. The activities recovered in the acetone and water washes are used in the bound water calculations, as explained in Section 5.3.5.

5.4 Conclusions

The partition coefficient K_{pw} is the (unitless) distribution coefficient of radioactivity in the pulp and water phases. The tritium can exchange with

exchangeable sites in the pulp such as hydroxyl and carboxylic acid groups and also with water associated with the pulp. Washing the tritium-loaded pulp with acetone removes the free water and the tritium associated with it. A subsequent water wash liberates the residual tritium from the pulp. This distinction is clearly seen in Figure 29 where progressive acetone washing reduces the activity in the wash acetone. When a water flush is used after the final acetone wash, the activity in the water rises sharply because the tritium in the bound water and in the pulp matrix now exchanges into it. Thus, with K_{pw} we can measure the hydrogen directly bound to the fiber.

CHAPTER 6: INITIAL RESULTS AND DISCUSSION OVERVIEW

6.1 Initial Studies

In order to prove the acetone method works experimentally and to standardize the experimental procedure, an initial refining study was performed. Refining alters the fibers in three primary ways. First, refining creates new surfaces, secondly, new particles are formed and thirdly, the fiber is altered through surface damage and modifications. The breaking of hydrogen bonds and covalent bonds causes these primary effects. Every time a bond breaks there is more hydrogen available for exchange with the surrounding liquid, thus an increase in refining results in an increase in tritium exchange. A study focusing on the impact of bleaching on refining was also conducted to see if the same general trends persist.

6.1.1   Fiber Source

The focus of this initial experiment was to observe large changes in fiber properties. By using northern bleached softwood kraft (BSWK) for the initial refining study, the fiber was primarily cellulose and impacts of lignin and hemicellulose were minimized. The dimensions of the softwood fiber allow for a larger span of refining levels. Receiving the pulp in slurry form eliminated any effects of drying, which can cause additional permanent hydrogen bonds, possibly altering results. To study the effect of bleaching, the same bleached softwood kraft along with bleached and unbleached hardwood kraft, all from StoraEnso's Wisconsin

Rapids mill, and an unbleached softwood kraft from International Paper's

Androscoggin mill in Androscoggin, Maine, was used.

6.1.2 Refining

The bleached softwood pulp was refined to five levels in a PFI mill; 0, 2500, 5000, 7500, and 10000 revolutions. This resulted in freeness levels of 676, 464, 358, 261, and 235 respectively. The hardwood pulps were refined at two levels 0 and 1250 revolutions and the unbleached softwood was refined at 0 and 7500 revolutions. These levels were chosen based on the results of the initial refining study.

6.1.2 Tritium Tracing

The processed pulp is spiked with a known amount of tritiated water. This solution is allowed to come to equilibrium before the excess water is drained off. The spiked pulp is then washed with acetone to remove any remaining free water. Then a known amount of water is added to the pulp and allowed to come to equilibrium. This water is drained and a sample is taken to determine the amount of tritium remaining with the pulp after removal of the free water. The water is added stage wise to ensure that most of the tritium is removed. Further description of tritium tracing is available in Chapter 5. These results were then compared with freeness and water retention values, tests performed as described in Chapter 4.

6.2 Refining Results

For every base unit of cellulose, there are six potential exchange points. These exchange points can be bound to other cellulose molecules in a crystalline structure, preventing all exchange, bound in an amorphous form or present on the surface of the fiber both of these forms facilitate exchange. Tritium can also exchange with the water bound to the fiber. This water is chemically bound to the fiber and is present after removing excess water from the system. This bound water causes the numbers to greatly exceed the potential accessibility of cellulose as the fibers create more surface area and bound water through the refining process.

Table 4: Initial Study Results

Refining level (revolutions)	CSF (mL)	K_{pw}	WRV (g/g)
0	676	0.09	1.78
2500	464	0.22	2.14
5000	358	0.32	2.26
7500	261	2.09	2.31
10000	235	3.54	2.37

Table 4 contains freeness, the averages of K_{pw}, and water retention values at the different freeness levels. The second measurement, K_{pw}, is the pulp/water partition coefficient. The partition coefficient is based on the selectivity of the tritium to exchange with the hydrogen in the pulp and bound water versus the hydrogen in the free water on a gram basis. Water retention values were performed for comparison of K_{pw} with other swelling methods. While freeness and water retention values trend somewhat linearly through the refining process, K_{pw} had a dramatic change in slope around 300 CSF. This jump is visually shown on the graph below. Figure 30 also includes fiber saturation points (FSP), reported by Scallan and Carles for spruce kraft with a 60 % yield.[48] Unlike the pulp used in this study, the Scallan pulp was unbleached. It is interesting to note how closely the FSP of Scallan and Carles' work trends with the K_{pw} (partition coefficients) of our study.
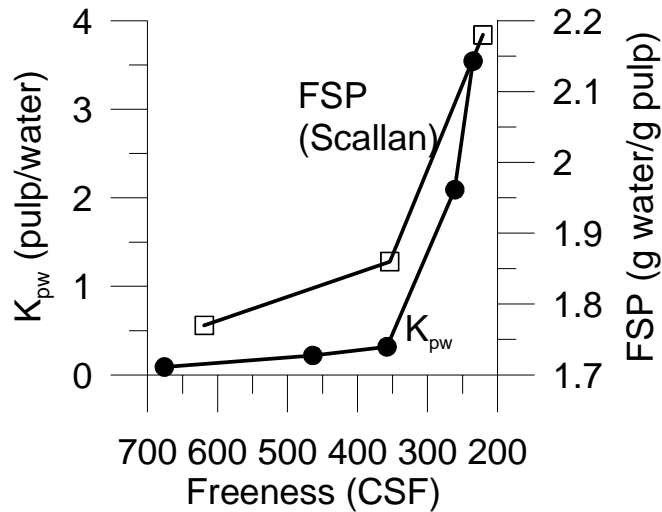
Figure 30: Effect of refining on K_{pw} and FSP
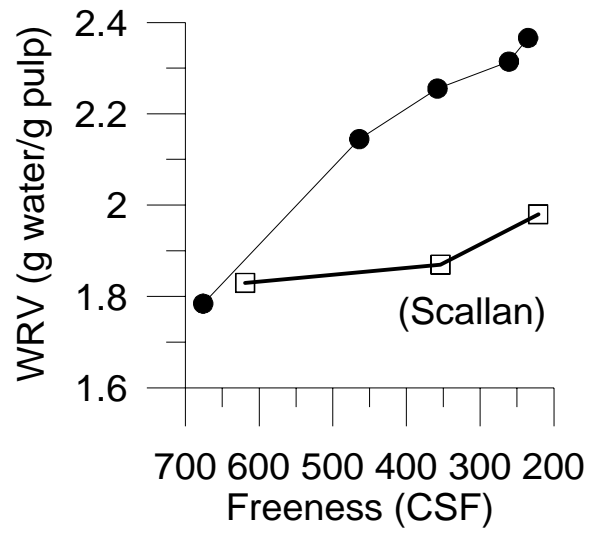
Figure 31: Effect of refining on WRV
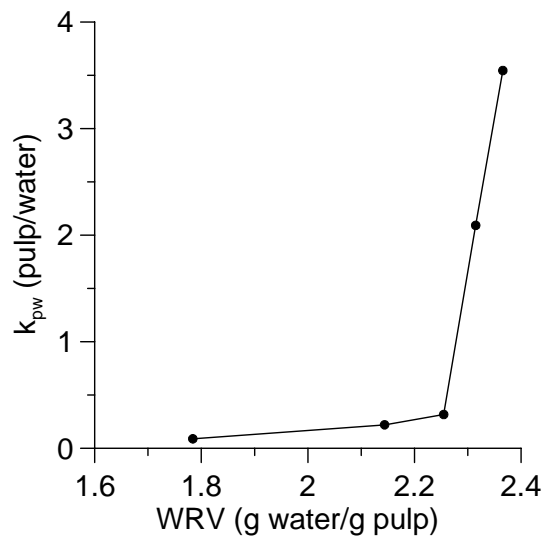
Figure 32: WRV K_{pw} Comparison

Scallan and Carles concluded that the discrepancy between WRV and FSP at higher refining levels was due to the compression of the swollen fiber under applied force.[48] Figure 31 displays a fairly linear relationship between WRV and freeness with both of the studies until fibers are refined blow 350 CSF, the results of this study are represented by the filled circles. However, both Scallan and Carles' FSP results and our K_{pw} results work in Figure 30 do not have a linear relationship with freeness implying that there are factors involved with K_{pw} and FSP that freeness and WRV measurements do not reflect. Figure 32 further illustrates the difference between K_{pw} and WRV.

It is also possible that the action of refining on the fiber reaches a threshold around 300 CSF causing the fiber surface to break open markedly creating more surface area as refining continues. This theory is visually confirmed through light microscopy performed by Rob Lowe. The slow increase in fibrillation of the fibers in Figure 33 correlates with the slight increase in K_{pw}. Beyond the threshold of 300 CSF, a dramatic difference in fibrillation is shown in Figure 34, also corresponding with the large increase in K_{pw}. The difference between the images of Figure 34 is approximately 100 CSF, but the change in fiber properties is extreme within this region. The changing nature of the fiber could lead to sheet breaks and other disruptions when producing products in this freeness range. Figure 35 displays the beginning stages of fiber destruction.
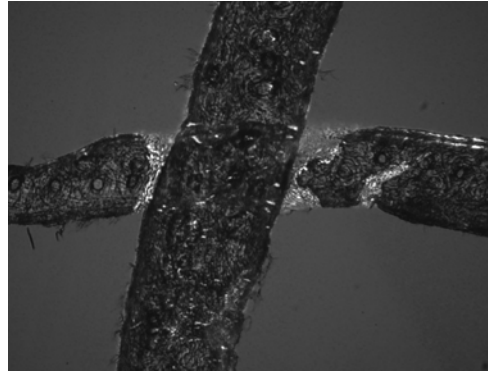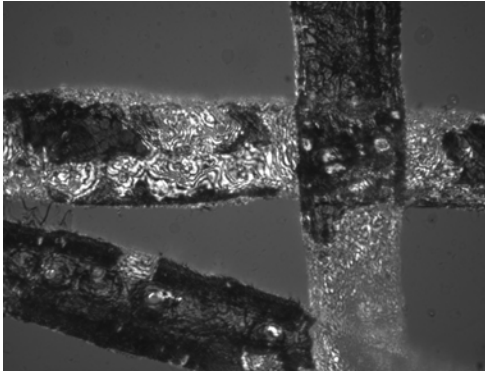
Figure 33: Unrefined, 676 CSF (left) and 2500 rev, 464 CSF (right)
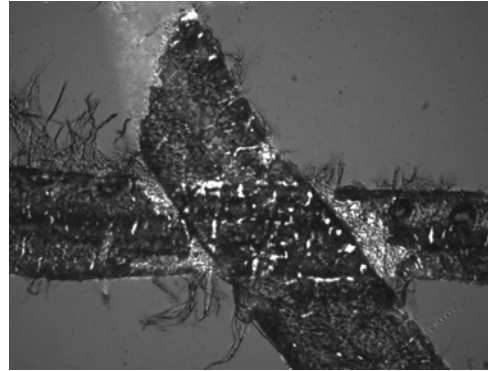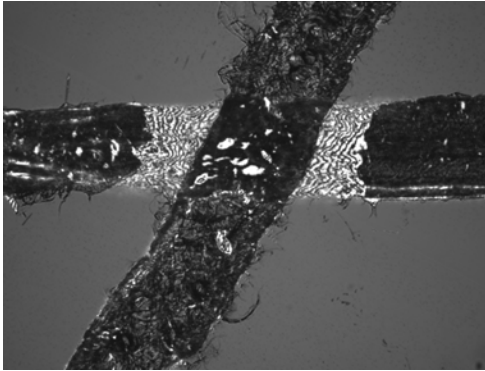
Figure 34: 5000 rev, 358 CSF (left) and 7500 rev, 261 CSF (right)
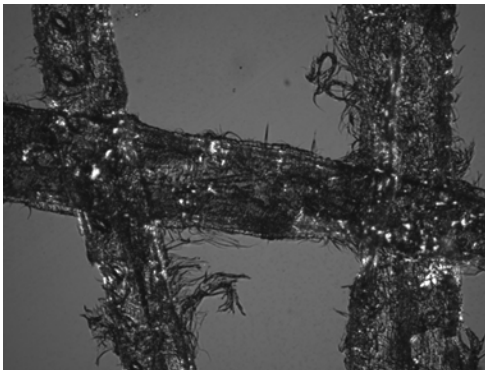
Figure 35: 10000 rev, 235 CSF

6.3 Refining Conclusions

K_{pw} provides a better understanding of how fiber structure changes with refining and offers a way to measure these changes with a single number. The practical benefit is likely to be a better selection of a target freeness value after refining. Presently, freeness is selected based on product quality and on some measure of runnability, *e.g.* machine speed, sheet breaks. Yet, there are other considerations. For, example, K_{pw} tracks the fiber saturation point in Figure 30, and an increase in FSP leads to an increase in dryer energy. A 50-point difference in freeness makes only a small difference to the FSP at the 400 CSF level, but a much larger impact at 350 CSF. It is the expectation, that the results of this study will enable a better selection of target freeness.

6.4 Experiments with bleached pulp

Studies with bleached pulp were conducted to see if the impact of bleaching on the fiber altered the conclusions made from the initial refining study. Since Scallan and Carles [48] FSP results with unbleached softwood trended closely with the K_{pw} results, FSP of the bleached and unbleached pulp was measured. Also, hardwood fiber was added to observe if K_{pw} trends differ between hardwood and softwood. All unbleached fiber studied was taken from the bleaching process stream and are thus considered bleachable grade pulps. For this study the hardwood pulps were obtained from the same source. Unfortunately, softwood pulp was not currently being produced at the Wisconsin Rapids mill so unbleached softwood was obtained from International Paper's Androscoggin mill. Therefore, while general conclusions can be made from the softwood comparison, the fibers are not directly related.

Table 5 compares the different fiber saturation results across all four pulp types used in the study. A general trend exists with increased refining, freeness decreases, while K_{pw}, FSP and WRV all increase. The only exception occurs with BHWK that had been refined at 1250 revolutions. The FSP decreases, but this is most likely an anomaly in the testing since both the K_{pw} and WRV increase slightly.

Of greater interest are the discrepancies that occur between the BHWK and UHWK after refining. One would assume that a bleached pulp with the same amount of refining as an unbleached pulp would have higher fiber saturation across all test methods.

Table 6 may provide some insight into the bleached / unbleached discrepancy. Table 6 contains the results of the fiber quality analysis. When comparing the bleached pulp to the unbleached pulp it is obvious that the pulp has gone through some high consistency stages during the bleaching process. The curl and kink index of the hardwood fibers after bleaching is almost double of the unbleached fibers. This doubling indicates that during the processing of bleaching the fibers the glass transition temperature of cellulose was possibly exceeded allowing kinks and water inaccessible regions to form. This processing would correlate with the lower fiber saturation results.

Table 5: Fiber Saturation Point Method Comparison

Type	Refining	CSF	K_{pw}	FSP	WRV
UHWK	0	439	0.11	1.64	1.80
UHWK	1250	259	1.21	2.04	2.02
BHWK	0	454	0.07	1.89	1.81
BHWK	1250	276	0.26	1.73	1.96
USWK	0	702	0.11	1.39	1.70
USWK	7500	242	1.71	2.18	2.39
BSWK	0	676	0.09	1.72	1.78
BSWK	2500	464	0.22	2.21	2.14
BSWK	7500	261	2.02	2.41	2.31

Table 6: Fiber Quality Analysis Averages

Type	Refining	Freeness	% Fines	Mean length (lw)	Curl	Kink index
UHWK	0	439	12.27	0.660	0.0517	0.89
UHWK	1250	259	9.18	0.689	0.0450	0.83
BHWK	0	454	12.37	0.624	0.0870	1.44
BHWK	1250	276	11.93	0.613	0.0803	1.29
USWK	0	702	5.38	2.743	0.0543	0.74
USWK	7500	242	7.74	2.627	0.0687	0.88
BSWK	0	676	10.80	2.105	0.0950	1.47
BSWK	2500	464	8.31	2.185	0.0635	0.99
BSWK	7500	261	9.83	2.140	0.0615	1.05

To observe what is happening to the fibers, SEM pictures were taken by Shaobo Pan as discussed in Chapter 4. Figure 36 displays the bleached fibers while Figure 37 shows the unbleached fibers. The stiff nature of the fibers is very apparent in Figure 36 with minimal fibrillation and no evidence of delamination. In Figure 37, there is evidence of internal delamination with crack formation and external delamination with fibrils extending from the fibers and matter separate from fibers. What is also evident is a more amorphous nature of the unbleached fibers with the number of collapsed fibers and general overall appearance.

6.5 Conclusions from the Bleached Pulp Experiments

As with the initial refining experiments, it was determined that K_{pw} is more sensitive than traditional methods in determining the overall condition of the fiber. In the case of the hardwood fibers, the effect of bleaching the fibers was evident in the lower K_{pw} of the refined hardwood bleached pulp. However, that effect may not be due to the chemical nature of bleaching but the processing conditions. The softwood pulps did not have the same correlation, but as they were produced in different mills, the effect of bleaching should not be analyzed. However, the same general increase in K_{pw} was present in both the unbleached and bleached softwood fibers.
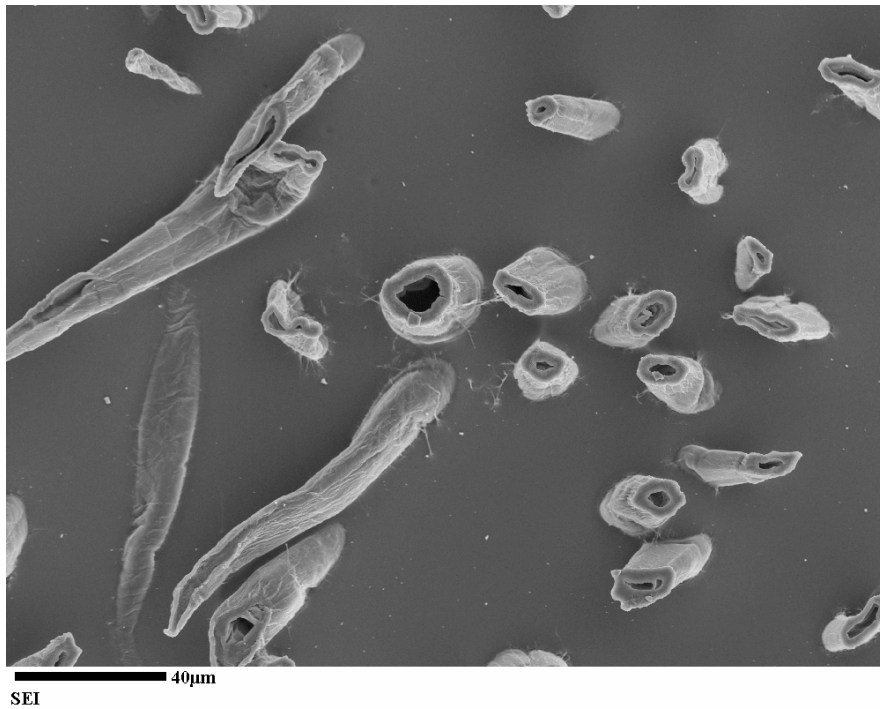
Figure 36: SEM of refined bleached hardwood pulp
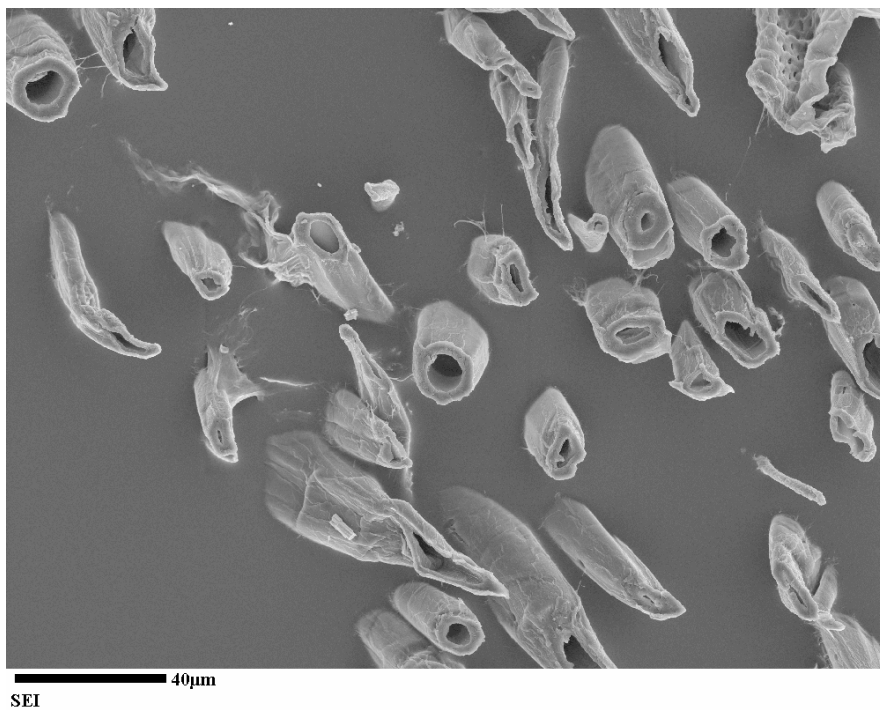
Figure 37: SEM of refined unbleached hardwood pulp

6.6 Discussion Overview

The following chapters contain portions of the work published from this thesis. Chapter 7 involves an analysis of monolayer water and a critique of current ways to determine bound water within the fiber. This work has been submitted to Holzforschung under the title "Measurement of monolayer water in pulp" [132]. Chapter 8 discusses the effects of refining on bleached softwood fiber utilizing K_{pw} and comparing this method to changes in fiber characteristics during refining measured using traditional techniques. The initial results of this study were presented at the 2006 Pan Pacific Conference in Seoul, Korea [133] and the complete study was submitted to Holzforschung under the title "Isotopic study of the effects of refining on internal fiber structure" [134].

Chapter 9, Impact of recycling, reports the findings of a study performed in conjunction with Adam Brancato. The results of this study will be presented at the 2006 TAPPI Engineering, Pulping, and Environmental Conference, November 5-8 in Atlanta, GA.

CHAPTER 7: FIBER SATURATION POINT STUDY

The amount of water associated with pulp is operationally defined. One measure is the water retention value (WRV), where fiber is separated from free water by centrifugation [47, 116]. Another index is the fiber saturation point (FSP) measured by the solute exclusion method [35, 45, 118, 119] where the volume of water inaccessible to a solute probe is measured. In this thesis a new technique is introduced for measuring tightly bound water, K_{pw}, which is most likely bound to the fiber surface as a monolayer. In this chapter the limitations of the procedure are defined, the procedure is compared to more conventional methods, and new insights provided by the technique are discussed. In Chapter 8 the technique is applied to pulp refining.

7.1 Materials and Methods

Bleached softwood pulp and bleached and unbleached hardwood pulp were obtained from Stora Enso's Wisconsin Rapids mill. Unbleached softwood pulp was acquired from International Paper's mill at Androscoggin, Maine. The pulps were not refined. Tritiated water was purchased from Amersham Biosciences.

Fiber:water distribution measurements (Kpw) were conducted as described in Chapter 5. WRV, freeness, and FSP and FQA were performed as described in Chapter 4.

7.2 Results and Discussion

Fiber:water partition coefficients (K_{pw}) and other properties of four virgin pulps are listed in Table 7. The K_{pw} values are all about 0.1; the corresponding WRV and FSP values are also relatively unchanged, although their values are much higher. It is

important to note that K_{pw} is much higher for refined pulp as discussed in Chapter 8. The

finding that K_{pw} is insensitive to the nature of the fiber (hardwood or softwood, bleached

or unbleached) suggests that the tritium primarily exchanges into the bound water rather

than into the exchangeable groups of the fiber. This is not surprising because there are

many more exchangeable protons in monolayer water than there are in the hydroxyl and

other groups on the surface that supports the monolayer water. Hence, K_{pw} should be

proportional to the bound water content of the fiber.

Table 7: Bound water content and other fiber properties

Type	K_{pw}[1] (sd)	FSP[1] (sd)	WRV[1] (sd)	Freeness (mL)	Fines[2] (percent)	Mean Length (mm, lw)[3]
UHWK	0.11 (0.06)	1.6 (0.1)	1.8 (0.2)	439	12.3	0.66
BHWK	0.07 (0.03)	1.9 (0.1)	1.8 (0.1)	454	12.4	0.624
USWK	0.11 (0.01)	1.4 (0.1)	1.7 (0.1)	702	5.4	2.743
BSWK	0.09 (0.01)	1.9 (0.1)	1.8 (0.2)	676	10.8	2.105

[1]average of four replicates
[2]Britt jar results
[3]FQA results

If exchange into the functional groups is neglected, then the K_{pw} value of 0.1

indicates that the fiber is associated with ten weight percent of water. The monomer unit

of cellulose is cellobiose, which consists of two glucose molecules joined by a β-1,4

linkage. If the fiber is approximated as a sequence of cellobiose units, each with a

molecular weight of 342 Da, then it follows (from the K_{pw} value of 0.1) that two

molecules of water (one-ninth of the cellobiose molecular weight) is associated with each

cellobiose unit. The FSP and WRV values in Table 1 average to a value of 1.72. This

translates to about thirty-three water molecules per cellobiose unit. It would seem that the additional thirty-one water molecules do not bind directly to the fiber matrix, but rather to the water layers adjoining the fiber. Presumably these thirty-one molecules must be associated through a multilayer arrangement as described by Caulfield or Goring [40, 41]. Thus, we have effectively classified the bound water fraction into strongly and weakly bound entities, comprising two and about thirty molecules of water, respectively, per cellobiose unit.

If the strongly bound water is assumed to be attached to the fiber surface as a monolayer, then an estimate of the surface area of a fiber can be obtained. Hines and Maddox [135] report the diameter of a water molecule to be 2.641 Å, which leads to a surface area of 1,830 m^2/g of water if the water were spread out as a single layer. Our K_{pw} values from Table 1 indicate that about 0.1 g of water is associated with each gram of fiber, which means that the water covers 183 m^2/g of pulp. This would then be the fiber surface area if the water is assumed to cover the entire surface as a monolayer.

Independent estimates for the surface area of a water film lead to similar results. In their study, Carles and Scallan [58] calculated the surface area of destructured water to be 0.90 mL/g, which leads to a value of 3,000 m^2/g for the surface area of a single layer of water. This value is higher than the Hines and Maddox [135] result because it includes the space between the water molecules. Use of the Carles and Scallan [58] estimate with our K_{pw} parameter leads to a value of 300 m^2/g for the surface area of fiber. These estimates of fiber surface area compare well with other internal surface area measurements as discussed by Herrington and Petzold [136]. It is important to recognize

that the surface area results for this study reflect wet conditions in contrast to some of those obtained from measurements where the fiber was first dried.

Bound water has been studied under a variety of names; here they will be generalized by terming them all interfacial water. Table 8 lists some earlier results along with corresponding FSPs where available. The K_{pw} measurement only considers water that cannot be displaced by acetone. It is possible that there is water in pores with openings too small for acetone to penetrate, but the proportion of this water, if any, should be quite small. Bound water has been variously defined. One definition is that it is water that cannot be mechanically removed by a device such as centrifuge. Another calls it surface-sorbed water. Clearly, the value one obtains can depend upon how one obtains it.

Goring [40] found the thermal expansion coefficient of wet cellulose or fiber to be three times greater that that of dry material. He attributed the effect to the expansion of water at the cellulose/water interface and calculated a value of 0.17 g of bound water per gram of cellulose. This result is considered to be close to ours given the very different assumptions and techniques involved.

Table 8: Historical interfacial water values

Material	FSP (g/g)	Interfacial water (g/g)	Determination	Method	Ref.
sulfite pulp		0.17	perturbed layer	thermal expansion coefficient	Goring, 1977 [40]
cotton bleached spruce bleached poplar bleached straw		0.05 / 0.05 0.06 / 0.06 0.06 / 0.07 0.07 / 0.06	monolayer coverage	water vapor adsorption	Hernadi, 1984 [54]
cotton, rayon		0.04-0.19	bound water	DSC	Mange, et al., 1947
cotton, rayon microcrystalline cellulose		0.14-0.31 0.2	total nonfreezing water	DSC	Mange, et al., 1947 [55]
cotton yarn cotton lint wood cellulose		0.14 0.18 0.19	nonfreezing bound water	DSC	Nakamura et al., 1981 [57]
cotton wood sulfite pulp kraft pulp	0.5 0.45 1.34 1.66	0.15 0.23 0.3 0.33	maximum bound water value	NMR	Carles and Scallan, 1973 [58]
Hardwood kraft Softwood kraft #1 Whatman filter		0.210 0.255 0.27	Total Bound Water	DSC	Nelson 1977 [61]

Caulfield [41] argued that water is structured in the presence of cellulose. Only the first layer of water is attracted strongly by the cellulose surface. The subsequent layers are associated with the preceding adsorbed layer. The attraction between each layer becomes progressively weaker until the layers are destructured by the surrounding water. Similar assumptions have been made by Grunwald [137] for solute-water interactions. Hence, the behavior of the first layer of water (the monolayer) should differ from that of additional layers. Hernadi [54] exploited this difference by measuring the sorption isotherms for water vapor on cellulose. He found a break in the isotherm and concluded that it was caused by a change from monolayer sorption to polymolecular sorption where the additional layers deposit on the first layer [54]. Hernadi's results are included in Table 8 and correlate well with the findings of this study. However, a point of difference is that Hernadi started with dry pulp where the pore structure within the fiber may have partially collapsed, lowering the overall surface area of the fiber. Hence, his low values could be partially due to a partial collapse of fiber structure, which would reduce the surface area.

Other researchers [55-57, 61] have used differential scanning calorimetry (DSC) to determine nonfreezing water. Limited molecular motion, kinetic effects, capillary forces in nanoscale pores, and site adsorption have been proposed to explain why water adjacent to fiber does not freeze [56]. The site adsorption theory is based on the premise that the amount of nonfreezing bound water corresponds to the number and type of accessible hydration sites in the fiber, mainly hydroxyl groups [56]. Nakamura et al. [57] characterize bound water as that restricted by the hydroxyl groups of the cellulose. Nonfreezing water is considered to be a subset of bound water; it is tightly associated

117

with cellulose and shows no detectable peak during the cooling and heating process associated with DSC. Nakamura et al. [57] calculated a value of 0.19 g/g for the nonfreezing water in wood cellulose. In his study, Nelson [61] also used DSC to determine the bound water content of various paper samples and found them to range between 0.21 to 0.27 g/g. As with the vapor pressure measurements, a potential difficulty with using DSC in this application is that the fiber structure is altered during measurement.

Carles and Scallan [58] used NMR to study bound water in a variety of fibers. Their results are higher than ours, but they state that due to experimental difficulties in determining the spin-spin relaxation times of protons in bound water, their values correspond to the maximum amount of bound water in the fiber. In other words, a clean distinction between monolayer water and water that is more loosely bound is not available from NMR.

These various results for bound water content are all of the same magnitude as our values. A closer comparison is not possible because of the differences in the nature of the substrates used. In order to unequivocally preserve fiber structure, a good measurement must work with wet rather than dry fiber. Of the techniques listed in Table 2 only NMR fulfills this requirement, but NMR is unable to cleanly distinguish between free and bound water. The K_{pw} approach actively separates free and bound water in wet fiber, the major assumption being that acetone is able to affect this separation.

7.3 Conclusions

This study has determined the fraction of water tightly bound to pulp through use of the fiber:water partition coefficient (K_{pw}) of the tritium ion. Bound water is operationally defined; this study classifies it as water that cannot be displaced from fiber by acetone. The values are at the low end of results obtained by other methods, but this is to be expected, since the technique should isolate water that is tightly bound, i.e. resistant to acetone displacement. The method perturbs the fiber to a much lower degree than more conventional techniques such as DSC or vapor adsorption. NMR is even more non-invasive, but it does not allow a clean distinction between the various forms of bound and free water to be made. At the limit, tightly bound water should correspond to monolayer coverage and should reflect the surface area of wet fiber. Surface area estimates obtained from these measurements appear to be in line with other results.

The method can be considered to be a refinement of the solute exclusion technique which measures the water present in pores larger than a probe molecule such as dextran. Acetone, by virtue of its smaller size, can remove water from pores that are too small for dextran to enter. Hence, the dextran method would lead to a higher estimate of bound water. This is evident from the FSP values in Table 2, which are all considerably higher than the estimates of bound water. At the limit, the tightly bound water should cover the fiber surface as a monolayer, in which case, it should correspond to the surface area. This seems to be the case by comparison with results obtained independently. The K_{pw} parameter is also a sensitive measure of the changes in fiber structure changes caused, for example, by refining, as discussed in Chapter 8.

CHAPTER 8: IMPACT OF REFINING

Refining is a complex process which alters both the external and internal structure of fiber [91]. The effects of refining are measured through parameters such as freeness, the water retention value (WRV), and the fiber saturation point (FSP). These properties reflect, in part, the increased water-carrying ability of the new fiber surface exposed upon refining. It is important to understand where the new surface is created. The desirable outcome would be for the surface to be developed at the exterior of the fiber where it can participate in hydrogen bonding and increase the strength of the mat. However, if the new surface is formed inside the fiber matrix, then it would increase water retention without increasing fiber strength, which is detrimental on many accounts.

Chapter 7 showed that K_{pw} is related to water that covers the pulp surface as a monolayer. It also provides a reasonable estimate of the wet surface area of fiber. Now the tritium technique is applied to study the effect of refining on monolayer water coverage and demonstrate that refining can be dissected into three discrete stages. Finally, a breakpoint is identified at which the benefits of refining begin to decrease.

8.1 Materials and Methods

Never dried bleached softwood kraft pulp was obtained from Stora Enso's Wisconsin Rapids Mill, Wisconsin Rapids, WI, USA. The pulp was refined in a PFI mill following CPPA Standard C.7 [113] to a number of refining levels ranging up to 15,000 revolutions. Freeness, FSP, WRV, SEM and FQA were determined as described in Chapter 4. K_{pw} was determined as described in Chapter 5.

8.2 Results and Discussion

Results from the effect of refining on pulp and fiber properties are presented in Table 9 and Table 10, respectively. The refining (or beater) curve is illustrated in Figure 38. This curve and the values in Table 10 demonstrate that conventionally measured properties of the fiber change as expected, and that the results to be discussed are not an artifact of refining. Figure 39 illustrates the relationship between several fiber properties and freeness. The vertical lines in Figure 39 emphasize the points of coincidence. For example, the position at which K_{pw} begins to rise (CSF 360 mL) and its maximum (CSF 220 mL) are inflexion points for all the other curves as well.

Table 9: Effect of refining on pulp properties

Refining level, rev	Freeness CSF, mL	FSP g/OD g	WRV g/OD g	K_{pw} (sd)	fines %
0	676	1.74	1.78	0.09 (0.01)	1.61
2,500	464	2.26	2.14	0.22 (0.11)	3.18
5,000	358	2.78	2.26	0.32 (0.09)	3.61
7,500	261	2.52	2.32	2.0 (0.4)	6.37
10,000	235	2.95	2.37	3.6 (0.8)	8.05
12,500	125	2.09	2.32	0.94 (0.6)	8.57
15,000	84	2.13	2.3	2.1 (1.9)	7.46

Table 10: Effect of refining on fiber properties

Refining level (rev)	Fiber length (mm)	Mean curl	Kink index (mm^{-1})
0	2.11	0.095	1.47
2,500	2.19	0.064	0.99
5,000	2.16	0.081	1.19
7,500	2.14	0.062	1.05
10,000	2.19	0.056	0.83
12,500	2.11	0.055	0.82
15,000	2.09	0.054	0.82
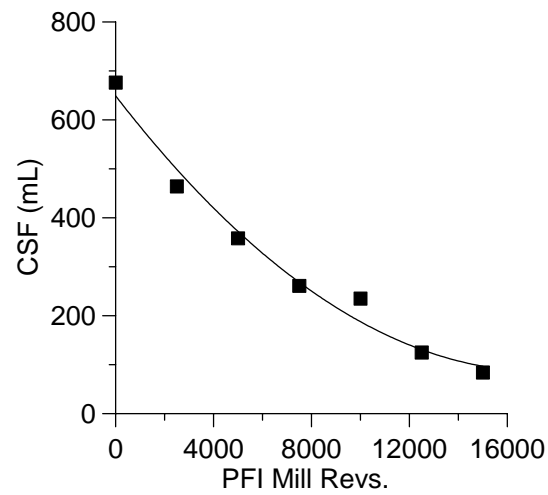
Figure 38: Refining curve for softwood pulp
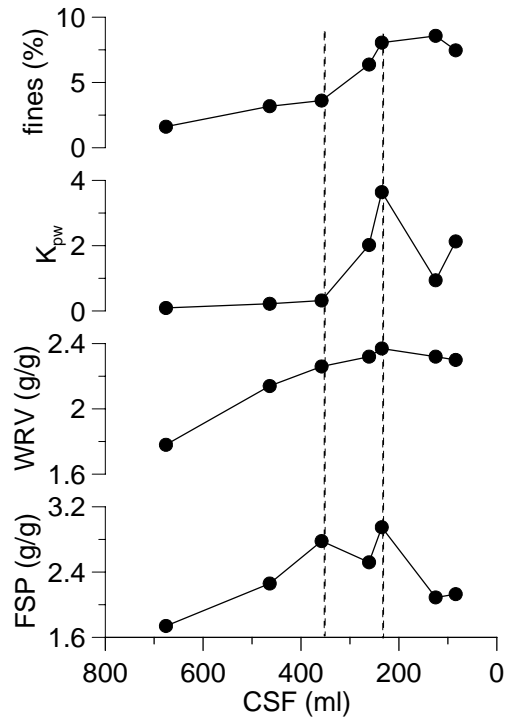
Figure 39: Effect of refining on fiber properties
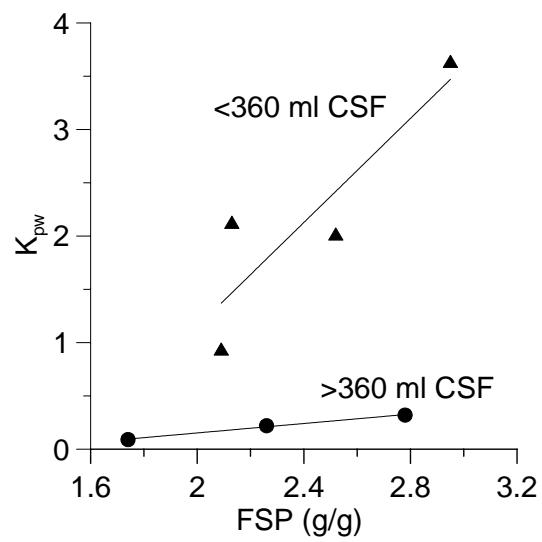
Figure 40: Relationship between FSP and Kpw
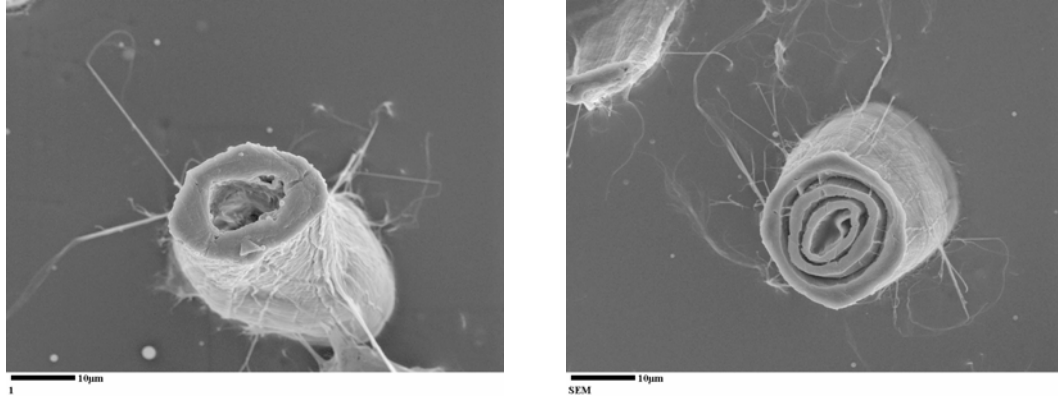
Figure 41: Typical SEM image of fibers refined to 358 CSF (left) and 261 CSF (right)

The FSP initially rises with decreasing freeness and then drops when the freeness falls below 220 mL. K_{pw} behaves very differently. It rises much more gradually at high freeness and then increases sharply at a 360 mL CSF. As shown in Figure 39, the fines content also steps up at this freeness value. Both FSP and K_{pw} are measures of fiber-associated water, but as discussed in Chapter 7, K_{pw} is believed to reflect mostly monolayer water (at least in unrefined pulp), whereas FSP includes additional layers of water. Consider the relationship between FSP and K_{pw} illustrated in Figure 40. Refining initially exposes more surface of the S2 layer, which increases the ability of the fiber to carry water. Hence, at high freeness (>360 mL CSF) both K_{pw} and the FSP increase linearly with each other. K_{pw} more than doubles in this region (Table 9), whereas FSP increases by about 50 %, which implies that refining increases monolayer water more than the water that is less strongly bound. This is reasonable because the initial cracks and tears created by refining are likely to be small, and a single layer of water is more likely to be accommodated than multiple layers in these small regions. A different relationship emerges upon further refining below 360 mL CSF. Although a rough linearity is still maintained, K_{pw} now increases much more sharply than does the FSP.

124

The increase in K_{pw} is almost fourfold in this range, whereas FSP rises by less than 50%. This indicates that the amount of monolayer water increases dramatically. It is remarkable that such a clear difference in behavior occurs at a freeness of 360 mL. While K_{pw} and FSP are linearly related on both sides of this value, there must be a sudden, rather than gradual change in fiber structure at this point.

Typical SEM images of fibers at and below the 360 mL CSF threshold are shown in Figure 41. Extensive internal delamination is clearly visible at 261 mL CSF. Such internal delamination is known to occur upon prolonged refining. Page and De Grace [138] have shown that kraft or sulfate pulp splits into two to four layers upon beating. Delaminations have also been observed by Williams [125]. Giertz [93] noted that removal of the primary wall and the S1 layer increases swelling within the fiber, which could promote delamination. Kibblewhite [139] observed cell wall removal during refining; a significant increase in S2 exposure occurred when either bleached or unbleached never-dried softwood pulps were refined to between 4,000 and 8,000 revolutions in a PFI mill. Kibblewhite [139] also reported an increase in the fines content, which is consistent with cell wall removal. The fines increase at 360 mL CSF in Figure 2 and level off when K_{pw} reaches a maximum. Hence, these results also support the onset of internal delamination at CSF 360 mL.

The most unusual feature of the K_{pw} profile is its sharp rise. The K_{pw} peak at about 3.6 indicates that a unit of dry fiber holds 3.6 units of water [134]. Clearly, this is well in excess of monolayer coverage, which raises the question of why such a large quantity of water resists being displaced by acetone. The Figure 41 images demonstrate that refining increases the internal surface and the water associated with this surface

could be considered to be confined by adjoining surfaces. An important property of confined water is that many more layers of water can be strongly bound to the structure than would be the case if the water were attached to a single surface [29].

Confined water can be found within the pores of a solid or between solid surfaces. The changes in behavior of water within these spaces is thought to be dependent on the size and geometry of the space [28]. The water may also be structured because of geometric constrains. One interesting attribute of confined water is its ability to supercool. Water within sol-gel silicas has the ability to supercool to between -15 and -25 ºC. When ice formation occurs within the silica the structure is cubic rather than the normal hexagonal shape [28]. As discussed in Chapter 7, supercooling occurs in cellulose fibers as well. This supercooled water is discussed under the terms nonfreezing bound water, and freezing bound water which freezes at a slightly depressed temperature. Nonfreezing water is most tightly associated with the cellulose and therefore has no detectable peak in the cooling or heating cycles associated with DSC [49, 57].

The size and shape of the confining space also reduce the ability for a water molecule to form all of its potential hydrogen bonds. This restriction is present until a separation of about ten water molecule diameters occurs between solid surfaces [29]. As the space between the surfaces decreases, the properties of water change from fluid-like to solid-like. Over approximately three hydration layers, or a separation of three water molecule diameters, the water retains fluid-like characteristics, although with increased shear viscosity. At a distance of one or two hydration layers, monolayer or bilayer ice can form [30]. Caulfield [41] also discussed the formation of 'ice-like' clusters from confined water in fibers. It is possible that acetone diffuses too slowly into this confined

region on our time scale. It is also possible that the water is very tightly bound to the surface. Regardless of the reason, it is clear that a large quantity of water strongly associates with the fiber surface at this low freeness.

As might be expected, the FSP also shows a maximum in the 350-450 mL CSF region although the peak is much shallower. The FSP measurement uses dextran as a probe, which, at a molecular weight of 2×10^6 is much larger than acetone and is able to access a smaller amount of the confined water. As a result, the FSP profile lacks the detail displayed in the K_{pw} curve. It is, of course, possible that acetone itself will also be excluded from some of the pore regions, but the degree of exclusion will be much lower than that for dextran. In any case, a reasonable; wet surface area can be calculated from K_{pw} [134], so the degree to which acetone is excluded cannot be high. Both FSP and K_{pw} decrease at less than 220 mL CSF. This is consistent with unraveling of the fiber structure where less of the water would be confined because the internal surfaces would open up and be exposed to the bulk water. The WRV tracks the FSP in the earlier stages of refining, but then levels off drops at the point at which K_{pw} reached a maximum. In contrast, the FSP drops at this point. The FSP falls upon prolonged refining for the same reason that K_{pw} does; the surface disintegrates and the proportion of confined water (the water held between surfaces) decreases. The WRV appears to be less sensitive to changes in the confined water.

K_{pw} is mainly a measurement of the water that cannot be displaced by acetone. Some of the tritium also exchanges with hydroxyl and other groups in the fiber matrix, but the proportion of these sites is small in comparison to the number of exchangeable sites present in the bound water [134]. Hence, the K_{pw} result depends on the size of the

molecule used to displace the water. Use of a compound larger than acetone to displace the water should give rise to a higher K_{pw}, because this larger molecule would be unable to enter some of the smaller pores and displace the water present there. The FSP is determined as the water that cannot mix with dextran. Thus, the main difference between the FSP and K_{pw} values is the size of the compound used to displace or mix with the water in the fiber. Dextran is much larger than acetone and it will be unable to enter some of the pores that will be accessible to acetone. As a result, the FSP is much higher than K_{pw} for unrefined pulp. The FSP and K_{pw} are very similar for refined pulp because the confined water does not interact with either compound and remains tightly bound to the fiber.

It appears that refining progresses through the three distinct stages shown in Figure 39, which are detected by both FSP and K_{pw}, although K_{pw} is more sensitive. The first stage of refining down to a CSF of about 360 mL removes the primary cell wall and S1 layer while swelling the S2 layer. At around 360 mL CSF, the fiber swelling reaches a maximum, increased refining creates internal delaminations within the cell wall thus developing regions of confined water. This confined water increases sharply as reflected by the spike in K_{pw} at 261 mL CSF. The outer area of the S2 layer as well as any remaining primary wall and S1 layer begin to form sheets of microfibrils extending from the fiber surface, similar to Neumann's 'dangling tail' theory [1]. Fiber destruction occurs in the final stage below a CSF of 220 mL where the internal surface opens up and the fraction of confined water decreases. The experimental uncertainty associated with K_{pw} increases at these low freeness values. Presumably, fiber destruction is not uniform.

The samples taken for K_{pw} measurements are quite small (~1.2 g) and fibers in multiple stages of destruction would add to measurement uncertainty.

The important feature of the K_{pw} profile is not the position of its maximum, but the freeness value of 360 mL CSF (in this case) where the curve breaks sharply upwards. It would appear that refining creates internal surface at lower freeness values, so the 360 mL CSF level should be an important cut-off point. Refining below this value will make dewatering and drying water removal more difficult without creating more useful surface. The 360 mL CSF is also optimum for minimizing fines. The K_{pw} identifies this breakpoint much more sharply than do the other parameters. Indeed, it suggests that small differences in freeness at this breakpoint will affect fiber properties significantly, a conclusion that is not obvious from the other more traditional measures of refining. Certainly, these features are absent in the traditional beater curve of Figure 38.

8.3 Conclusions

In conclusion, it has been shown that changes in internal fiber structure can be followed with the fiber:water partition coefficient (K_{pw}) of tritiated water. This study offers evidence that refining leads to three distinctly different stages. The primary cell wall and S1 layer is first removed. Further refining leads to internal delamination, which is signaled by a sharp increase in K_{pw}. Below this threshold K_{pw} is believed to represent monolayer water; above it, it also includes water confined between surfaces in the internal fiber structure. The rise in K_{pw} coincides with the beginning of internal delamination as confirmed by SEM imaging. It is suggested that the benefits of refining begin to decrease at this point. The fiber finally disintegrates when refined further.

Virgin fiber is rarely beaten to the low freeness levels where K_{pw} changes the most, so our work will mainly apply to recycle material.

CHAPTER 9: IMPACT OF RECYCLING

The work for this portion of the thesis was performed in collaboration with Adam Brancato. Adam's thesis work involves using the AFM to detect changes in a sheet surface during recycling. This study was performed to determine if changes in the sheet surface were also apparent in the bulk wet state. For this study the effect of hornification was analyzed.

9.1 Materials and Methods

Again never dried bleached softwood kraft pulp was obtained from Stora Enso's Wisconsin Rapids Mill, Wisconsin Rapids, WI. The pulp was refined to three different levels, unrefined, medium refining, and high refining in a valley beater following TAPPI Test Method T 200 [140]. For this study, the fibers at each refining level were recycled three times in a controlled manner. Throughout the recycling process, the sheets were restrain-dried as described in TAPPI Test Method T 205 [114], therefore the effect of heat during the drying process is minimized. Further information including all experimental procedures can be found in Chapter 4.

9.2 Results and Discussion

This study measured the effects of hornification on bleached softwood kraft at three refining levels, unrefined, a medium refining level (415 mL CSF), and a low refining level (222 mL CSF). The objectives of this study were to determine if K_{pw} and AFM are viable methods to study hornification. Based on the results of the refining study discussed in Chapter 8, three refining levels were chosen to determine if the different

stages of refining affect the level of hornification. The first, unrefined, was used as a

control. The second level at approximately 400 mL CSF should provide a swollen fiber

and with the high refining level, internal delamination should be present in the fiber.

However, in this study the fiber was refined using a valley beater due to the large

quantities of fiber needed for the study. Thus, the refining effects could be different from

those observed earlier with PFI mill refining.

Traditionally, the degree of hornification has been determined from the WRV

results [104, 117]. Table 11 provides hornification results from recent studies in the

literature. Wistara and Young [103] prepared bleached black spruce kraft pulp and

refined it at 10 % in a PFI mill to a freeness of approximately 400 mL CSF. Tze and

Gardner [107] used hardwood bleached kraft pulp in their experiments; no freeness

information given. Both of these studies fully dried the sheets during recycling [103,

107]. In Table 11 RX represents the number of recycles, X. Weise, Maloney and

Paulapuro [49] studied 'wet hornification'. In a previous study they determined that wet

hornification only occurred after 30% solids [141]. In this study they determined that

after that critical point, hornification will occur until the moisture content reaches a

minimum of around 60 % solids, where hornification no longer occurs [49]. The degree

of hornification was determined using Equation 24. Where WRV_{R0} is the WRV of the

virgin fiber and WRV_{RX} is the WRV of the fiber after X recycling cycles.

Equation 24: Degree of hornification

$$Degree\ of\ hornification = \frac{(WRV_{R0} - WRV_{RX})}{WRV_{R0}} * 100$$

Table 11: Recent hornification results in the literature

Reference	Pulp	Recycling level	WRV g/g	Degree of hornification %
Wistara and Young [103]	Bleached black spruce kraft	R0	2.19	0
		R1	1.90	13.24
		R2	1.81	17.35
Tze and Gardner [107]	Hardwood bleached kraft	R0	1.92	0
		R1	1.10	42.71
Weise, Maloney and Paulapuro [49]	Beaten HW bleached kraft	20-35%	2.74	0
		60-75%	1.75	36.3
	Beaten, Unbleached kraft, no fines	20-35%	2.05	0
		60-75%	1.55	24.5

Table 12: Comparison of methods during refining

Recycling level	Freeness mL	WRV g/g	Degree of hornification %	K_{pw} (sd)	AFM nN
RU0	676	1.79	0	0.11 (0.08)	27.55
RU1	677	1.73	3.35	0.21 (0.05)	68.26
RU2	672	1.65	7.82	0.18 (0.05)	84.96
RU3	670	1.65	7.82	0.12 (0.02)	93.98
RM0	415	2.06	0	1.02 (0.4)	34.62
RM1	428	1.48	28.16	0.43 (0.4)	68.80
RM2	424	1.38	33.01	0.46 (.03)	93.46
RM3	424	1.38	33.01	0.65 (0.4)	106.39
RH0	222	2.41	0	0.72 (0.3)	28.55
RH1	245	1.73	28.22	0.83 (0.3)	82.16
RH2	247	1.64	31.95	0.69 (0.4)	92.55
RH3	246	1.66	31.12	0.82 (0.4)	98.02

Table 12 contains the results of this study. The first set of data is for the unrefined sheets (RUX). The second is for the sheets with medium refining (RMX) and the third set of data is the results of the highly refined samples (RHX). The numbers, X, reflect how many times that sample has been recycled. Within this study the freeness was not affected by recycling.

The next two columns contain the traditional hornification data. Refining the fiber increases the degree of hornification, but after the first recycle, the degree of hornification seems to stabilize. The amount of hornification that is occurring appears to be independent of the amount of refining, at least at the refining levels chosen for this study. The degree of hornification in the refined pulp of this study is greater than the amount determined by Wistara and Young [103]. However, our results maybe slightly increased due to the method of obtaining the WRV samples. Most likely, a portion of the fines in the pulp were lost during sheet formation lowering WRV results. Weise, Maloney and Paulapuro [49] followed a similar method in performing their WRV testing and their degree of hornification results compare closely, even though a different base fiber is used.

The K_{pw} results and AFM results finish out Table 12. AFM measures the hydrophilicity of the surface of a sheet of paper by determining the strength of the forces present between the surface and the AFM tip. Both the K_{pw} and AFM results will be discussed in detail in the following paragraphs.

As determined in Chapter 8, when refined the interior water within the fiber begins to dominate the amount of water bound to the fiber as determined by K_{pw}. The

effect of the interior water on hornification is very apparent by examining both the WRV and K_{pw} results. For the unrefined fiber, there is essentially no change in the WRV or K_{pw} during the recycling process. The effects of recycling can be more clearly understood by examining Figure 42. Figure 42 contains the results for AFM, K_{pw}, and WRV for the unrefined pulp across all recycles. While, both the K_{pw} and WRV results remain relatively unchanged through repeated recycling, the AFM results increase steadily with each recycle.
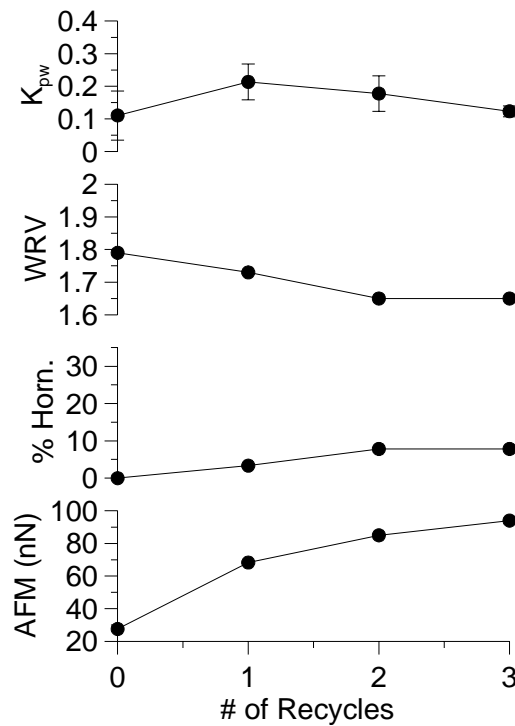
Figure 42: Effect of recycling unrefined pulp

Figure 43 and Figure 44 display the trends for the refined pulps. The medium refined K_{pw} results (Figure 43) follow the same trend as seen with the WRV results, indicating that both of these results are affected by the amount of interior water within the

135

fiber. In Chapter 8 the effect of interior water or confined water on K_{pw} results was discussed in detail. With the recycling results, interior water becomes a critical factor in determining WRV as well. The collapse of internal pores during drying is well documented in the literature [50, 104, 142-144]. This collapse of pore structure is quantified by the lowering of both WRV and K_{pw} results during recycling.
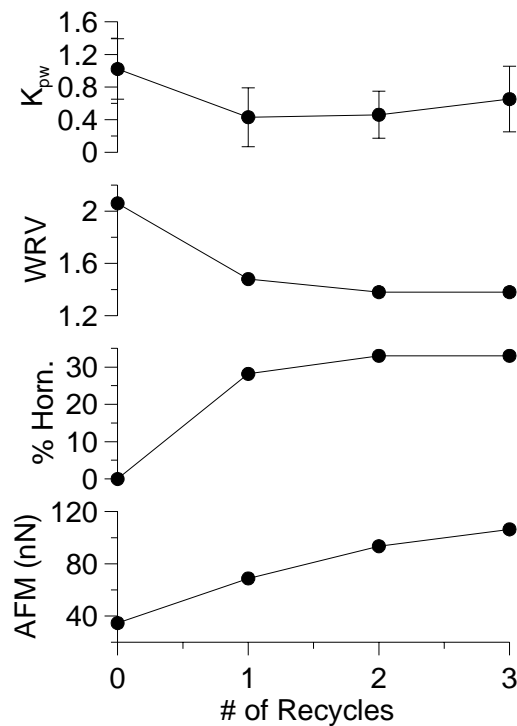
Figure 43: Effect of recycling on pulp refined to 400 mL CSF

Today hornification is also defined chemically by the formation of irreversible internal hydrogen bonding [6, 49, 77, 104]. The hydrogen bonds formed between and within fibers during the drying process cause shrinkage and an increased rigidity of the fibers. There are a number of theories on the formation of these hydrogen bonds. Researchers have theorized that the formation results from the crystallization of

amorphous regions of the fiber [53] to cocrystallization between adjacent crystallization regions or microfibrils [106]. Tze and Gardner quantified the reduction in available hydroxyl groups through acetyl substitution [107]. They found a significant difference in hydroxyl number between the virgin, 261, and recycled pulp, 177, a 32 % decrease. On the whole, the decrease in K_{pw} and WRV indicate a lower amount of available hydroxyl groups through the bulk of the pulp

However, the results are not as clear with the highly refined pulp, Figure 44. The K_{pw} results are highly variable and show no general trend, while the WRV decreases as expected. This is where the method of water removal is highlighted. For WRV, water is physically removed and for K_{pw} excess water is chemically displaced. At this point in the refining curve, the fiber could easily be in the destruction phase. This reduces the amount of interior water due to the large amount of delamination and fiber separation occurring, thus lowering the K_{pw} values from the previous refining level (Chapter 8). The K_{pw} values here indicate that the overall association of fiber with water has not changed by recycling at the high freeness level, but as indicated by WRV and AFM where the association occurs has changed.
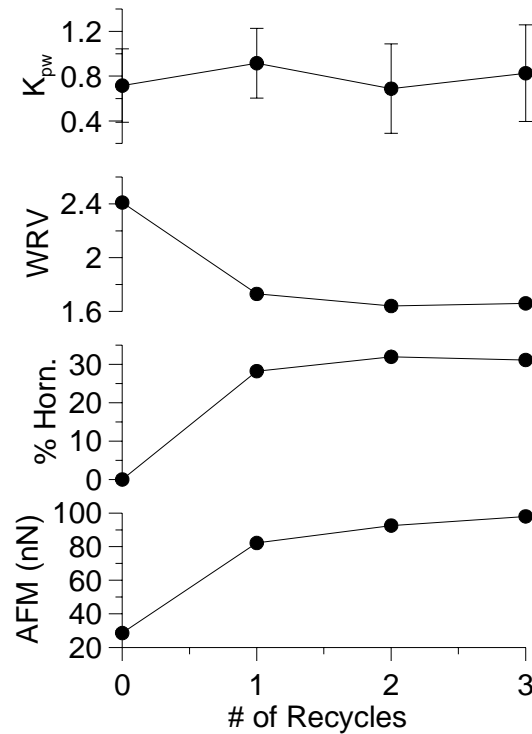
Figure 44: Effect of recycling on pulp refined to 200 mL CSF

AFM, being a dry measurement only focuses on the external properties of the sheet. What is apparent across all refining levels is the increase in the hydrophilicity of the surface with recycling. Microstructural changes within the fiber are also possible during hornification [103]. These changes may influence the interaction between fibers and water [103]. Wistara et al, found that recycling changes the surface free energy of a pulp, increasing the acid component and decreasing the base [145]. These changes gave the pulp an improved wettablilty, but the changes at the surface did not affect the overall properties of the pulp [145]. The AFM results also found an increase in the hydrophilicity of the surface of the pulp at all refining levels, confirming the Wistara results.

9.3 Conclusions

Through this study it became apparent that the method of determination determines the outcome of the research.

WRV is a measure of the physical water carrying ability of a fiber mat. Through the WRV results it is evident that the amount of water retained decreases with recycling. It appears however that after a certain refining level the percentage decrease with recycling does not change. This is the expected behavior.

AFM and K_{pw} however, are measures of the chemical interaction of water with fiber. AFM overall shows an increase in the activity of the fiber surface with recycling. These results confirm the earlier work of Wistara et al [145]. However, the AFM results do not change with progressive refining. This is probably because the changes induced by refining are on a scale that is much larger than the nanoscale.

The K_{pw} results are more difficult to decipher as the internal chemical reactivity also plays a role in the K_{pw} result. The internally available hydrogen sites can override the affect of the external hydrogen bonding sites. Through recycling, the internal surface area decreases lowering the internal hydrogen accessibility, while the hydrophilicity of the surface increases as shown through AFM. The K_{pw} results appear to stem from a combination of both the internal and external bonding sites. With the unrefined and highly refined pulp, the overall chemical reactivity as shown by K_{pw} remains constant. But, at 400 mL CSF, Kpw decreases in correlation with WRV values. This change in response may correspond to the internal state of the refined fiber. With the unrefined fiber having little internally chemically attached water, the medium refined fiber having a much larger quantity of internal water possibly stemming from delaminations within the

fiber, and the highly refined fiber lowering the amount of chemically attached water through fiber separation.

Thus, there are two main components at work during hornification, the chemical nature of the fiber and the physical nature of the fiber.

CHAPTER 10: OVERALL CONCLUSIONS

A new technique for measuring the water content of fiber was presented in this thesis. Within this technique, tritiated water is added to a pulp/water suspension whereupon the tritium partitions between the bulk water and the pulp. Thus, a fiber:water partition coefficient is developed, K_{pw}. This thesis covered the development of the K_{pw} procedure and three different case studies.

The first study involves comparing K_{pw} to traditional methods of fiber water content. The procedure provides a value of ten percent for the tightly bound water content of unrefined hardwood or softwood kraft fiber, either bleached or unbleached. If this water is assumed to cover the fiber surface as a monolayer, then an estimate of the wet surface area of fiber can be obtained. This estimate compares well to independent measurements of surface area.

K_{pw} has also been found to be valuable in furthering the understanding of refining. Based on the study, it is proposed that refining occurs in three discrete stages. First, refining removes the primary cell wall and S1 layer while beginning to swell the S2 layer. Next, internal delamination occurs within the S2 layer. Finally, fiber destruction occurs at high refining levels. By using K_{pw}, the three stages of refining are clearly recognized.

Lastly, K_{pw} is used to study the effect of hornification on bleached softwood kraft fiber. For this study samples were refined to three levels and recycled three times, testing was performed during each recycle. The recycling effects at each refining level were characterized by K_{pw} and followed closely the findings of the refining study. At low and high refining levels, the impact of recycling was minimal according to K_{pw} results, but at

400 mL csf the impact of recycling was much more pronounced. This could be attributed to the closing of internal delaminations within the fiber.

Overall, K_{pw} provides a new method for characterizing the fiber – water relationship. K_{pw} indicates the chemical interaction between fiber and water which is an advancement over traditional methods that physically characterize this interaction.

REFERENCES

1.   Neuman, R.D., *Surface Force Measurement in Paper Making Systems*. Products of Papermaking, ed. C.F. Baker. Vol. 2. 1993, Leatherhead: Pira International. 969-1021.

2.   Clark, J.d.A., *Pulp technology and treatment for paper*. 2nd ed. 1985, San Francisco, California: Miller Freeman Publications, Inc. 878.

3.   Kibblewhite, R.P., *Effects of beating on wet web behavior.* Appita Journal, 1973. **26**: p. 341.

4.   Alince, B., *Deposition of cationic polymeric pigments on pulp fibers.* Journal of Colloid Interface Science, 1979. **69**: p. 367.

5.   Dimmel, D.R., *A6130 Wood and Fiber Science, Lecture 7 Wood Components*. 2001, Institute of Paper Science and Technology.

6.   Smook, G.A., *Handbook for Pulp and Paper Technologists*, ed. M.J. Kocurek. 1982, Montreal, Quebec Canada: TAPPI and CPPA. 395.

7.   Brown, et al. *Cellulose biosynthesis in higher plants*. 2002 [cited 2002; Available from: http://www.botany.utexas.edu/infores/cen/library/recpub/.

8.   Grinsted, M.J. and A.T. Wilson, *Hydrogen Isotopic Chemistry of Cellulose and Other Organic Material of Geochemical Interest.* New Zealand Journal of Science, 1979. **22**(3): p. 281-287.

9.   Fahlen, J. and L. Salmen, *Cross-sectional structure of the secondary wall of wood fibers as affected by processing.* Journal of Materials Science, 2003. **38**: p. 119-126.

10.   Nissan, A.H. *General principles of adhesion with particular reference to the hydrogen bond*. in *Formation and Structure of Paper, trans. IInd Fund. Res. Symp.* 1961. Oxford: FRC.

11.   Retulainen, E., *The role of fibre bonding in paper properties*, in *Department of Forest Products Technology*. 1997, Helsinki University of Technology: Helsinki, Finland. p. 63.

12.   Liitia, T., S.L. Maunu, and B. Hortling, *Solid State NMR Studies on Cellulose Crystallinity in Fines and Bulk Fibres Separated from Refined Kraft Pulp.* Holzforschung, 2000. **54**(6): p. 618-624.

13.   Child, T.F. and D.W. Jones, *Broad-Line NMR Measurement of Water accessibility in Cotton and Woodpulp Celluloses.* Cellulose Chemistry and Technology, 1973. **7**: p. 525-534.

14.   Biermann, C.J., *Handbook of Pulping and Papermaking.* 1996, Academic Press: San Diego, California. p. 754.

15.   Mark, R.E., *Cell wall mechanics of tracheids.* 1967, New Haven and London: Yale University Press. 310.

16.   Christensen, P.K. and H.W. Giertz. *The cellulose/water relationship.* in *Consolidation of the Paper Web, Trans. IIIrd Fund. Res. Symp.* 1965. Cambridge: FRC.

17.   Ring, G., *Introduction to Pulp and Paper Properties, Paper Properties Notes.* 1999, University of Wisconsin - Stevens Point.

18.   Higgins, H., *Sticking together - how interfibre cohesion works The magic of hydrogen bonds.* Appita Journal, 2002. **55**(3): p. 187.

19.   Pelton, R., et al., *The role of surface polymer compability in the formation of fiber/fiber bonds in paper.* Nordic Pulp and Paper Journal, 2000. **15**(5): p. 400-406.

20.   Corte, V.H. and H. Schaschek, *Physikalische Natur der Papierfestigkeit.* Das Papier, 1955. **9**(21/22): p. 519-530.

21.   Haddad, Y.M., *A theoretical approach to interfiber bonding of cellulose.* Journal of Colloid and Interface Science, 1980. **76**(2): p. 490 - 501.

22.   Nilsson, A. and L.G.M. Pettersson, *Chemical bonding on surfaces probed by X-ray emission spectroscopy and density functional theory.* Surface Science Reports, 2004. **55**: p. 49-167.

23.   Jacob, T. and W.A. Goddard III, *Agnostic interactions and dissociation in the first layer of water on Pt(111).* Journal of the American Chemical Society, 2004. **126**(30): p. 9360-9368.

24.   Michaelides, A., A. Alavi, and D.A. King, *Different surface chemistries of water on Ru{0001}: from monomer adsorption to partially dissociated bilayers.* Journal of the American Chemical Society, 2003. **125**: p. 2746-2755.

25.   Ping, Z.H., et al., *States of water in different hydrophilic polymers - DSC and FTIR studies.* Polymer, 2001. **42**: p. 8461-8467.

26.   Adams, B. and L. Lerner, *Observation of hydroxyl protons of sucrose in aqueous solution: no evidence for persistent intramolecular hydrogen bonds.* Journal of the American Chemical Society, 1992. **114**: p. 4827-4829.

27. Wong, T.C. and T.T. Ang, *Study of molecular dynamics of water adsorbed on macroscopically oriented cellulose by deuteron nuclear magnetic relaxation.* Journal of Physical Chemistry, 1985. **89**(19): p. 4047-4051.

28. Crupi, V., et al., *Dynamic properties of liquids in restricted geometeries.* Journal of Molecular Liquids, 2005. **117**: p. 165-171.

29. Urbic, T., V. Vlachy, and K.A. Dill, *Confined water: A Mercedes-Benz model study.* Journal of Physical Chemistry B, 2006. **110**(10): p. 4963-4970.

30. Leng, Y. and P.T. Cummings, *Hydration structure of water confined between mica surfaces.* The Journal of Chemical Physics, 2006. **124**: p. 074711.

31. Israelachvili, J.N. and R.M. Pashley, *Molecular layering of water at surfaces and origin of repulsive hydration forces.* Nature, 1983. **306**(17): p. 249 - 250.

32. Derjaguin, B.V. and L. Landau, Acta Physicochim URS, 1941. **14**: p. 633-662.

33. Verwey, E.J.W. and J.T.G. Overbeek, *Theory of the Stability of Lyophobic Colloids.* 1948, Amsterdam: Elsevier.

34. Child, T.F., *Pulsed n.m.r. study of molecular motion and environment of sorbed water on cellulose.* Polymer, 1972. **13**: p. 259-264.

35. Stone, J.E. and A.M. Scallan, *The effect of component removal upon the porous structure of the cell wall of wood. II. Swelling in water and the fiber saturation point.* TAPPI Journal, 1967. **50**(10): p. 496-501.

36. Stamm, A.J., *Wood and cellulose science.* 1964, New York: Ronald Press. 549.

37. Berthold, J., et al., *Types of adsorbed water in relation to the ionic groups and their counter-ions for some cellulose derivatives.* Polymer, 1994. **35**(26): p. 5729-5736.

38. Salmen, L. and J. Berthold. *The swelling ability of pulp fibers.* in *The Fundementals of papermaking Materials, XIth Fund. Res. Symp.* 1997. Cambridge: FRS.

39. Kimura, M., H. Hatakeyama, and M. Usuda, *Studies on adsorbed water in cellulose by broad-line NMR.* Journal of Applied Polymer Science, 1972. **16**: p. 1749-1759.

40. Goring, D.A.I. *The effect of cellulose on the structure of water: view 1.* in *Fiber-Water Interactions in Paper-Making, VIth Fun. Res. Symp.* . 1977. Oxford: FRC.

41. Caulfield, D.F. *The effect of cellulose on the structure of water: view 2.* in *Fiber-Water Interactions in Paper-Making, VIth Fun. Res. Symp.* . 1977. Oxford: FRC.

42. Hartley, I.D., F.A. Kamke, and H. Peemoeller, *Cluster theory for water sorption in wood.* Wood Science and Technology, 1992. **26**: p. 83-99.

43. Brunauer, S., P.H. Emmett, and E. Teller, *Adsorption of gases in multimolecular layers.* Journal of the American Chemical Society, 1938. **60**: p. 309-319.

44. Dent, R.W., *A multilayer theory for gas sorption. I. Sorption of a single gas.* Textile Research Journal, 1977. **47**: p. 145-152.

45. Stone, J.E., A.M. Scallan, and B. Abrahamson, *Influence of Beating on Cell Wall Swelling and Internal Fibrillation.* Svensk Papperstidning, 1968. **71**(19).

46. Tiemann, H., *Bull. No. 70: Effect of moisture upon the strength and stiffness of wood.* 1906, US Department of Agriculture, Forest Service

47. TAPPI, *UM 256 Water Retention Value (WRV),* in *TAPPI Useful Methods.* 1991, TAPPI Press: Atlanta, GA. p. 54-56.

48. Scallan, A.M. and J.E. Carles, *Correlation of the Water Retention Value with the Fiber Saturation Point.* Svensk Papperstidning, 1972. **75**(17): p. 699-703.

49. Weise, U., T.C. Maloney, and H. Paulapuro, *Quantification of water in different states of interaction with wood pulp fibers.* Cellulose, 1996. **3**: p. 189-202.

50. Scallan, A.M. *Accommodation of water within pulp fibers.* in *BPBIF Symposium - Fiber Water Interactions in Papermaking.* 1977. Oxford.

51. Aggebrandt, L.G. and O. Samuelson, *Penetration of water-soluble polymers into cellulose fibers.* Journal of Applied Polymer Science, 1964. **8**: p. 2801-2812.

52. Nanko, H., *A6130 Wood and Fiber Science, Lecture 21 Effect of Beating on Fiber Properties II.* 2001, Institute of Paper Science and Technology.

53. Somwang, K., et al., *Changes in crystallinity and re-swelling capability of pulp fibers by recycling treatment.* Japan Tappi, 2002. **56**(6): p. 868-869.

54. Hernadi, A., *Accessibility and specific surface of cellulose measured by water vapor sorption.* Cellulose Chemistry and Technology, 1984. **18**: p. 115-124.

55. Magne, F.C., H.J. Portas, and H. Wakeham, *A calorimetric investigation of moisture in textile fibers.* Journal of the American Chemical Society, 1947. **69**: p. 1896-1902.

56. Maloney, T.C., H. Paulapuro, and P. Stenius, *Hydration and swelling of pulp fibers measured with differential scanning calorimetry.* Nordic Pulp and Paper Research Journal, 1998. **13**(1): p. 31-36.

57. Nakamura, K., T. Hatakeyama, and H. Hatakeyama, *Studies on bound water of cellulose by differential scanning calorimetry.* Textile Research Journal, 1981. **51**(9): p. 607-613.

58. Carles, J.E. and A.M. Scallan, *The determination of the amount of bound water within cellulosic gels by NMR spectroscopy.* Journal of Applied Polymer Science, 1973. **17**: p. 1855-1865.

59. Jeffries, R., *Sorption of water by cellulose and eight other textile polymers. I. The sorption of water by celluloses below 100.* Journal of the Textile Institute, 1960. **51**: p. T339-T374.

60. de Boer, J.H. and C. Zwikker, *Adsorption as a result of polarization. The Adsorption isotherm.* Zeitschrift fuer Physikalische Chemie, Abeteilung B, 1929. **3**: p. 407-18.

61. Nelson, R.A., *The determination of moisture transitions in cellulosic materials using differential scanning calorimetry.* Journal of Applied Polymer Science, 1977. **21**: p. 645-654.

62. Hatakeyama, T., K. Nakamura, and H. Hatakeyama, *Vaporization of bound water associated with cellulose fibres.* Thermchimica Acta, 2000. **352-353**: p. 233-239.

63. Froix, M.F. and R. Nelson, *The interaction of water with cellulose from nuclear magnetic resonance relaxation times.* Macromolecules, 1975. **8**(6): p. 726-730.

64. Niskanen, K., *Paper Physics.* Papermaking Science and Technology, ed. J. Gullichsen and H. Paulapuro. Vol. 16. 1998, Helsinki, Finland: Fapet Oy. 324.

65. McKenzie, A.W., *The structure and properties of paper Part XXI: The diffusion theory of adhesion applied to interfibre bonding.* Appita, 1984. **37**(7): p. 580 - 583.

66. Byrd, V.L., *How much moisture is needed to develop strength in dry-formed handsheets?* TAPPI, 1974. **57**(4): p. 131 - 133.

67. Johansson, A., *The linear free energy relation of the acid-base interactions between cellulose and organic molecules. A possible for characterizing new pulp qualities.* Holzforschung, 1990. **44**(2): p. 103-106.

68. Byrd, V.L., *Bonding of air-laid webs: Critical amount of moisture necessary.* TAPPI, 1982. **65**(5): p. 153 - 155.

69. Robertson, A.A., *Interactions of liquids with cellulose.* TAPPI, 1970. **53**(7): p. 1331-1339.

70. Campbell, B.W., *The mechanism of bonding.* TAPPI, 1959. **42**(12): p. 999-1001.

71.   Campbell, B.W., *Hydration and beating of cellulose pulps.* Industrial and Engineering Chemistry, 1934. **26**(2): p. 218-219.

72.   Voyutskii, S.S., *Autohesion and adhesion of high polymers.* Polymer reviews, ed. V.L. Vakula. Vol. 4. 1963, New York: Wiley. 272.

73.   Paavilainen, L., *Conformability - flexibility and collapsibility - of sulphate pulp fibers.* Paperi ja Puu, 1993. **75**(9-10): p. 689-702.

74.   *isotope*, in *Merriam-Webster's Collegiate Dictionary*, F.C. Mish, Editor. 1995, Merriam-Webster, inc.: Springfield, Massachusetts. p. 1559.

75.   Hishikawa, Y., et al., *Characterization of amorphous domains in cellulosic materials using a FTIR deuteration monitoring analysis.* Polymer, 1999. **40**: p. 7117-7124.

76.   Rousselle, M.-A. and M.L. Nelson, *Accessibility of cotton cellulose by deuterium exchange.* Textile Research Journal, 1971. **41**(7): p. 599-604.

77.   Hatakeyama, H. and T. Hatakeyama, *Structural change of amorphous cellulose by water- and heat-treatment.* Reports on Progress in Polymer Physics in Japan, 1979. **22**: p. 169-170.

78.   Guthrie, J.D. and D.C. Heinzelman, *Determination of the accessibility of cellulose by use of $D_2^{18}O$ and mass spectroscopy.* Textile Research Journal, 1970. **40**(12): p. 1133.

79.   Ioelovitch, M. and M. Gordeev, *Crystillinity of cellulose and its accessibility during deuteration.* Acta Polymer, 1994. **45**: p. 121-123.

80.   Li, T., *2H-NMR spectra for D2O adsorbed on oriented cellulose fibers.* Applied Spectroscopy, 1996. **50**(12): p. 1512-1518.

81.   Tsuchikawa, S. and H.W. Siesler, *Near-infrared spectroscopic monitoring of the diffusion process of deuterium-labeled molecules in wood: Part 1 - Softwood.* Applied Spectroscopy, 2003. **57**(6): p. 667-674.

82.   Tsuchikawa, S. and H.W. Siesler, *Near-infrared spectroscopic monitoring of the diffusion process of deuterium-labeled molecules in wood: Part 2 - Hardwood.* Applied Spectroscopy, 2003. **57**(6): p. 675-681.

83.   Guthrie, J.D. and D.C. Heinzelman, *Deuterium-hydrogen-exchange accessibility of cellulose by use of $D_2^{18}O$ and mass spectroscopy.* Textile Research Journal, 1974. **44**(12): p. 981-985.

84.   Frilette, V.J., J. Hanle, and H. Mark, *Rate exchange of cellulose with heavy water.* Journal of the American Chemical Society, 1948. **70**(3): p. 1107-1113.

85.   Jeffries, R., *The amorphous fraction of cellulose and its relation to moisture sorption* Journal of Applied Polymer Science, 1964. **8**(3): p. 1213-1220.

86.   Schott, H., *Direct comparison of the strength of hydrogen bonds formed by H_2O and D_2O.* Journal of Macromolecular Science - Physics, 1988. **B27**(1): p. 119-123.

87.   Sakai, K., et al., *Determination of pore radius of hollow-fiber dialysis membranes using tritium-labeled water.* Journal of Chemical Engineering of Japan, 1988. **21**(2): p. 207-210.

88.   Sumi, Y., et al., *Accessibility of wood and wood carbohydrates measured with tritated water.* TAPPI Journal, 1964. **47**(10): p. 621-624.

89.   Wahid, A.K. and J.H. Ali, *Determination of molecular weight for cellulose by tracer technique.* Cellulose Chemistry and Technology, 1986. **20**: p. 153-156.

90.   Jacobson, A., *Diffusion of chemicals into green wood*, in *Ph.D. thesis*. 2006, Georgia Institute of Technology: Atlanta, GA. p. 121.

91.   Page, D.H. *The beating of chemical pulps - the action and the effects*. in *Fundamentals of Papermaking, 9th Fundamental Research Symposium*. 1989. Cambridge: FRC.

92.   Emerton, H.W., *Fundamentals of the beating process*. 1957, Kenley, Eng.: The British Paper and Board Industry Research Association. 198.

93.   Giertz, H.W., *The effects of beating on individual fibres*, in *Fundamentals of Papermaking Fibres, 1st Fundamental Research Symposium*, F. Bolam, Editor. 1957, FRC: Cambridge. p. 389-409.

94.   Batchelor, W., *Refining and the development of fibre properties.* Nordic Pulp and Paper Journal, 1999. **14**(4): p. 285-291.

95.   Fahey, M.D., *Mechanical treatment of chemical pulps.* TAPPI Journal, 1970. **53**(11): p. 2050-2064.

96.   Gallay, W. *Some aspects of the theory of the beating process*. in *Fundamentals of Papermaking Fibres, Tras. Ist Fund. Res. Symp.* 1957. Cambridge: FRC.

97.   Hietanen, S. and K. Ebeling, *Fundamental Aspects of the Refining Process.* Paperi ja Puu, 1990. **72**(2): p. 158-170.

98.   Higgins, H.G. and J. de Yong. *The beating process - primary effects and their influence on pulp and paper processes*. in *Formation and Structure of Paper, 2nd Fundamental Research Symposium*. 1961. Oxford: FRC.

99.   Strachan, J., *Hydration of cellulose in paper making.* Paper Industry, 1926. **8**: p. 235-237.

100.   Nanko, H., J. Ohsawa, and A. Okagawa, *How to see interfibre bonding in paper sheets.* Journal of Pulp and Paper Science, 1989. **15**(1): p. J17-J23.

101.   Robertson, A.A. *A note on the permeability method for determining surface development and swelling during beating and refining.* in *Fundamentals of Papermaking Fibres, Trans. Ist Fund. Res. Symp.* 1957. Cambridge: FRC.

102.   Hult, et al., *A CP/MAS 13C-NMR Study of Cellulose Structure on the Surface of Refined Kraft Pulp Fibers.* Carbohydrate Polymers, 2002. **49**(2): p. 231-234.

103.   Wistara, N. and R.A. Young, *Properties and treatments of pulps from recycled paper. Part I. Physical and chemical properties of pulps.* Cellulose, 1999. **6**(1): p. 291-324.

104.   Fernandes Diniz, J.M.B., M.H. Gil, and J.A.A.M. Castro, *Hornification - its origins and interpretation in wood pulps.* Wood Science and Technology, 2004. **37**: p. 489-494.

105.   Jayme, G. and E. Roffael, *Die Anwendung des WRV-Wertes zur Erfassung von Strukturanderungen der Cellulose.* Das Papier, 1970. **24**(6): p. 335-340.

106.   Newman, R.H., *Carbon-13 NMR evidence for cocrystallization of cellulose as a mechanism for hornification of bleached kraft pulp.* Cellulose, 2004. **11**: p. 45-52.

107.   Tze, W.T. and D.J. Gardner, *Swelling of recycled wood pulp fibers: Effect on hydroxyl availability and surface chemistry.* Wood and Fiber Science, 2001. **33**(3): p. 364-376.

108.   Baum, G.A., *A6130 Wood and Fiber Science, Lecture 26 Section 4 Fiber Cell Wall Models.* 2001, Institute of Paper Science and Technology.

109.   Page, D.H., *Personal Communication, Institute of Paper Science and Technology*, F.L. Jacobson, Editor. 2002: Atlanta, GA.

110.   Berry, S.L. and M.L. Roderick, *Plant-water relations and the fibre saturation point.* New Phytologist, 2005. **168**(1): p. 25-37.

111.   Nanko, H., *A6130 Wood and Fiber Science, Lecture 20 Effect of Beating on Fiber Properties I.* 2001, Institute of Paper Science and Technology.

112.   IPST, *Procedure No. 401B: PFI Refining - CPPA Procedure.* 2002, Institute of Paper Science and Technology. p. 4.

113.   PAPTAC, *Pulp and Paper Technical Association of Canada Standard Testing Methods.* 1998, Montreal, Canada.

114.	TAPPI, *T 205 sp-02: Forming handsheets for physical tests of pulp*, in *2004-2005 TAPPI Test Methods*. 2004, TAPPI Press: Atlanta, GA. p. 9.

115.	TAPPI, *T 272 sp-02: Forming handsheets for reflectance testing of pulp (sheet machine procedure)*, in *2004-2005 TAPPI Test Methods*. 2004, TAPPI Press: Atlanta, GA. p. 6.

116.	IPST, *Procedure No. 416: Water Retention Value of Pulp*. 2000, Institute of Paper Science and Technology.

117.	Jayme, G., *Properties of Wood Celluloses II. Determination and Significance of Water Retention Value.* TAPPI Journal, 1958. **41**(11): p. 180-183.

118.	Frazier, J.A., *Evaluation of physico-chemical mechanisms by which residual cooking liquor retards kraft delignification*. 2001, Institute of Paper Science and Technology: Atlanta, Georgia. p. 125.

119.	Bottger, J., L. Thi, and T. Krause, *Untersuchungen zur Porenstruktur von Zellstoffasern.* Das Papier, 1983. **37**(10A): p. V 14 - V 21.

120.	Garcia, R. and R. Perez, *Dynamic atomic force microscopy methods.* Surface Science Reports, 2002. **47**: p. 197-301.

121.	Brancato, A., *AFM procedure, emailed to Frances L Walsh June 28, 2006*. 2006: Atlanta, GA.

122.	*The fiber quality analyzer code LDA96 32-bit software operation manual.* 1999, Hawekesbury, Ontario, Canada: OpTest Equipment Inc. 67.

123.	Lowe, R., A. Ragauskas, and D.H. Page. *Imaging Fibre Deformations*. in *Advances in Paper Science and Technology, 13th Fun. Res. Symp. .* 2005. Cambridge: FRC.

124.	Williams, G.J. and J.G. Drummond, *Preparation of large sections for the microscopical study of paper structure.* Journal of Pulp and Paper Science, 2000. **26**(5): p. 188-193.

125.	Williams, G.J., J.G. Drummond, and H.A. Cisneros, *A Microscopical approach for examining fibre and paper structures.* Journal of Pulp and Paper Science, 1994. **20**(4): p. J110-J114.

126.	Pan, S., *SEM Procedure, email to Frances L Walsh, May 11, 2006*: Atlanta, GA.

127.	Chiang, Y., et al., *Kinetic isotope effects on the hydroxide ion catalyzed enolization of acetone: Relationship between deuterium and tritium isotope effects.* Journal of the American Chemical Society, 1992. **114**: p. 3981-3982.

128. Mantanis, G.I., R.A. Young, and R.M. Rowell, *Swelling of compressed cellulose fiber webs in organic liquids.* Cellulose, 1995. **2**: p. 1-22.

129. Li, T.-Q., et al., *Water diffusion in wood pulp cellulose fibers studied by means of the pulsed gradient spin-echo method.* Journal of Colloid and Interface Science, 1992. **154**(2): p. 305-315.

130. Crank, J., *Figure 5.7*, in *Mathematics of Diffusion*. 1956, Clarendon Press: Oxford. p. 78.

131. PerkinElmer, *QuantaSmart for the TriCarb Liquid Scintillation Analyzer Getting Started Manual*. A ed. 2004, Downers Grove, IL: PerkinElmer, Inc. 88.

132. Walsh, F.L. and S. Banerjee, *Measurement of monolayer water in pulp.* Holzforschung submitted, 2006.

133. Walsh, F.L. and S. Banerjee. *An isotopic study of the effects of refining on fiber*. in *2006 Pan Pacific Conference Advances in Pulp & Paper Sciences and Technologies* 2006. Seoul, Korea: Korea TAPPI.

134. Walsh, F.L. and S. Banerjee, *Isotopic study of the effects of refining on internal fiber structure.* Holzforschung submitted, 2006.

135. Hines, A.L. and R.N. Maddox, *Mass Transfer: fundamentals and applications*. Prentice Hall International Series in the Physical and Chemical Engineering Series, ed. N.R. Amundson. 1985, Upper Saddle River, New Jersey: Prentice Hall PTR. p. 21.

136. Herrington, T.M. and J.C. Petzold, *Surface area of papermaking woodpulps used by the British paper industry.* Cellulose, 1995. **2**: p. 83-94.

137. Grunwald, E.J., *Thermodynamic properties, propensity laws, and solvent models in solutions in self-associating solvents. Application to aqueous alcohol solutions.* Journal of the American Chemical Society, 1986. **106**: p. 5414-5420.

138. Page, D.H. and J.H. De Grace, *The delamination of fiber walls by beating and refining.* TAPPI, 1967. **50**(10): p. 489-495.

139. Kibblewhite, R.P., *Interrelations between pulp refining treatments, fibre and fines quality, and pulp freeness.* Paperi ja Puu, 1975. **57**(8): p. 519-526.

140. TAPPI, *T 200 sp-06: Laboratory beating of pulp (Valley beater method)*, in *2004-2005 TAPPI Test Methods*. 2004, TAPPI Press: Atlanta, GA. p. 9.

141. Weise, U. and H. Paulapuro, *Der Zusammenhang zwichen Faserschrumpfung und Verhornung.* Das Papier, 1996. **50**(6): p. 328-333.

142. Stone, J.E. and A.M. Scallan. *Influence of drying on the pore structures of the cell wall*. in *Consolidation of the Paper Web, Trans. IIIrd Fund. Res. Symp.* 1965. Cambridge: FRC.

143. Topgaard, D. and O. Soderman, *Changes of cellulose fiber wall structure during drying investigated using NMR self-diffusion and relaxation experiments.* Cellulose, 2002. **9**: p. 139-147.

144. Norberg, P.H., *Electron Microscopy Observations of the Effects of Drying on Cellulose Fibers.* Svensk Papperstidning, 1970. **73**(7): p. 208-214.

145. Wistara, N., X. Zhang, and R.A. Young, *Properties and treatments of pulps from recycled paper. Part II. Surface properties and crystallinity of fibers and fines.* Cellulose, 1999. **6**(2): p. 325-348.